

博士論文

Application of endometrial stromal cells in engineered tissue constructs to promote uterine regeneration and early implantation of embryo

(子宮再生および胚の初期着床を
促進するための組織形成における
子宮内膜細胞の適用)

キム ジョンヒョン



東京大学
THE UNIVERSITY OF TOKYO

**Application of endometrial stromal cells in
engineered tissue constructs to promote uterine
regeneration and early implantation of embryo**

Ph.D. Eng. Thesis

By: **Jeonghyun Kim**

Supervised by
Associate Professor Katsuko S. Furukawa

August 2017

Department of Mechanical Engineering
Graduate School of Engineering
The University of Tokyo

Table of Contents

1. Introduction	7
1.1 Introduction	7
1.2 Motivation	7
1.3 Objective	8
2. Background	10
2.1.1 What is uterus?	10
2.1.2 Anatomy of Uterus	11
2.1.3 Development of uterus	12
2.1.4 Menstrual cycle	12
2.1.5 Implantation	14
2.1.6 Uterine disease	16
2.1.7 In-vitro Fertilization (IVF)	18
2.2 Tissue engineering	20
2.2.1 Cell source	20
2.2.2 Mechanical stimuli on tissue engineering	26
2.2.3 Mechanotransduction cell signaling	32
2.2.4 Bioreactor using mechanical stimuli	34
2.2.5 Decellularization	35
3. Methodology	38
3.1 Cell culture	38
3.2 Embryo isolation	39
3.3 Mechanical stimulated dynamic culture (Flexcell)	41
3.4 Histological Analysis	42
3.4.1 Sample preparation.....	42
3.4.2 Metachromatic staining.....	43
3.4.3 Immunostaining.....	46
3.5 Biochemical analysis	47
3.5.1 Sample preparation.....	47
3.5.2 DNA quantification	48
3.6 Gene expression analysis	48
4. Study. 1: Enhancement of smooth muscle cells in human endometrial stromal cells by mechanical stimuli for uterine regeneration	50
4.1 Purpose	50

4.2 Materials and Methods	51
4.2.1 Isolation and culture of hESCs.....	51
4.2.2 Uniaxial cyclic strain loading.....	51
4.2.3 rt-PCR.....	52
4.2.4 Immunostaining.....	53
4.2.5 Measurement of cell reorientation against cyclic strain.....	53
4.2.6 Cyclic adenosine monophosphate (cAMP) measurement.....	53
4.2.7 Cell contraction assay.....	54
4.2.8 Statistical analysis.....	54
4.3 Results	54
4.3.1 Up-regulation of uterine smooth muscle cell markers in hESCs in response to uniaxial strain.....	54
4.3.2. Reorientation of hESCs after applying 7 days of uniaxial cyclic strain.....	57
4.3.3 Induction of cAMP production by cyclic strain in hESCs.....	58
4.3.4 Inhibitor test using SQ22536 and H-89.....	59
4.3.5 Effect of oxytocin on hESCs-mediated collaged I gel with regard to its contractile ability.....	61
4.4 Discussion	62
5. Study 2: Reconstruction and evaluation of scaffold-free tissue for partial uterine regeneration in murine model	67
5.1 Purpose	67
5.2 Method	68
5.2.1 Isolation and culture of rESCs.....	68
5.2.2 Collecting embryo.....	69
5.2.3 Fabrication of scaffold free tissue (SFT) using rESCs.....	69
5.2.4 Cocultivation of embryo on SFT.....	70
5.2.5 Transplantation of SFT.....	71
5.2.6 Immunostaining.....	72
5.3 Results	73
5.3.1 Need for a monolayer formed underneath the scaffold-free tissue.....	73
5.3.2 Reconstruction and evaluation of SFT using rESC.....	74
5.3.3 Rat embryo incubation on rESC SFT <i>in vitro</i>	75
5.3.4 Establishing a defect model for partial uterine regeneration.....	77
5.3.5 Transplantation of rESC SFT into the defect model.....	79
5.4 Discussion	86

6. Study 3: Novel <i>in vitro</i> application of scaffold-free tissue using human endometrial stromal cells for early implantation of embryo.....	89
6.1 Purpose.....	89
6.2 Materials and Methods.....	90
6.2.1 Isolation and culture of hESCs	90
6.2.2 Scaffold-free tissue constructs	90
6.2.3 Actin staining	91
6.2.4 Histological analysis.....	91
6.2.5 Immunohistochemical staining.....	91
6.2.6 rt -PCR	92
6.2.7 Collecting embryo	93
6.2.8 Embryos coculturing on SFT	93
6.2.9 Applying cyclic strain on the SFT	94
6.2.10 Statistical analysis	94
6.3 Results.....	94
6.3.1 Utilization of Y27632 to fabricate the scaffold-free tissue.....	94
6.3.2 Gene expression changes in hESCs after treating with Y27632	95
6.3.3 Histological assay and immunochemistry staining.....	96
6.3.4 Incubating rat embryo on hESC SFT for 24 hour.....	98
6.3.5 Gene expression changes between hESC monolayer and SFT.....	101
6.3.6 Applying cyclic strain in hESC monolayer and SFT	102
6.4 Discussion.....	103
7. Conclusion	109
7.1 Summary of Studies.....	109
7.2 Concluding Remarks	110
8. Future Work.....	113
8.1 Elucidation of mechanosensors in endometrial stromal cells and application of bioreactor for total uterine regeneration.....	113
8.2 Verification of specific genes involving early implantation of embryo using scaffold-free tissue.....	113
8.3 Scale-up of scaffold-free tissue for total uterine regeneration	114
References	115
Protocol.....	131
Cell culture.....	131

Animal experiments	133
Rat endometrial stromal cells	133
Rat behavioral Core Protocols	135
Tissue engineered construct preparation	137
Making scaffold-free tissue	137
Dynamic culture	140
Applying cyclic strain.....	140
Histological Analysis	142
Cryosectioning	142
Hematoxylin & Eosin (HE) staining.....	144
Toluidine Blue (Tb) staining.....	145
Masson's Trichrome (MT) staining.....	146
Verhoeff-Van Gieson (VVG) staining.....	148
Immunohistochemistry (IHC)	150
Immunocytochemistry/immunofluorescence (ICC/IF)	152
Reverse transcription - Polymerase chain reaction (rt-PCR)	154

List of Abbreviations

Aa: Antibiotic-antimycotic
BSA: Bovine serum albumin
cAMP: Cyclic adenosine monophosphate
COL2: Type II collagen
DAB: 3,3'-Diaminobenzidine
DMEM: Dulbecco's Modified Eagle's Medium
ECM: Extracellular matrix
ESC: endometrial stromal cells
HE: Hematoxylin & Eosin
FBS: fetal bovine serum
IVF: *In-vitro* fertilization
KRT18: cytokeratin 18
MSC: mesenchymal stem cell
MT: Masson's trichrome
PBS: Phosphate-buffered saline
PCR: Polymerase chain reaction
ROCK: Rho-associated protein kinase
SD rat: Sprague Dawley rat
SEM: Scanning electron microscope
SFT: Scaffold-free tissue
SMC: Smooth muscle actin
STR: Cyclic strain
TB: Toluidine Blue
Vim: Vimentin

1. Introduction

1.1 Introduction

Uterus is an essential organ for embryo/fetus to grow until women give birth. Recently, the rate of uterine diseases has been tremendously increased, further causing decrease in pregnancy rate. When the uterine diseases such as gynecological cancer, asherman's syndrome, adenomyosis, etc, become severe, most of the patients are subjected to hysterectomy that refers to a removal of uterus with the defects or malignant tumors. This surgical procedure, however, results in permanent infertility from the patients.

On the other hand, as many women give birth to their first baby at late age, the rate of pregnancy also decreases. In 1970's, the technique of *in-vitro* fertilization (IVF) was first established by Professor Robert G. Edwards from Cambridge university¹. His great achievement for the development of IVF made him award the Nobel prize in Physiology or Medicine in 2010. The IVF refers to the method to fertilize sperms and eggs *in vitro*, and the zygote fertilized is transplanted to the uterus of women, so that it allows for the women to become pregnant²⁻⁴. The assisted hatching was carried out during IVF in order to help induce the hatching of the embryo artificially and further to make the embryo being able to attach on the endometrium^{5,6}.

1.2 Motivation

In order to solve aforementioned issues, tissue engineering approaches have been discussed by many researchers. For uterine regeneration, our group has attempted to utilize decellularized scaffold that is fabricated by high hydrostatic pressure⁷. We showed that the decellularized scaffold helped the uterine tissue in murine model regenerated after 1 month of transplantation, but the total uterine regeneration was not completely achieved particularly in smooth muscle layer. The motivation of this research was to find out a new model for uterine regeneration.

Although the role of mechanical stimuli in cell models has been highlighted, only limited studies are conducted for uterine cells. While the myometrium undergoes a contractile movement under the hormone control, the effect of its mechanical movement on the inner layer of uterus wall, endometrium, has not been fully understood. Understanding of this mechanism in the uterus is thought to contribute to reveal the differentiation mechanism of cells in the uterus. Furthermore, it is expected to apply into tissue engineering approaches leading to three-dimensional reconstruction of uterine tissue by utilizing bioreactors.

On the other hand, while the IVF has highlighted for the patients who are suffering from infertility, it still remains several issues. When the assisted hatching was performed during IVF procedure, it sometime damages the fertilized zygote, or the zygote sometimes degenerated *in vitro* while the zygote is usually required to be cultured on the culture dish for its development for 2 – 6 days during the IVF. Moreover, one of the main reasons in the IVF failure refers to the low success rate of implantation onto the endometrium after the cultured embryo is transferred to the patient^{8,9}. Hence, those issues left in the techniques of IVF are required to be solved in order to promote its success rate and further to overcome the infertility.

1.3 Objective

The aim of this dissertation is to develop a novel model for uterine tissue engineering by applying mechanical stimuli as well as tissue engineered constructs. The effect of cyclic strain on endometrial stromal cells was first examined to check the behavior of cells in response to mechanical stimuli, further suggesting the possibility as cell source for uterine regeneration. Then, the novel method to reconstruct the tissue engineered construct, such as scaffold-free tissue, was established by using endometrial stromal cells. By utilizing the early stage of embryo, we evaluated its early implantation, one of uterine functions, *in vitro*. Finally, the tissue-engineered construct is *evaluated in vivo* using murine model. The three studies carried out in this dissertation are as follows;

- **Study 1:** Enhancement of smooth muscle cell in human endometrial stromal cells by mechanical stimuli for uterine regeneration
- **Study 2:** Reconstruction and evaluation of scaffold-free tissue for partial uterine regeneration in murine model
- **Study 3:** Novel *in vitro* application of scaffold-free tissue using human endometrial stromal cells for early implantation of embryo

2. Background

2.1.1 What is uterus?

The uterus refers to a female sex organ of mammals including human, which is sensitive to hormones. During pregnancy, it supports the development of the embryo in this uterus by supplying a room for the embryo to grow up for a certain period depending on species of mammals. For human uterus, the uterine cervical is located in the inside of vagina at the end, and the two oviducts are connected to the other ends. On the other hand, the rodent uterus has a Y-shape with two ovaries connected to the ends while cervix of the uterus is located in between the other ends. Female rats have two tubed-shape horns as shown in Fig. 1.

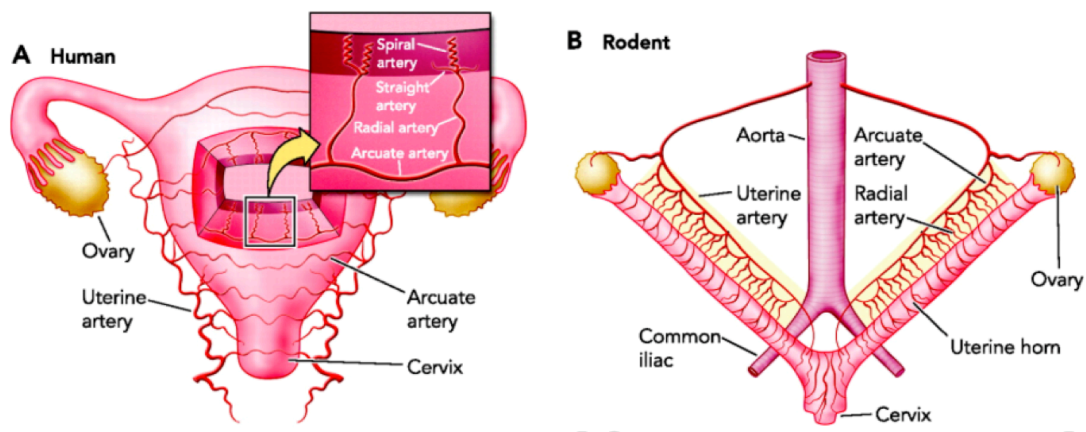


Figure 1 Anatomy of uterus in (A) human and (B) rodent.¹⁰

2.1.2 Anatomy of Uterus

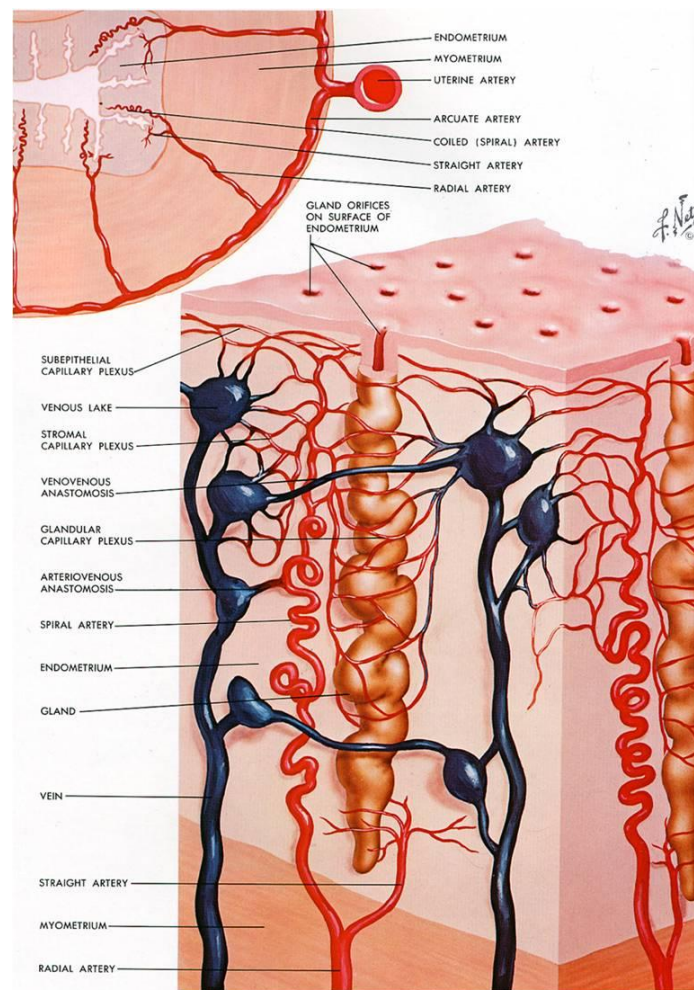


Figure 2 Endometrium blood supply¹¹

The uterus wall consists of multilayers; endometrium, myometrium, and perimetrium. Endometrium is the most inner layer of uterus wall that is mainly composed of epithelial cells and stromal cells. Endometrium is also functionally subdivided into two layers of stratum functionalis and stratum basalis. The superficial layer of stratum functionalis is thickened and vascularized through proliferative and secretory phase in the menstrual cycle. During the menstruation, the thickened wall is sloughed off. The inner layer of endometrium, called stratum basalis, always stores the stem cells that differentiate into stromal cells to replenish the functional layer. The stratum basalis is always preserved during the menstruation since it is less responsive to the hormonal stimuli. The thickest middle layer of the uterus wall is defined as myometrium, that is mainly composed of smooth muscle cells in order to induce the uterine contractions. On

top of the myometrium, the perimetrium covers around the uterus with its loose connective tissue. By simply classifying with the types of cells, the uterus wall has multilayer of epithelial cells (inner), stromal cells (middle), and smooth muscle cells (outer).

2.1.3 Development of uterus

During early fetal life, the uterus is formed from paramesonephric ducts (Müllerian ducts). Paramesonephric ducts are present in both male and female embryo. As a result of Anti-Müllerian hormone (AMH) produced by testes in male embryo, the paramesonephric ducts are regressed. Whereas, the absence of AMH in female embryo allows the development of paramesonephric ducts into uterine tubes, uterus, cervix, and the upper of the vagina^{12,13}.

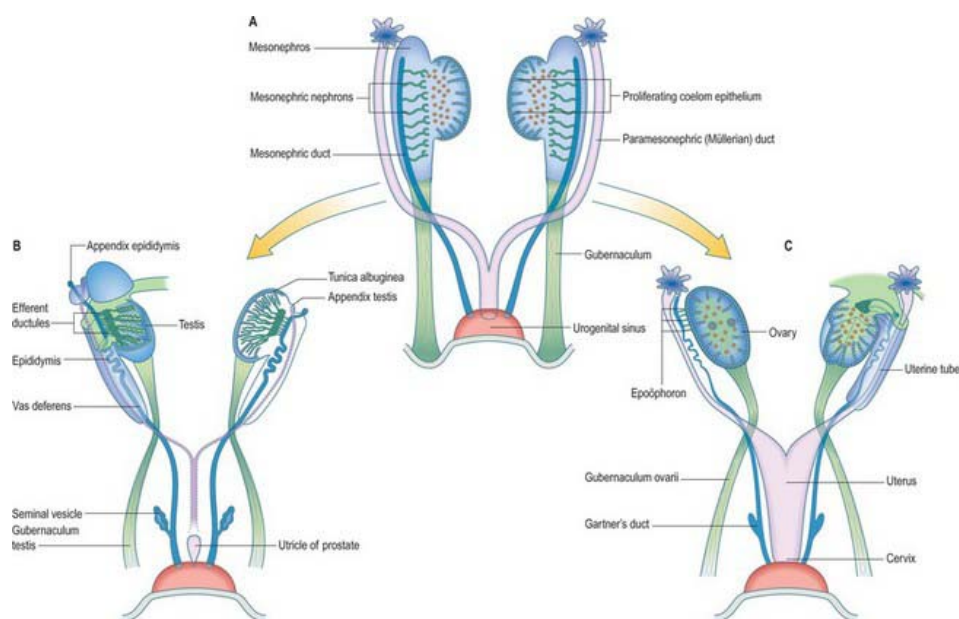
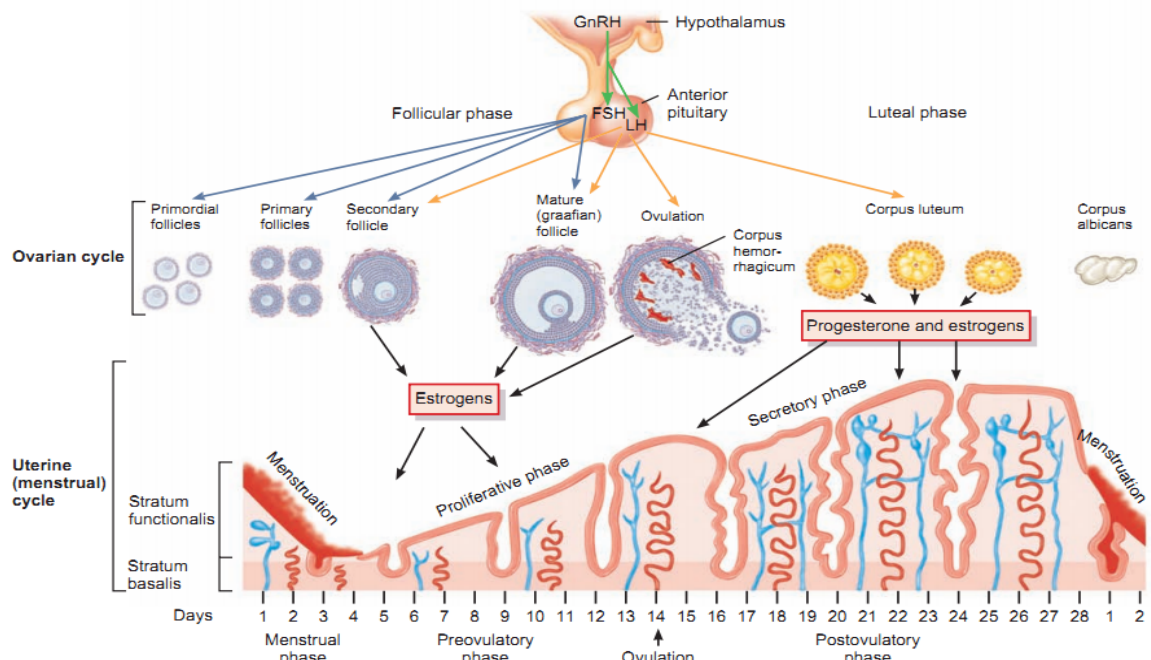
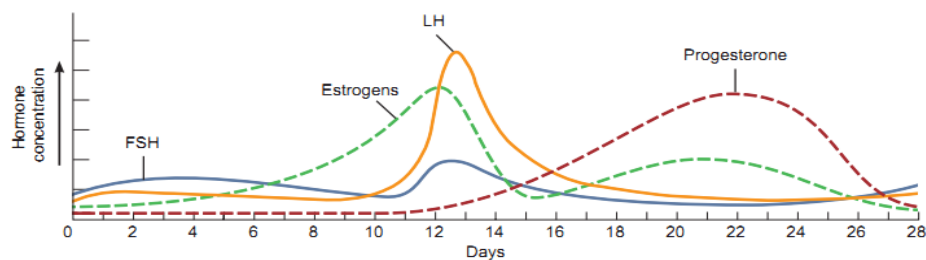


Figure 3 Paramesonephric (Müllerian) ducts ¹⁴

2.1.4 Menstrual cycle



(a) Hormonal regulation of changes in the ovary and uterus



(b) Changes in concentration of anterior pituitary and ovarian hormones

Figure 4 ovarian and uterine cycle¹⁵

Menstrual cycle, or called uterine cycle, is an essential 28-days cycle of the ovary and uterine for sex reproduction. According to the menstrual cycles due to the different level of expression in hormones such as estrogen and progesterone, the development or shedding of stratum functionalis in endometrium occurs. Depending on the status of the ovary or uterine, it has been classified into three different phases each for the ovary (follicular phase, ovulation, and luteal phase) and the uterus (menstruation, proliferative phase, and secretory phase). All the phases for both ovary and uterus counts on the expression of hormones.

Pituitary gland releases the hormone called follicle stimulating hormone (FSH) that induces the growth of ovarian follicles, resulting in the release of estrogen. This cycle last for two weeks and is known as follicular phase (preovulatory

phase). On day 14, the adenohypophysis of the pituitary gland also starts releasing luteinizing hormone (LH) allowing the egg to pop out of the ovarian follicle. The LH is highly secreted to result in the ovulation. At the same time, the release of estrogen from ovarian follicles makes the uterine wall thicker (proliferative phase).

After two weeks of follicular phase, the same ovarian follicle after ovulation is called the corpus luteum. The secretion of LH allows the corpus luteum to secrete the mostly progesterone and some estrogen, resulting in development of stratum functionalis in the endometrium, which is called secretory phase. Since LH is highly secreted in this period, it is also called luteal phase (Postovulatory phase).

If the egg is not fertilized by day 28, LH is no longer secreted from the pituitary gland and the corpus luteum becomes shriveled up, called corpus albicans. Then, it leads to the transient decrease in progesterone, resulting in the shedding of the endometrial lining. In menstruation, the blood vessel at the stratum functionalis constrict, blocking the supply of nutrition to the stromal cells and further causing death. Lastly, the dead cells are shed with blood vessel.

2.1.5 Implantation

For human, implantation indicates the attachment of embryo (blastocyst) onto the uterine wall in the early pregnant status. From the implantation, it enables the embryo to receive the oxygen and nutrition. In order for the blastocyst to be implanted onto the uterine wall, the uterus is required to undertake the adaptation.

Predecidualization

The endometrium become enlarged and vascularized by glands. This change lasts and is maximized on 7th days after ovulation. Moreover, the surface of endometrium produces large and round cells termed decidual cells. The surface

of endometrium is covered with the decidual cells. It happens 9 or 10 days after ovulation (during late secretory phase). The decidual cells were shed off in the menstruation unless pregnancy occurs. This process is known as predecidualization.

Decidualization

Once the pregnancy (implantation) was successfully occurred, predecidualization is followed by decidualization. Decidual reaction is shown where the blastocyst encounters the decida in the endometrium in the early period of pregnant. The function is to promote the secretion of stromal cell in and around the part of implantation occurred. Decidualization is an essential process of differentiation in endometrial stromal cells, which is caused by progesterone hormone. It thickens the uterine wall and induces the development of blood vessels. Moreover, the surface of endometrium produces large and round cells termed decidual cells. The surface of endometrium is covered with the decidual cells due to glycogen and lipid accumulation in the cytoplasm, supplying nutrition to the embryo implanted. Hence, this type of deformed endometrial stromal cell is termed decidual cell, and the phenomena of this deformation is called decidual reaction.

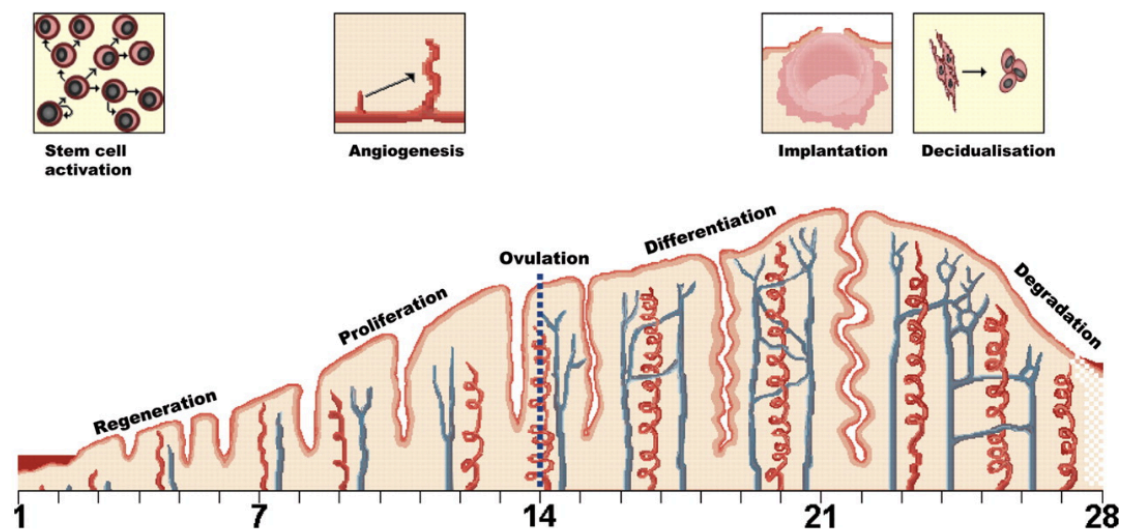


Figure 5 Decidualization of human endometrial stromal cells ¹⁶

2.1.6 Uterine disease

Endometrial cancer

Endometrial cancer is the cancer arose from the endometrium. It has a characteristic invading its cancer cell originated from the endometrium into the myometrium. It is known that endometrial cancer is caused by excessive estrogen exposure, high blood pressure, and diabetes indicating that many of cases are related to the obesity^{17,18}. The most common type of the endometrial cancer accounting for more than 80% is endometrioid carcinoma. The endometrioid carcinoma originates from the epithelial layer in the endometrium^{19,20}. Fig. 6 represents the endometrial cancer according to its severity.

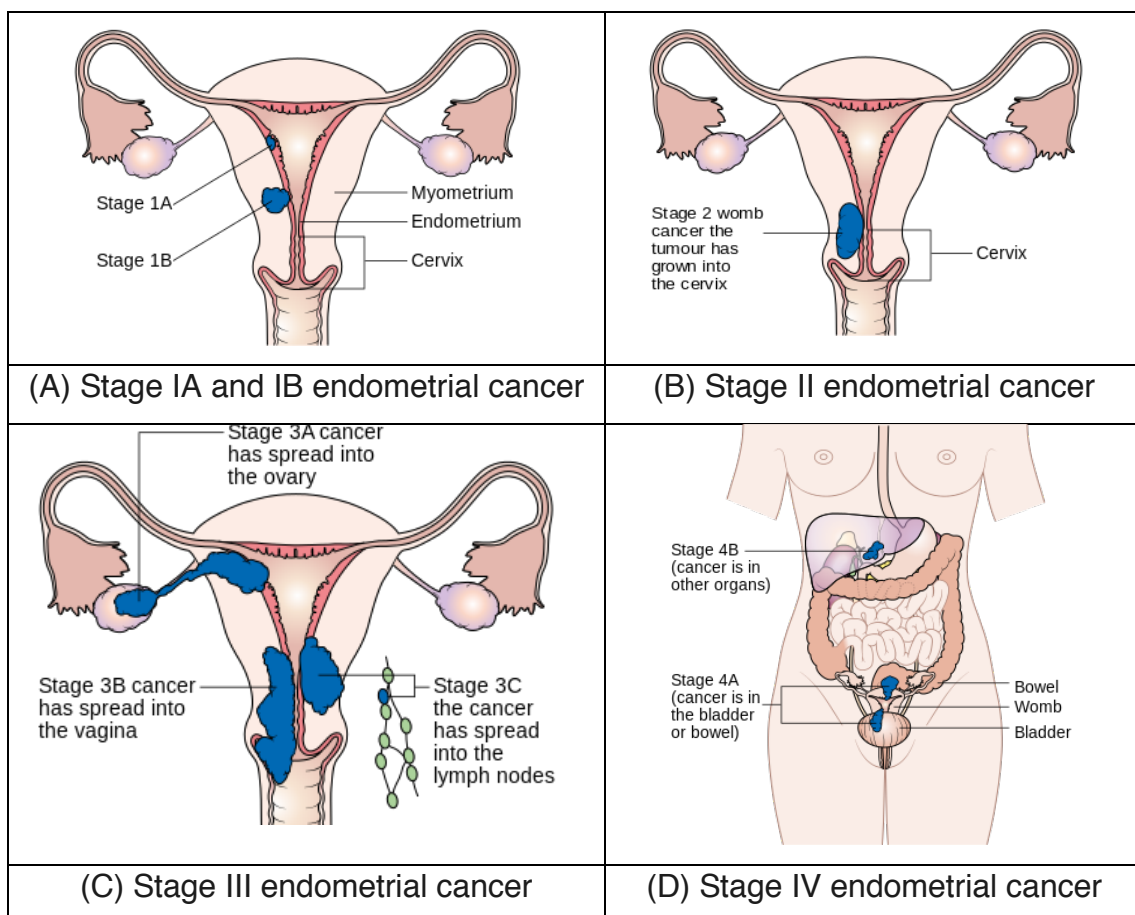


Figure 6 endometrial cancer ²⁰

Adenomyosis

Adenomyosis indicates ectopic endometrial tissue invading into the myometrium, resulting in the abnormal enlargement of the uterus. Since the endometrial glands are placed within the myometrium, it brings about pain due to the lack of increased blood^{21,22}. The cause of adenomyosis has not been clearly clarified yet. For the current treatment, it undergoes hysterectomy that removes the uterus totally from the patient whereas it prescribes some medication to relieve its pain.

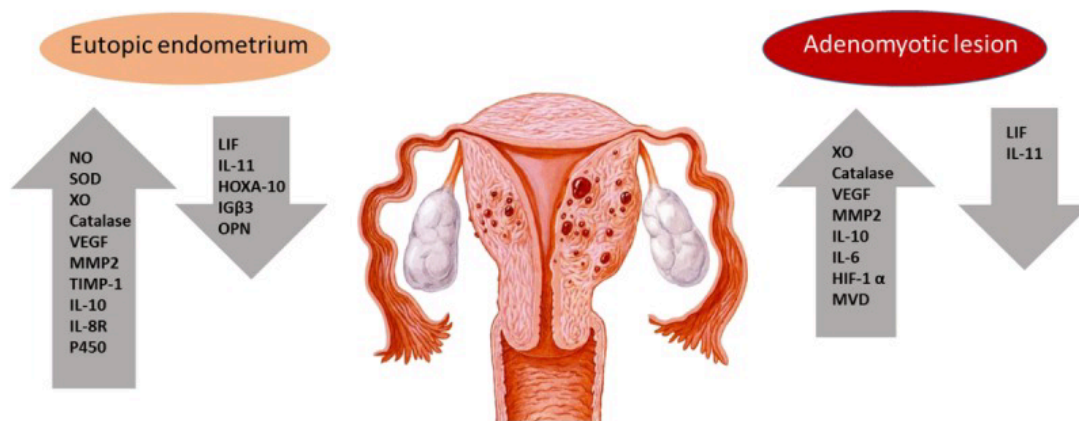


Figure 7 Adenomyosis ²³

Asherman's syndrome

Asherman's syndrome refers to intrauterine adhesions in the uterine cavity. It is also known as Fritsch syndrome. One of the most common reasons to induce this disease is by dilation and curettage (D&C)²⁴. The D&C indicates a gynecological procedure usually performed when the patient has a cancer or malignant tumor in the uterus wall, so that the cervix of uterus is opened followed by removal of the cancer/tumor embedded inside the uterus wall by scrapping. The scarred tissue inside the uterine left attach partially and gradually to the normal uterine wall after the surgery as illustrated in Fig. 8. When this disease becomes severe, the front and back walls of uterus stick completely, resulting in infertility.

Clinical pathology correlation of Asherman syndrome.

Location of the pathology of Asherman's syndrome

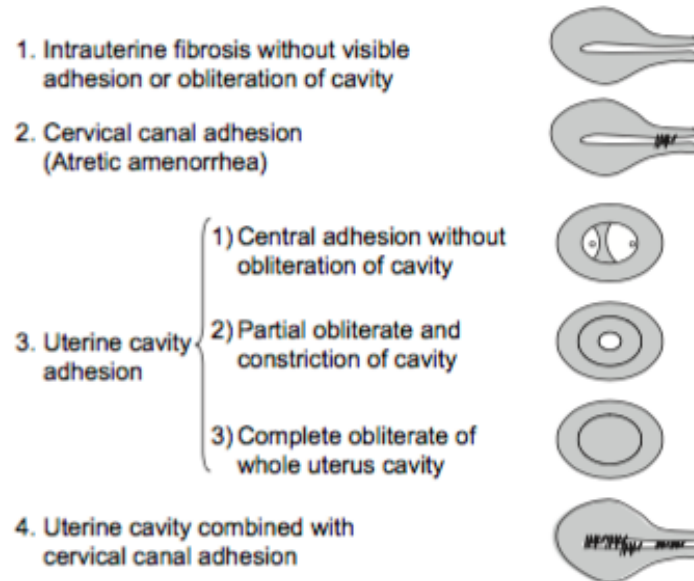


Figure 8 Asherman's Syndrome ²⁵

2.1.7 In-vitro Fertilization (IVF)

The method of *in-vitro* fertilization (IVF) was first introduced and established by Professor Robert G. Edwards in 1970s. The first IVF baby, Louise Brown, was born in England and turns 37 years old in 2017. Since she was firstly born by using the IVF, it has allowed for many women to give birth for last four decades. The process of IVF consists of four processes; 1. Collecting follicles (eggs) from ovary of the woman, 2. Fertilizing eggs *in vitro* with sperm obtained from the man, 3. Incubating the fertilized egg (zygote/embryo) for development within 2 - 6 days, and 4. Transferring embryo to the uterus of the woman. The most common failure during IVF is due to the low success rate of implantation by transferred embryo into the uterus. When the number of the eggs obtained from the woman is sufficient, the fertilized eggs/embryos developed *in vitro* are usually stored by cryopreservation for next trial. While the success rate of IVF still remains low about 29%, the expense of IVF is \$10,000 - \$15,000 in the USA.

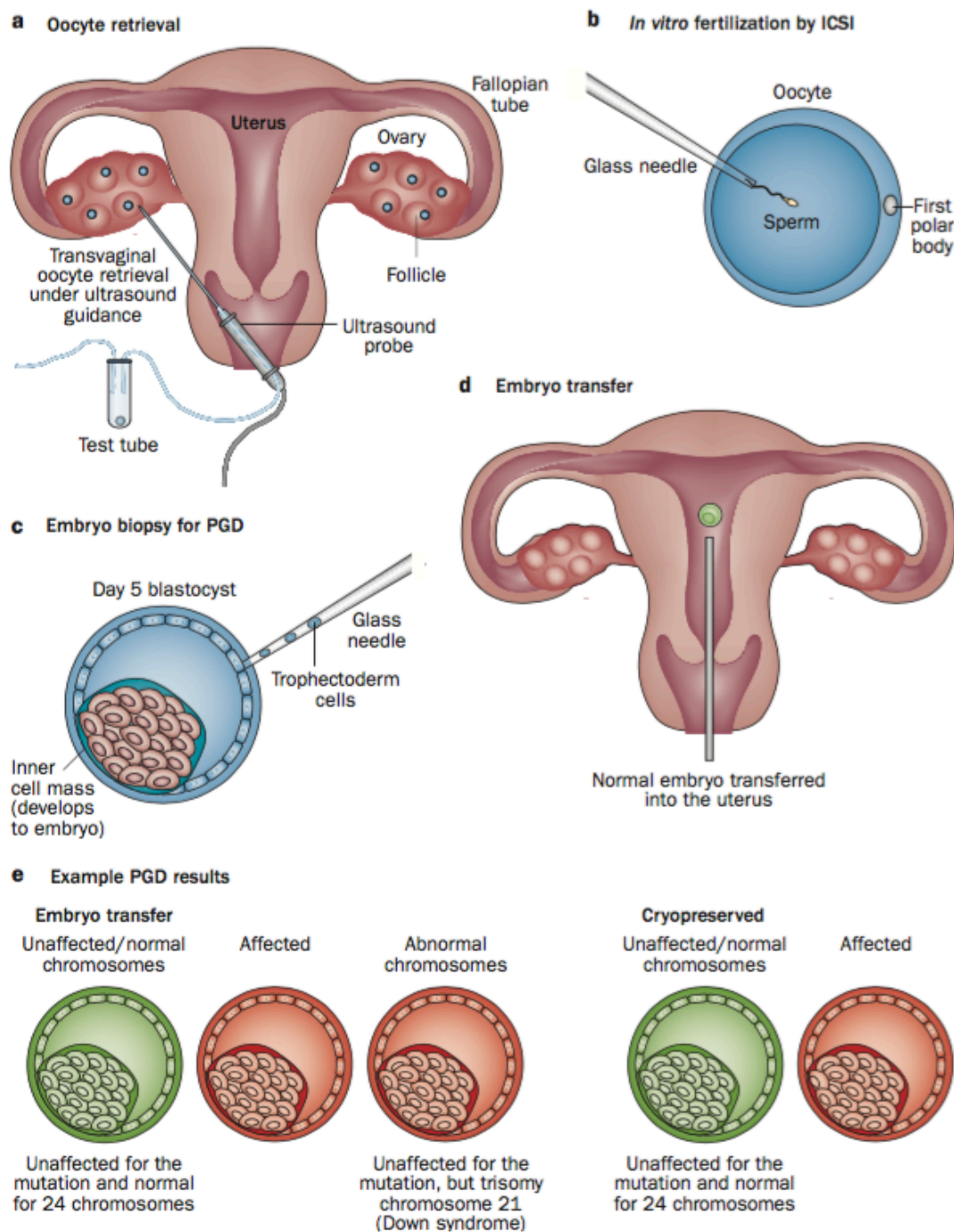


Figure 9 Schematic diagram of IVF ²⁶

Assisted hatching

One of the main reasons for failure of implantation of the embryo is caused by failure of hatching in embryo. Hatching refers to a removal of glycoprotein outer

layer of embryo, called zona pellucida. It is regarded as a necessary step for embryo to undergo the implantation. In order to overcome this problem, an assisted hatching is often carried out by opening the zona pellucida of the embryo mechanically with a micro needle (zona drilling), laser, or acidified Tyrode's solution^{6,27-29}. Fig. 10 represents the laser assisted hatching. The assisted hatching is usually carried out after 2 – 6 days after fertilization. As the assisted hatching has been known to help the embryo to implant efficiently, there is a report that may induce higher risk of having multiple pregnancies due to the assisted hatching^{30,31}.

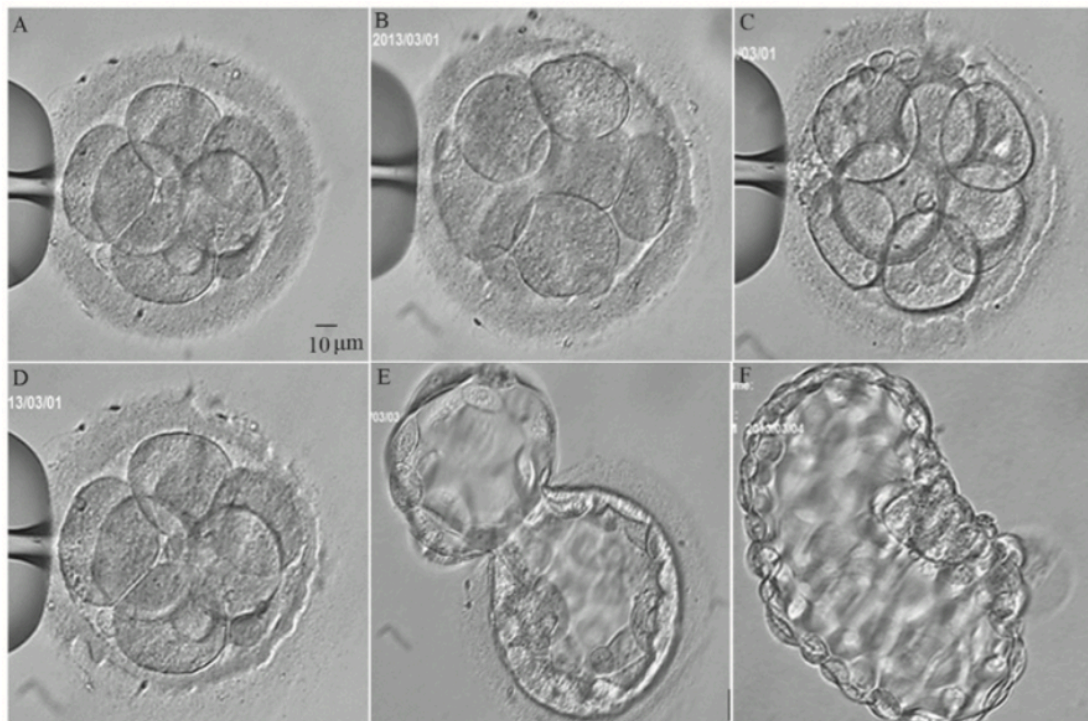


Figure 10 Assisted hatching by laser during IVF ³²

2.2 Tissue engineering

2.2.1 Cell source

2.2.1.1 Endometrial stromal cells (ESCs)

Most of studies in uterine regenerative medicine have been currently using endometrial stromal cells as cell source. For primary human endometrial

stromal cells, a method for cell harvesting has been established for last two decades³³⁻³⁵. The purity of cells becomes above 98%. These primary cells were stained by CD10 (endometrial stromal cell marker) whereas they were negative stained by cytokeratin 18 (epithelial cell marker) or SMA (smooth muscle cell marker). By using this certain cell source with extremely low risk of cell contamination, most of groups have been conducting uterine regeneration.

2.2.1.2 Mesenchymal stromal cells (MSCs)

While the use of mesenchymal stem cells (MSCs) made a breakthrough in the field of regenerative medicine, there is no report on specific MSCs for the uterus. Some groups used bone marrow derived MSCc to induce uterine regeneration³⁶⁻³⁸, but appropriate cell sources for the uterus have not been established other than ESCs.

MSCs, often referred to as multipotent mesenchymal stromal cells, has a distinct ability to differentiate into specific end-stage cell types such as bone (osteogenesis), cartilage (chondrogenesis), muscle (myogenesis), marrow, tendon/ligament (tendogenesis/ligamentogenesis), or fat tissues (adiopogenesis) as shown in djouad's diagram³⁹. Due to their distinct ability, many approaches using MSCs have been studied and discussed as cell source for tissue engineering or regenerative medicine⁴⁰.

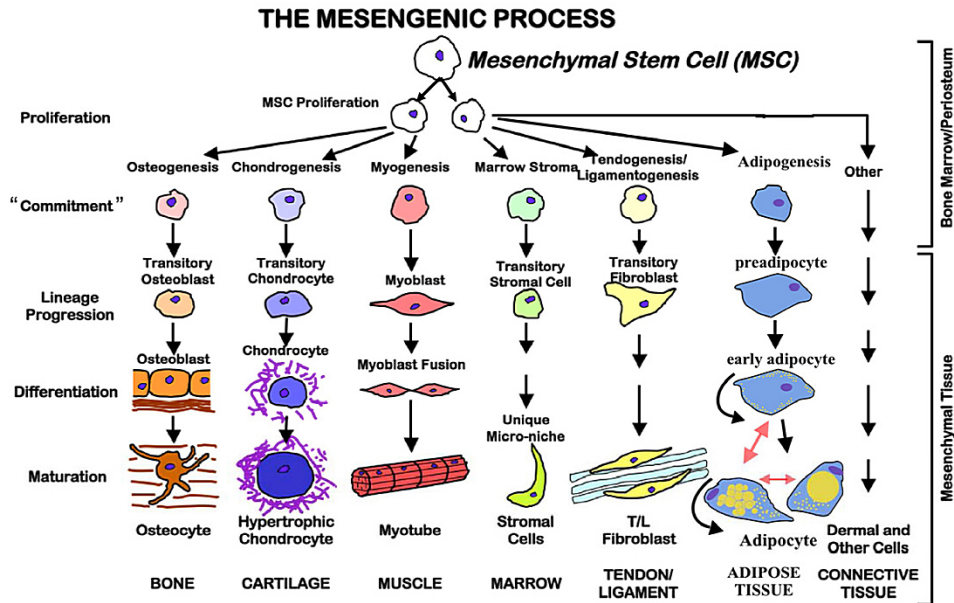


Figure 11 Mesengenic process of mesenchymal stem cell ³⁹

Other than their distinct pluripotent ability, it also implements their functions including maintenance, exhaustion, expansion, self-renewal, and differentiation. These functions are modulated by intracellular and extracellular gene regulator networks (e.g. cell surface molecules or secreted proteins) *in vivo* as shown in Fig. 12.

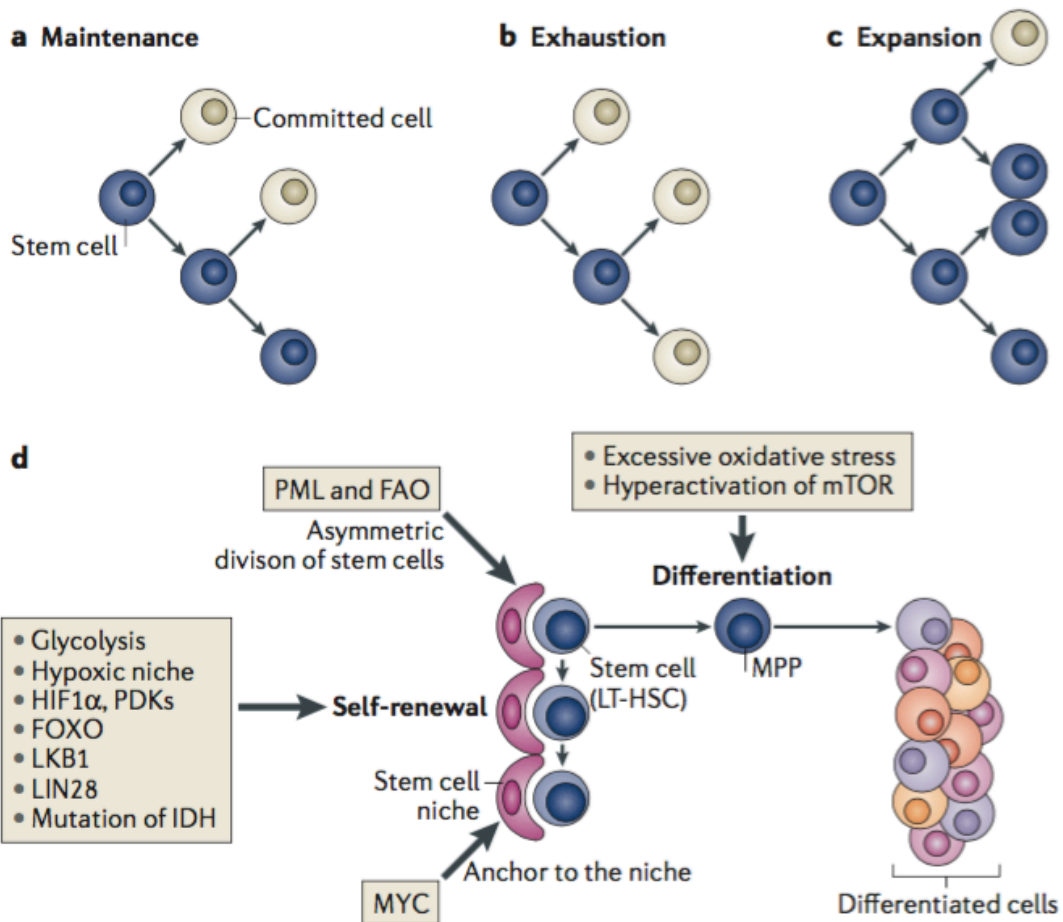


Figure 12 Stem cell fates ⁴¹

In vivo, the MSCs are located in different tissues and organs. The circumstances in which the MSCs are located are thought to give rise to the differentiation of MSCs such as biochemical factors secreted from surrounding cells/tissues, mechanical factors from tissues, or its microenvironment. In order to modulate the differentiation of MSCs into certain cell types *in vitro*, many researchers have attempted and revealed using biochemical factors as well as mechanical stimuli or substrate. While the effect of biochemical stimuli onto MSC differentiation have been studied by many researchers for several decades, the effect of mechanical stimuli or culturing on the substrates were relatively unknown and understanding of its mechanism is still limited.

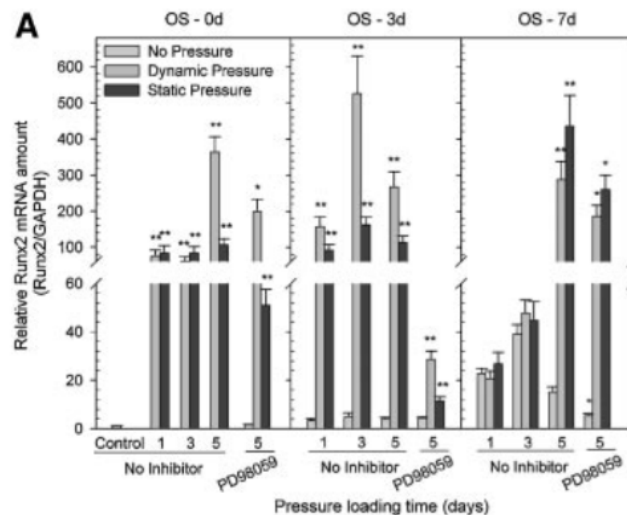


Figure 13 Expression of osteogenesis-related transcription factors affected by dynamic and static pressure for 1 - 5 days or plus PD98059 pretreatment for 5 days. ⁴²

There are several reports with regard to the effect of mechanical stimuli on MSC differentiation. Compression loading in the physiological range promotes chondrogenesis of MSCs. In Huang's study, cyclic compressive loading with a magnitude of 15% at 1 Hz 4 hours daily for 2 days induced early responsive genes of chondrogenesis, *SOX9*, in rabbit bone marrow-derived MSCs⁴³. Moreover, there is a report on the effect of hydrostatic pressure on MSCs. In Fig. 13, the result suggested that loading either static or dynamic hydrostatic pressure induced the elevation of initial osteogenesis markers (*Runx2*, *Osterix*, *Msx2*, and *Dlx5*) of MSCs⁴².

The role of substrate in where cells were cultured has been highlighted by several researchers. In Fig. 14, the elasticity of substrate significantly affects the differentiation of MSCs⁴⁴. The softer substrate with low stiffness induced neurogenesis while the stiffer substrate help MSCs differentiate into osteogenesis. Seo's group also reported that the topography of the substrates also plays an important role in regulation of differentiation for stem cells⁴⁵. The small change in forces of cytoskeleton or contraction force subjected by topography may influence on the gene expressions for differentiation markers of stem cells⁴⁶. Types of material for scaffold also exert its effect on a certain stem-cell fate of MSCs. Wu developed a novel bioactive hydrogel conjugating

Polyphosphate onto hyaluronic acid polymer⁴⁷. The material eventually elevated its osteogenesis markers in MSCs. Thus, the different substrate with different topology significantly affects the cell-fate of MSCs.

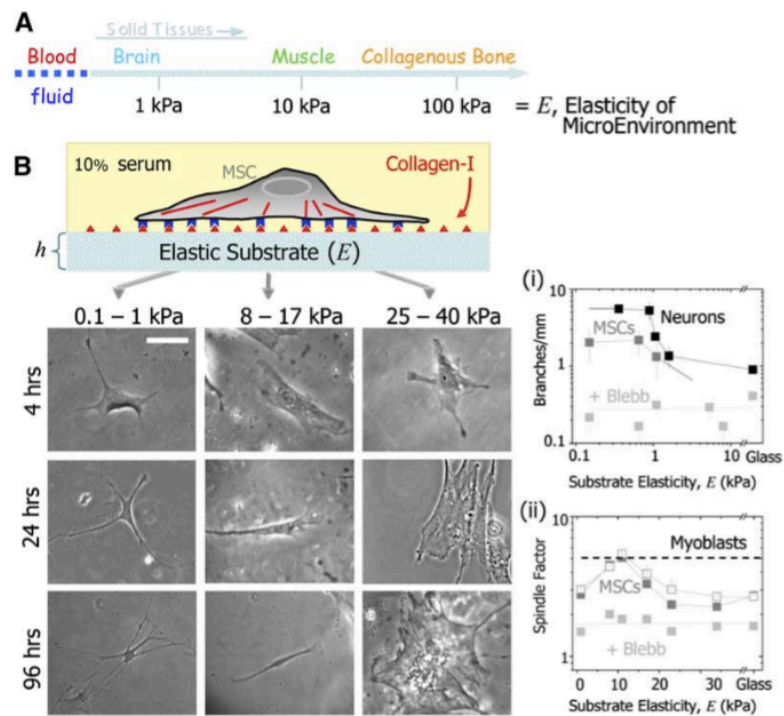


Figure 14 Tissue elasticity and differentiation of native MSCs. ⁴⁴

Despite its promising function as pluripotency, the number of MSCs is age-dependent as indicated in Fig. 15 ⁴⁰. With aging, the number of MSCs becomes remarkably declined. The reason of its decrease, however, has not been revealed yet. Thus, the use of MSCs for tissue engineering or regenerative medicines is still limited especially for the elderly patients.

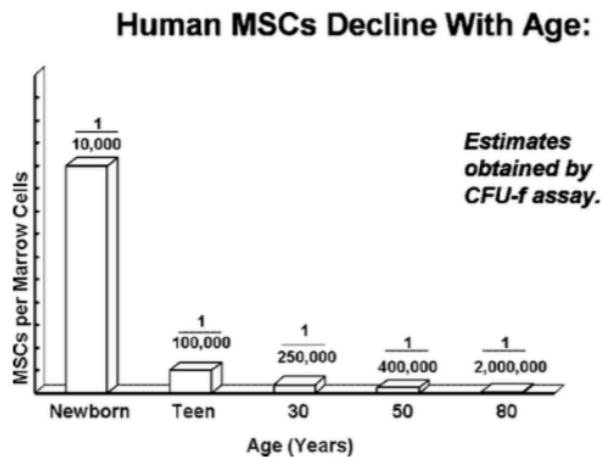


Figure 15 Human MSCs decline with age ⁴⁰

2.2.2 Mechanical stimuli on tissue engineering

Application of mechanical stimuli onto cell/tissue engineering has been widely studied in various cell models and regarded as a significant factor for the field of regenerative medicines and tissue engineering. In the cell engineering, the effects of various mechanical stimuli onto tissue have been discussed. In order to reveal its effects, the samples were prepared as monolayer or 3D tissue either with or without scaffolds.

Among various mechanical factors, applying compression loading has been studied in the chondrocyte models. The compression loading is known to play a critical role in the development of articular cartilage while the knee is always subjected to mechanical compression loading from physical activities such as walking or jumping. Hence, there are many studies reporting its positive effect on chondrocytes⁴⁸⁻⁵². Fig. 16 represented that human chondrocytes seeded with Poly(ethylene glycol terephthalate) and poly(butylene terephthalate) scaffold were subjected to dynamic compression with 5% strain offset at 0.1 Hz, 10 hours daily for 3 days or 17 days. As a result, it enhanced collagen II mRNA expression as well as GAG accumulation level after 3 days and 17 days.

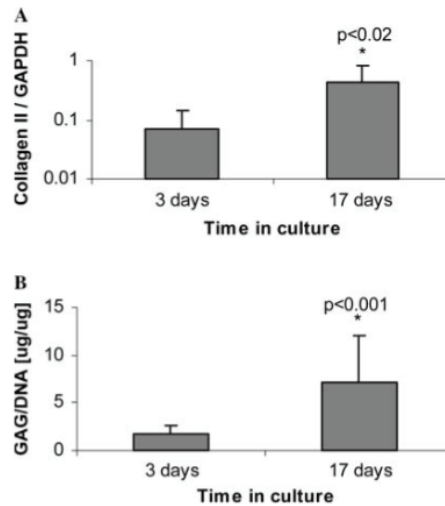


Figure 16 Effects of time in culture on (A) collagen II mRNA expression and (B) GAG accumulation in engineered cartilage constructs cultured in defined serum-free medium ⁴⁸.

On the other hand, the effects of mechanical stimuli such as fluidic shear stress onto blood vessel model have been widely researched from 1980s ⁵³. The shear stress is now known as an essential factor among mechanical stimuli for vascular tissue engineering.⁵⁴ As shown in Fig 17, shear stress is applied into human umbilical vein endothelial cells (HUVECs) for 24 hours⁵⁵. After loading shear stress, the cells were reoriented in the direction of shear flow. Moreover, it enhanced the expression of *VCAM-1* (vascular cell adhesion molecule-1) as well as nitric oxide and thrombomodulin. Thus, the shear stress plays a key role in regeneration of vascular tissue engineering. Furthermore, the effects of shear stress have also been widely studied in many other cell models⁵⁶⁻⁵⁸.

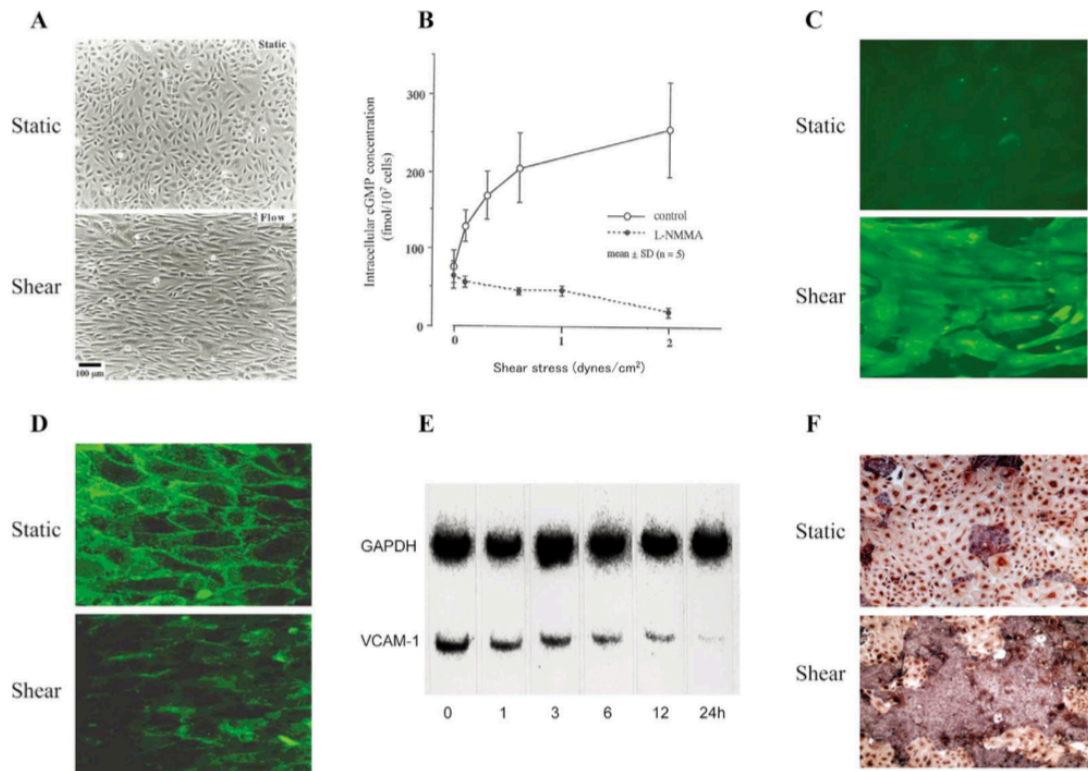


Figure 17 Endothelial cells response to shear stress ⁵⁵

Hydrostatic pressure (HP) is also often used as mechanical stimuli applying onto the field of tissue engineering. As well as compression loading and shear stress, many studies on articular cartilage has been carried out using HP. The cartilage consists of 60-80% of water and is also covered by synovial fluid inside the knee, so that compressing cartilage gives rise to interstitial fluid pressure onto chondrocytes in the cartilage. Hence, there are many reports loading physiological range of HP on the chondrocytes, exerting its positive effect with regard to regeneration⁵⁹⁻⁶¹. Fig. 18 showed that loading 5 MPa of dynamic HP at 0.5 Hz for 4 hours daily for 4 days onto bovine chondrocytes (Passage 3)⁶². As a result of Polymerase Chain Reaction (PCR), it significantly up-regulated the mRNA expressions of chondrogenesis markers, *Aggrecan* and *Type II collagen*.

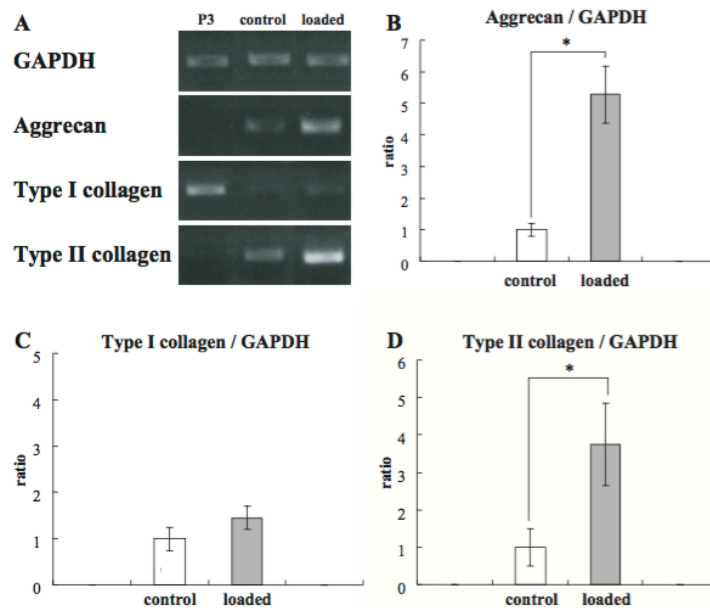


Figure 18 Effect of cyclic hydrostatic pressure on aggrecan, type I collagen, and type II collagen mRNA levels ⁶³.

Ultrasound is often introduced in the field of tissue engineering. Fig. 19 showed that the group developed a bioreactor applying low-intensity pulsed ultrasound (LIPUS) onto the samples⁶⁴. They loaded 1 MHz of LIPUS over 10 days onto bovine articular chondrocytes. By evaluating changes with regard to histology, immunostaining, proteoglycan and total collagen protein production level, it showed increase in cartilage matrix production as well as proteoglycan and total collagen protein production level. The group also suggested the introduction of ultrasound on dedifferentiated chondrocytes can be used to redifferentiate them and further suppress the hypertrophic development.

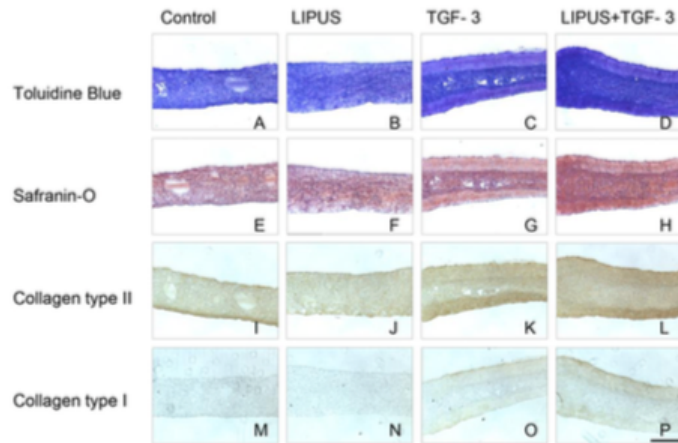


Figure 19 Comparison of matrix synthesis and localization in constructs exposed to low-intensity pulsed ultrasound (LIPUS) with or without TGF- β 3⁶⁴

The effect of cyclic strain has been widely studied in the field of cell engineering particularly in certain cell models such as blood vessels and smooth muscle cells^{54,65}. Due to the fact that those cell models are always subjected to strain forces by outer layer of its smooth muscle layer *in vivo*, there are many reports on the effect of cyclic strain on the cells with regard to its gene expression in both short and long term experiment. In Collin's study represented in Fig. 21, the group showed that cyclic strain regulated the expression of endothelial Occludin and ZO-1 in bovine aortic endothelial cells⁶⁶. Hence, cyclic strain has been highlighted in the vascular tissue engineering as a significant factor to regulate the gene expressions that may further modulate its physiological change involving its differentiation or proliferation.

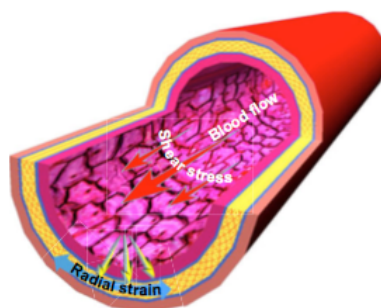


Figure 20 Mechanical forces in native blood vessels⁵⁴

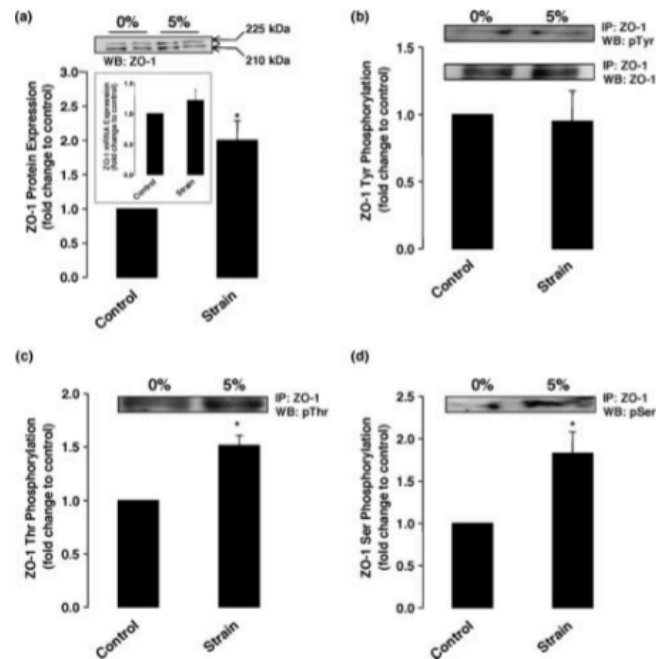


Figure 21 Effect of cyclic strain on ZO-1 expression and phosphorylation in bovine aortic endothelial cells⁶⁶

2.2.2.1 Mechanical stimuli on the uterus

While the role of mechanical stimuli has been highlighted in tissue engineering, there are only limited studies reporting the effect of mechanical stimuli onto the uterus. As mechanical stimuli conducted for those studies on the uterus, it utilized Flexercell Tension system to load cyclic stretching. In Harada's study, they showed that mechanical stretch highly up-regulated *IGFBP-1* (insulin-like growth factor-binding protein-1), a decidualization marker, in decidualized endometrial stromal cells (ESCs)⁶⁷ in Fig. 22. The group also found out that mRNA expression of Interleukin-8 (*IL-8*) is induced by loading mechanical stretching onto ESCs in as short as 2 hours⁶⁸. Izumi's group also reported that applying cyclic stretching onto ESCs up-regulated neutrophil chemokine factors (*CXCL1* & *CXCL8*), Matrix Metalloproteinases (*MMP-1*, *MMP-2*, & *MMP-3*), and Activin A secretion level. Those studies focused only on certain gene expressions after loading mechanical stretching, so that there are no reports on the effect of mechanical stimuli onto uterus with regard to its differentiation or regeneration.

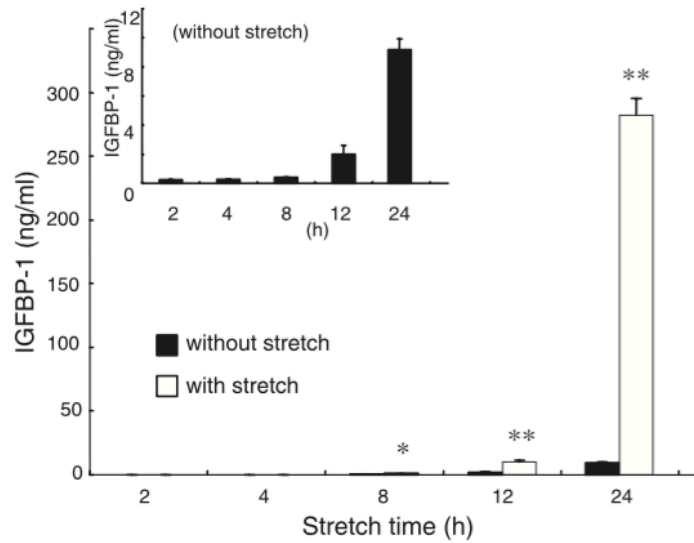


Figure 22 Effects of cyclic stretch on the secretion of insulin-like growth factor-binding protein-1 (IGFBP-1) from decidualized endometrial stromal cells ⁶⁷

2.2.3 Mechanotransduction cell signaling

Mechanotransduction is a term combining of two words; ‘mechano’ and ‘transduction’. It means a mechanism by which cells convert any mechanical stimuli into an intracellular electrical and biochemical change. During the process, mechanosensitive ion channel becomes open due to the activation of mechanoreceptors, leading to a change in an electrical transduction current on the membrane potential of cells⁶⁹. The mechanosensitive ion channel is also known as a cation-specific channel depolarized when the ion passes through the channel.

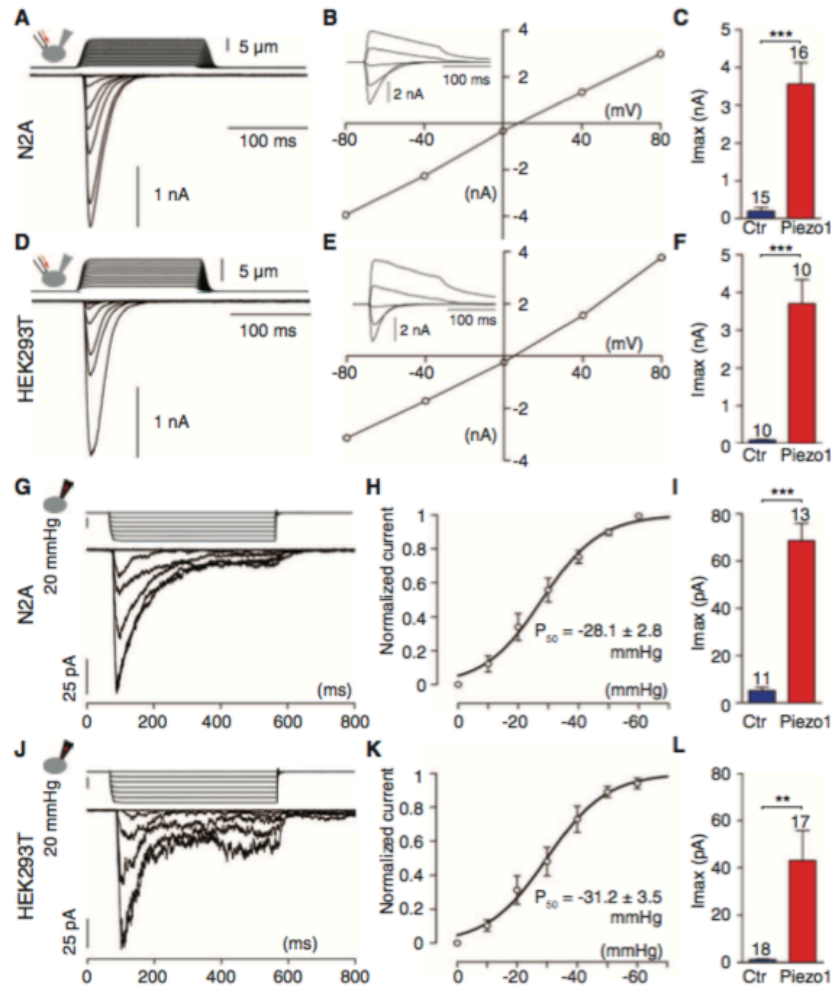


Figure 23 Large mechanical activated currents from cells overexpressing Piezo 1. ⁷⁰

While the interests in mechanosensitive ion channels has been addressed by many researchers after its first finding in 1980s, Kim's group identified that Piezo1 and Piezo2 respond to mechanical forces in the membrane of cells, which are also able to form in various cell types⁷¹. In Coste's study shown in Fig. 24, the mechanically activated cation channel was highly induced by expression of Piezo1 and RNA interference knockdown of the gene⁷⁰. On the other hand, there was a report on an inhibitor or channel blocker for the mechanically gated cation channel, a peptide GsMTx4⁷².

Other than those mechanosensitive ion channels, there are many genes or proteins that highly respond to mechanical forces. G-protein-coupled receptors (GPCRs) are located on the cell membrane and capable of sensing molecular

signaling from outside the cells and induce intracellular signaling pathways⁷³. Although GPCRs are involved in significant signaling pathways such as cAMP signal pathway and phosphatidylinositol, it also is respond to mechanical stimuli such as shear stress, cyclic stretch, compression loading, etc.⁷⁴. Moreover, it involves various mechanoreceptors, such as the integrins, cadherins, and stretch-activated Ca channels, regulating gene expressions and further leading to the differentiation or proliferation of cells in various cell models^{75,76}. While many studies on mechanotransduction are ongoing in many cell types, there is few studies focusing on mechanotransduction in uterine tissues, particularly on any reporting on its change in cell differentiation in response to mechanical stimuli.

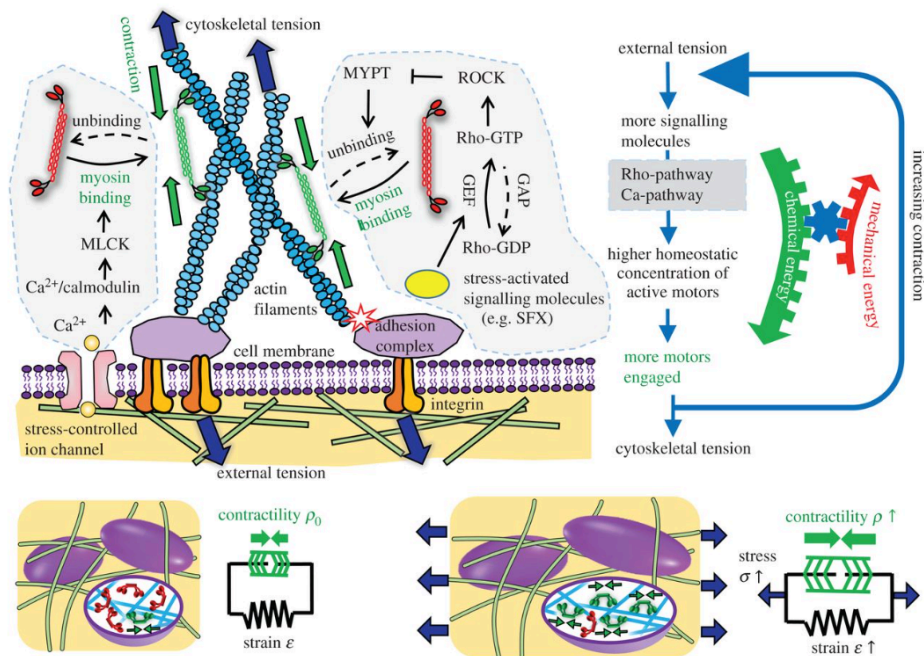


Figure 24 Schematic depiction of the chemo-mechanical coupling and stress-dependent feedback mechanisms⁷⁷

2.2.4 Bioreactor using mechanical stimuli

During 3D tissue reconstruction under the static condition such as an incubator, tissue culturing of such a great number of cells is restricted due to the lack of nutrients or oxygen supply. Not like monolayer condition, the tissues were not

capable of maintaining its tissue functions or degrade. Hence, various types of bioreactors were introduced to solve this issue through tissue engineering approaches. The bioreactors are referred to as devices which enable to control pressure, perfusion of nutrients or gas, waste removal or to monitor changes in temperature or pH in medium^{78,79}. Fig. 25 represented the various bioreactors utilized in the field of tissue engineering. Furthermore, it highly promotes the efficiency of seeding cells into three-dimensional scaffold. The use of bioreactor in the field of tissue engineering has been regarded as a promising success with regard to enhanced tissue function. There are various types of mechanical stimuli generated by the bioreactors in the field of tissue engineering, such as shear force, compression loading, hydrostatic pressure, ultrasound, etc.

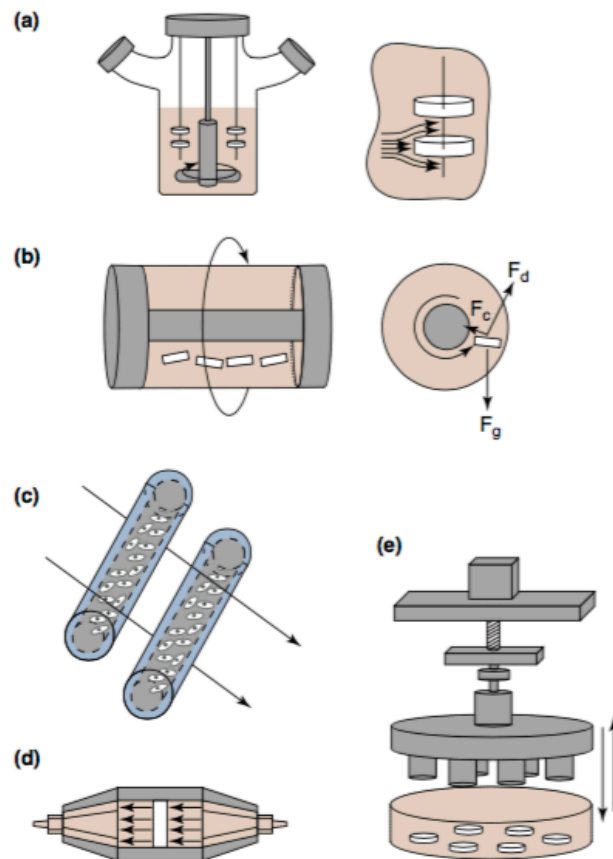


Figure 25 Representative bioreactors for tissue engineering applications ⁷⁸

2.2.5 Decellularization

Decellularization refers to as a process isolating cells from the tissues as shown in Fig 26. The products obtained from decellularization have a potency to use as biological scaffold. The decellularization is conducted by three different methods⁸⁰;

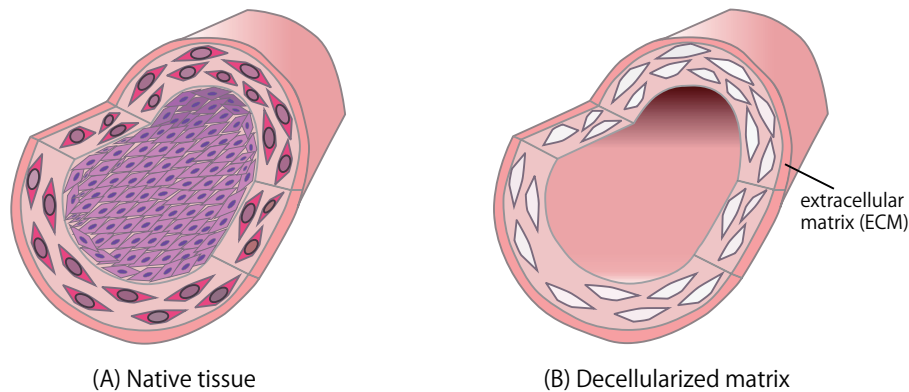


Figure 26 Decellularization; (A) Native tissue (B) Decellularized matrix

- 1) Physical method: Snap freezing, pressure, mechanical agitation, etc
- 2) Chemical method: Triton-X, Sodium dodecyl sulfate (SDS), etc
- 3) Enzymatic method: Trypsin, etc

The advantage of using decellularized matrix is to provide microvascular structure by preserving its original tissues. It allows for cells to supply nutrients and oxygen efficiently after reseeding cell back into the decellularized matrix. Furthermore, it does not induce a severe foreign body reaction since it is a biological scaffold obtained from tissues. Currently, the decellularized matrix has been widely applied into many models including heart, kidney, blood vessel, cartilage, etc. While conventional scaffolds are restricted to apply only into organs that has relatively simple structure such as blood vessel and cartilage in Fig. 27^{81,82}. The utilization of decellularized matrix has suggested a new solution for complex vascularized organs. Hence, various animal experiments and clinical trials are currently attempted for the use of decellularized matrix.

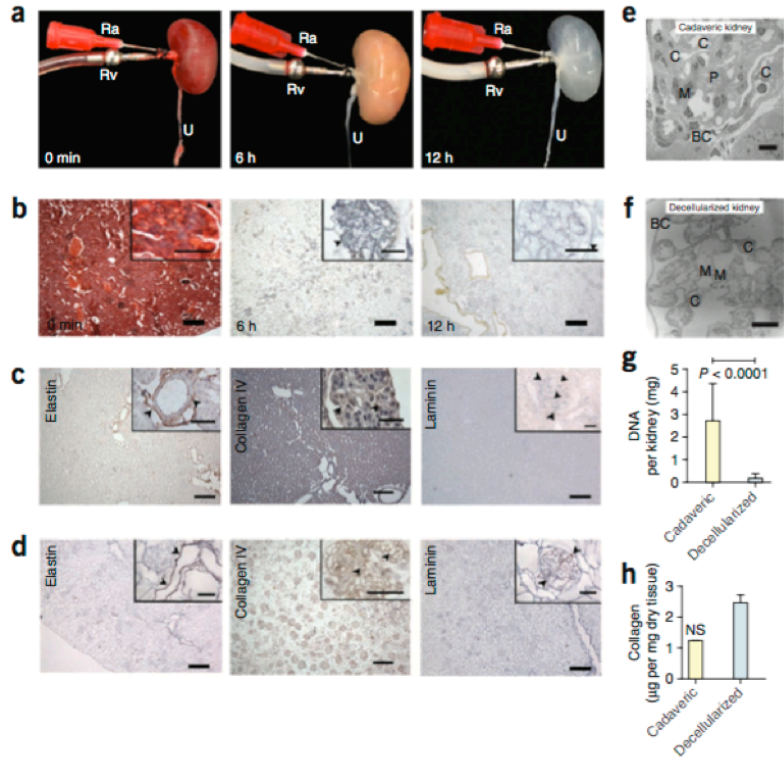


Figure 27 Perfusion decellularization of whole rat kidney ⁸²

2.2.5.1 Decellularization by using HHP

Hydrostatic pressure does not only exert a strong influence in tissue engineering, but it is also conducted for decellularization. By loading high hydrostatic pressure above 600 MPa to tissues, it enables to disrupt cells embedded inside the tissues while preserving its extracellular matrices that is potentially used for scaffolds. As shown in Funamoto's study, their protocol controlling temperature during pressurizing allowed to successfully obtain a decellularized matrix using porcine aortic blood vessels⁸³. Compared to conventional treatments using chemicals such as Sodium dodecyl sulfate (SDS), it showed that the HHP decellularized matrix reduced the inflammation during implantation. Since it does not use any chemicals during treatments, it is superior to retain its extracellular matrices. In Fig.28, it first reported the application of this HHP decellularized matrix for uterine tissues⁷. They suggested a strong evidence of

potential possibility using HHP decellularized matrix as scaffold for uterine regeneration in the future.

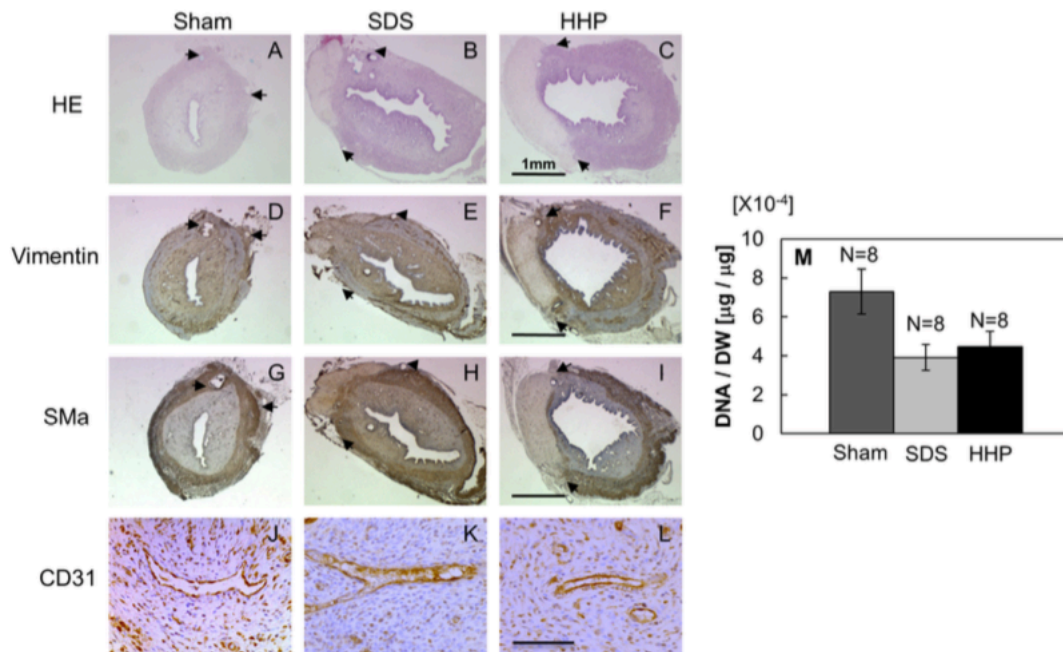


Figure 28 Qualitative observation of reconstructed uterus for tissue regeneration at day 30 (H&E, vimentin and α -SMA) and blood vessels (CD31), respectively, in sham (A,D,G, and I), SDS 1% for 1 hour (B, E, H, and K) and HHP 30 - 4 (C,F, I and L), and quantitative analysis of DNA contents (M).⁷

3. Methodology

3.1 Cell culture

While the cell lines has been widely used due to its easiness of use allowing to subculture for up to about 80 passages, the primary cells are preferentially used at early passage numbers because they have a limited proliferation capability as the passage number increases. Although the cell lines are easily handled and preferred by many scientists, the use of primary cells has been highly demanded to achieve more biologically relevant results rather than cell lines. In this study, we conducted our studies utilizing human and rat primary cells including endometrial stromal cells (ESCs) and bone marrow derived mesenchymal stem cells (bmMSCs). Human ESCs were isolated from endometrial biopsies obtained

from female patients who has regular menstrual cycles by cooperation of obstetrics and gynecology team from the medical school of Tokyo University as reported³³. Rat ESCs were isolated from 9 weeks old female Sprague Dawley rat (SD rat). The SD rat is also used to isolate biopsies for rat bmMSCs. Human MSCs were isolated directly from human knee joints and cultured *in vitro*. Details of culture methods for each cell types including culture medium compositions were reported in each of the following chapters.

3.2 Embryo isolation

Although it would be ideal to use human embryo in this study, this was not possible due to ethical issues as well as practical reason. In this study, we utilized rat embryos collected from SD rat that is purchased from CLEA Japan. The menstrual cycle of female SD rats was monitored and mated with a male SD rat. Once the mating was confirmed by identification of sperms in the vagina in Fig 30, the female rat was sacrificed using isoflurane gas. The embryos were collected from two uterine horns obtained from one SD rat under aseptic condition in a clean bench as shown in Fig 29. In this study, we utilized various experiments using rat embryos as described in Fig. 31 that have an early stage of embryo, morula or blastocyst.

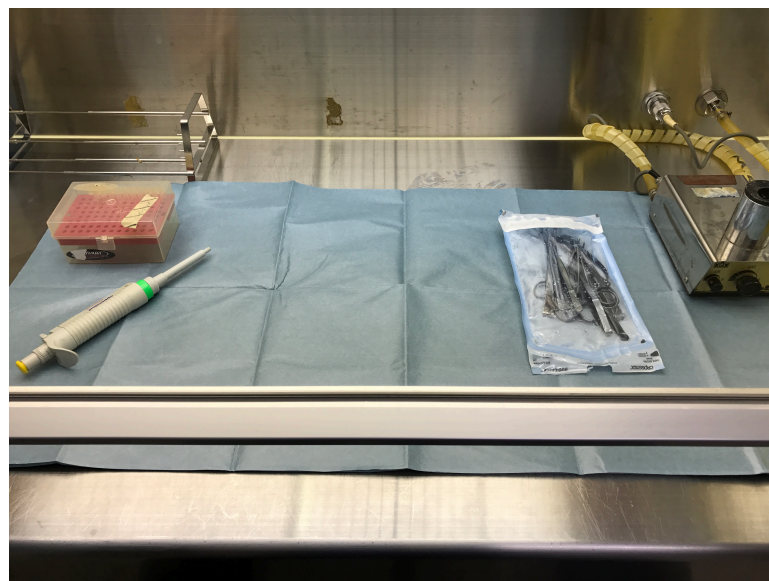


Figure 29 Clean bench set up for isolating embryos from the SD rat.

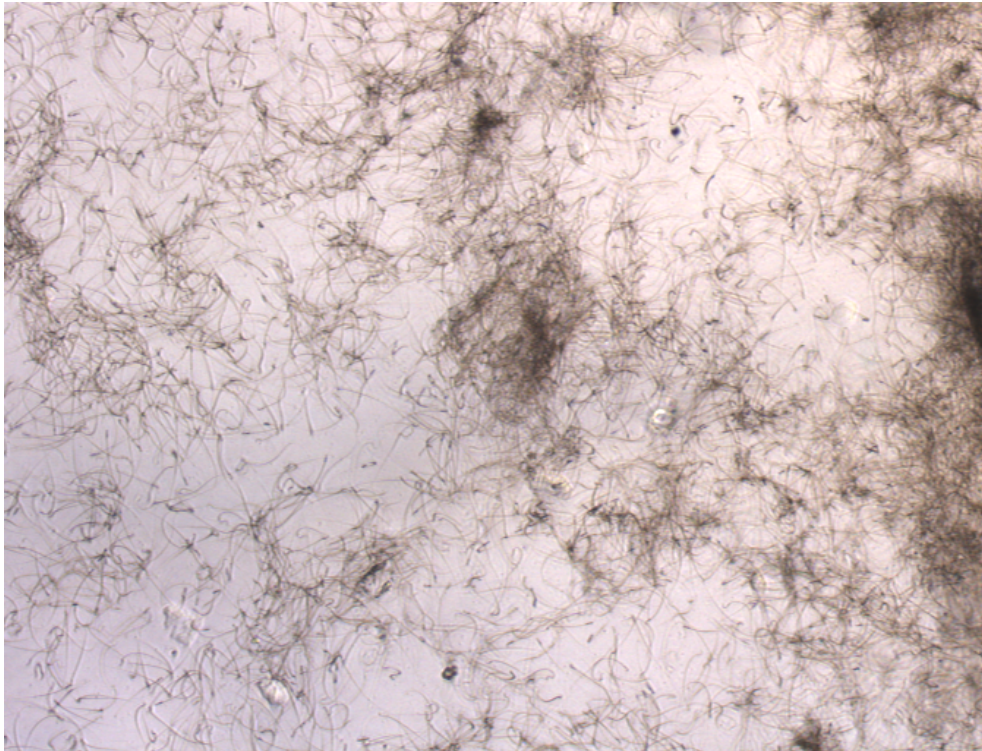


Figure 30 Rat sperms identified by vaginal smear after mating.

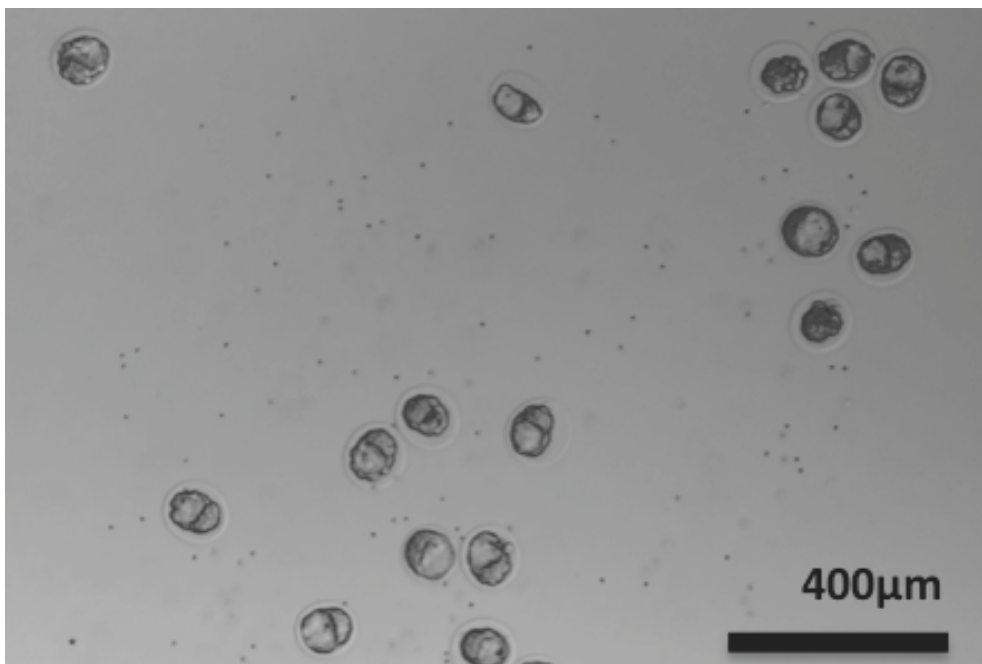


Figure 31 Rat embryos with a stage of morula or blastula obtained from a female SD rat.

3.3 Mechanical stimulated dynamic culture (Flexcell)

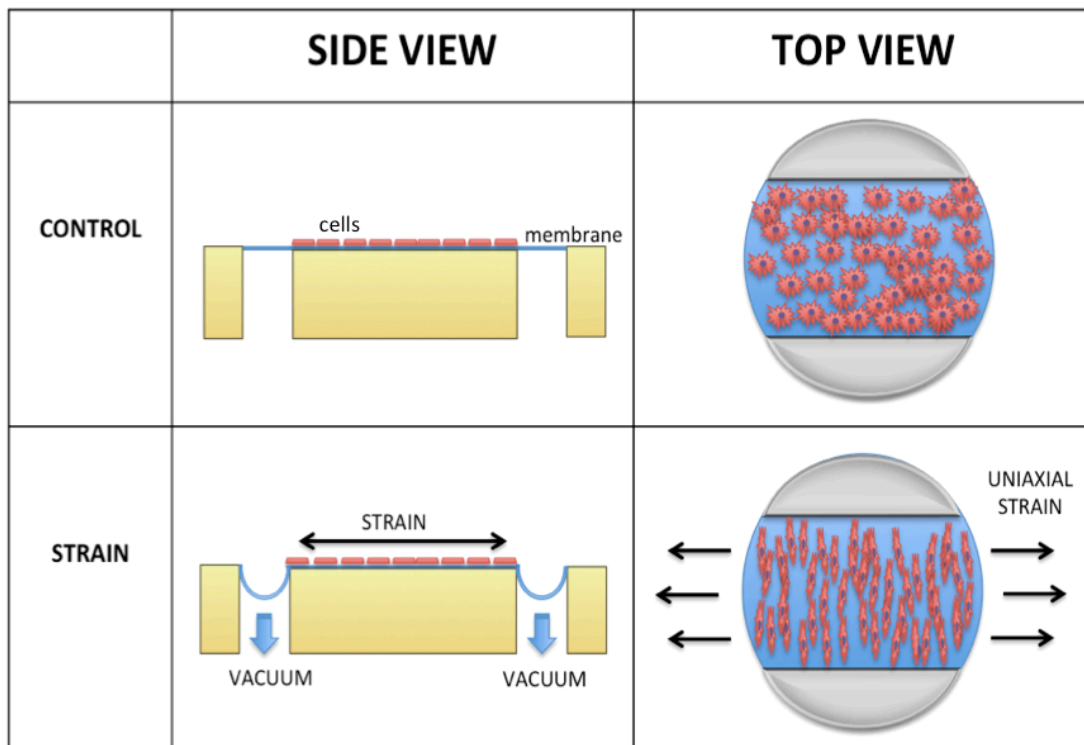


Figure 32 Uniaxial strain application to a bioartificial tissue construct

The flexcell system (FX-4000TM; Flexcell International Corporation) allows for cells to be subjected to cyclic strain. As shown in Fig 32, a vacuum pump connected to the system pulls down a PDMS membrane in flexcell culture plates, leading to strain forces on to the cells seeded on the membrane. In Fig 33 (A) and (C), it is automatically controlled by a computer program, so that it enables to change its amplitude or frequency of cyclic strain. In Fig 33 (B), the flexcell system is located inside the incubator to keep in a humidified incubator at 37°C with 5% CO₂ during the experiment. In this study, we only utilize a certain type of flexcell plate to apply uniaxial cyclic strain loading onto the sample (cells).

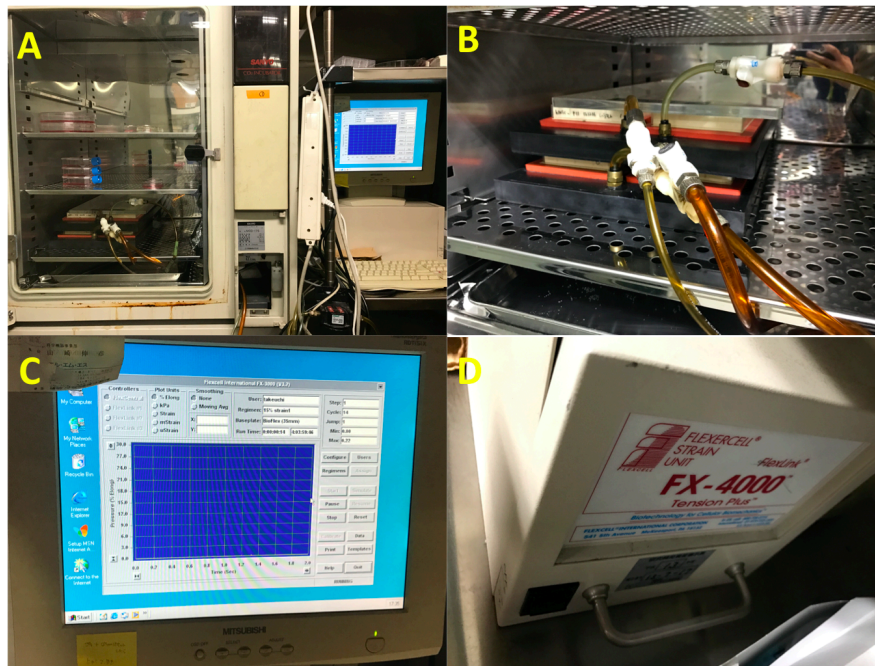


Figure 33 Flexcell tension system

3.4 Histological Analysis

Histological analysis is regarded as one of powerful tools in the biological field because it enables to visualize or identify the microscopic structure of cells and tissues under a microscope. By elucidating the microstructure of the sample, it allows for users to observe the morphology of the sample directly and to examine the sample qualitatively.

3.4.1 Sample preparation

For sample preparation prior to staining, fixation process is required to preserve tissues and prevent from autolysis by enzymes or putrefaction by microorganisms. 10% neutral buffered formalin or 4% formaldehyde in phosphate buffered saline (PBS) are commonly used as fixatives. After fixation of the tissue, the sample is subjected to cryoprotection by immersing into sucrose solution so that it can prevent from the ice crystal formation during the freezing. Then, the sample is externally embedded into OCT compound placed into molds, followed by freezing using isopentane and liquid nitrogen. Frozen samples are sliced by a cryostat and mounted on a glass slides for

staining by using a cryostat (CM1850; Leica). The section of the sample has a thickness of 5 – 10 μm . Cryosectioning has such an advantage of the fastest method to have samples ready for staining, but it sometimes remains an issue of poor morphology preserved after sectioning.

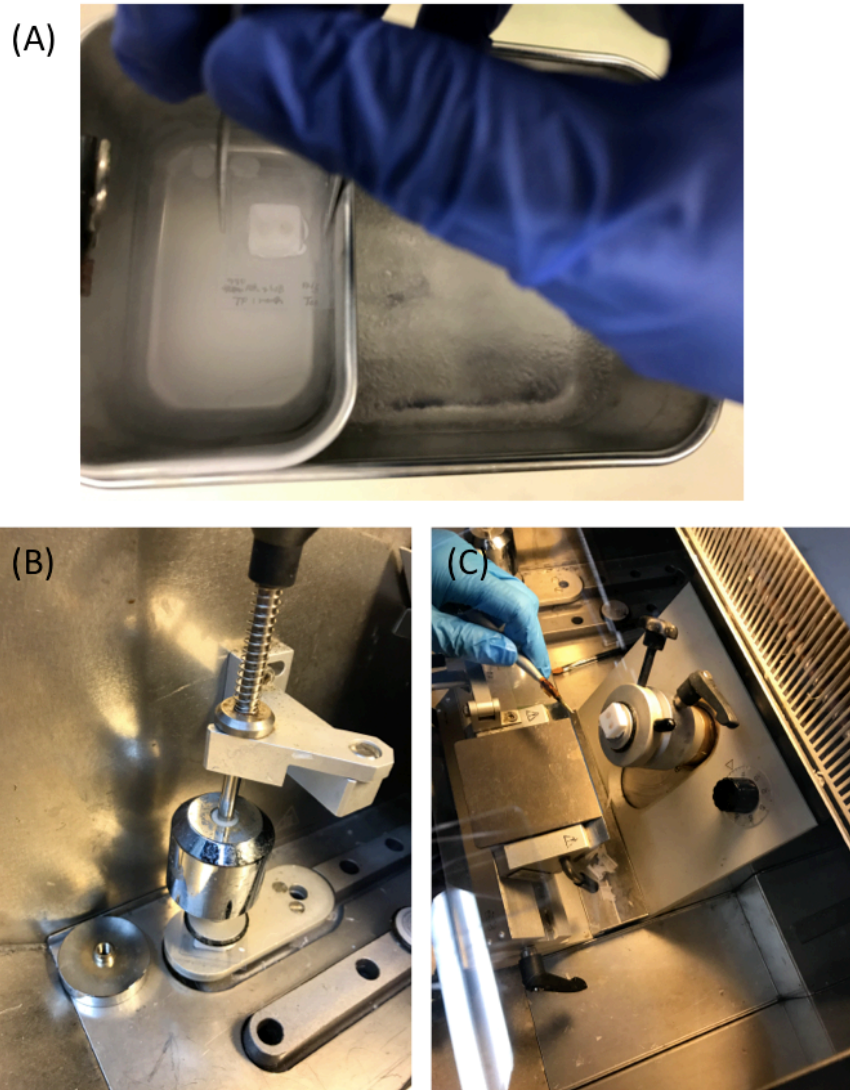


Figure 34 Sample preparation for cryosectioning

3.4.2 Metachromatic staining

Metachromatic staining refers to a staining widely conducted for biological tissues by binding stains to chromotropes inside the nucleus or extracellular proteins. Depending on properties of the components in the tissue sample, its stained color varies, distinguishing its tissue morphology. In this study, we

carried out hematoxylin and eosin (HE) staining, toluidine blue (Tb) staining, and Masson's trichrome (MT) staining.

Hematoxylin and eosin (HE) staining is one of the most widely used metachromatic stain in order to observe morphology of cells and tissues. Hematoxylin binds to DNA/RNA inside tissues where involve acidic and negatively charged basophilic substances. On the other hand, eosin binds to positively charged acidophilic substances, so that it stained protein non-specifically in the extracellular matrix (ECM) inside the tissues. Hence, the nuclei is stained a dark blue or violet while the cytoplasm is stained pink.

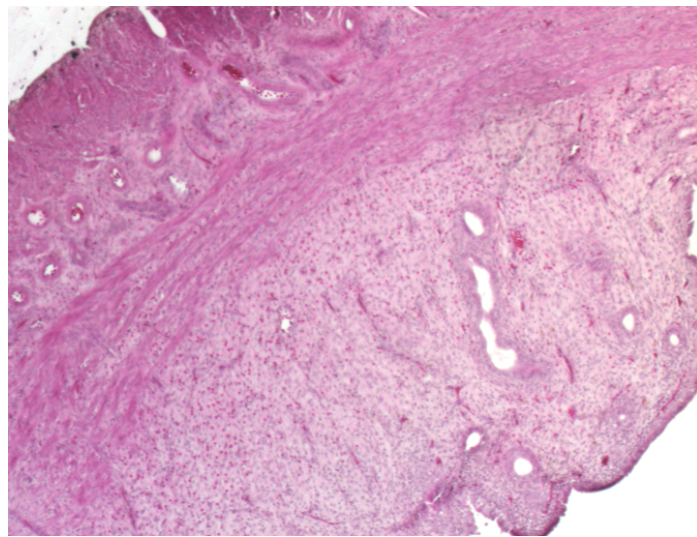


Figure 35 Hematoxylin & Eosin staining image of rat native uterine tissue

Toluidine blue (Tb) staining is another basic metachromatic staining binding to negatively charged acidic components in tissues such as DNA/RNA. While it stained sulphated glycosaminoglycans (sGAG) purple, non-proteoglycan substances are stained light blue.

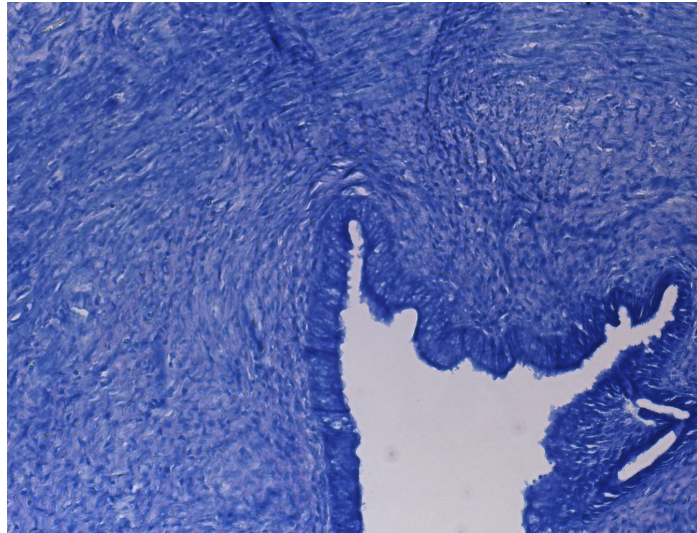


Figure 36 Toluidine blue staining image of rat native uterine tissue

Masson's trichrome (MT) staining is a three color staining used to distinguish between collagen and smooth muscle from tissues. While cell nuclei are stained black by Weigert's hematoxylin, collagen fiber is stained blue. Keratin and muscle fibers are also stained red.

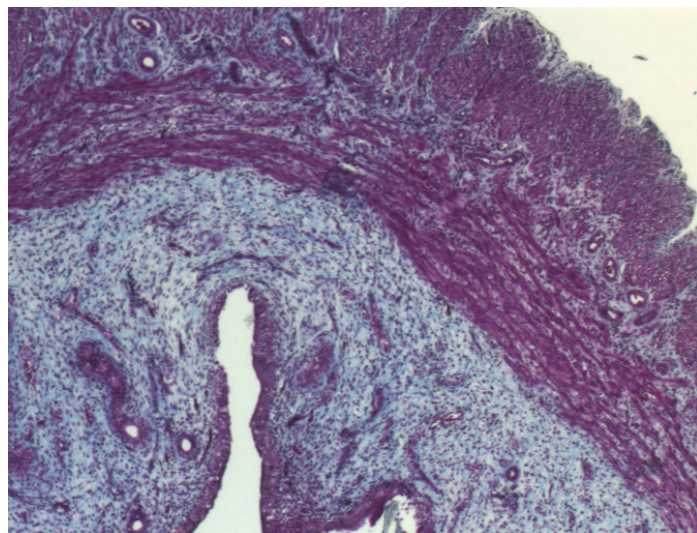


Figure 37 Masson's trichrome staining image of rat native uterine tissue

3.4.3 Immunostaining

Immunostaining refers to an antibody-based method of staining to exhibit a specific target protein in cell/tissue sample. As the most commonly applied immunostaining technique, it conducts immunohistochemistry (IHC) and immunocytochemistry (ICC) that stain for tissue and cell samples, respectively. The samples for immunostaining are prepared as the same process for metachromatic staining. The samples are fixed with 10% neutral buffered formalin or 4% formaldehyde in phosphate buffered saline (PBS). By using citrate buffer, the sample is then subjected to antigen retrieval to enhance the detection of the antigen. The sample is then pre-treated with blocking reagent to prevent from false positive. The primary antibody is labeled onto the sample by incubating it diluted in 1% TBST (Tris-buffered saline, 0.1% Tween 20), followed by the secondary antibody to assist and sort the target antigen. With regard to the secondary antibody, it is recommended to utilize the one conjugating horseradish peroxidase (HRP) enzyme to enhance and amplify a weak signal of the target antigen. In order to visualize the antibody labeled on the sample, a chromogenic substrate such as DAB (3,3'-dianubibenzidine) is finally added in order for the HRP enzyme to catalyze with it, coloring the sample into dark brown. For multi-staining, it usually uses a fluorephore conjugated to the secondary antibody to detect multiple antibodies in the cell/tissue sample.



Figure 38 Immunostaining image of cytokeratin 18 indicating epithelial cells in the native uterine tissue

Table 1 Antibodies used for immunostaining in uterine studies

Antibody	Marker	Vender	Catalogue number	Reactivity	Dilution
Cytokeratin 18 (krt18)	Epithelial cell	Abcam	ab181597	mouse, rat, human	1:500
Vimentin (Vim)	Stromal cell	Abcam	ab92547	mouse, rat, human	1:500
Smooth muscle actin (SMa)	Smooth muscle cell	Abcam	ab5694	mouse, rat, human	1:500
Ki67	Ki67 (proliferation)	Abcam	ab15580	mouse, rat, human	1:500
Collagen I (col1)	Type I collagen	Abcam	ab34710	mouse, rat, human	1:500
Estrogen receptor (ER)	Estrogen receptor	Abcam	ab32063	mouse, rat, human	1:200

3.5 Biochemical analysis

In order to quantify the amount of DNA in tissue-engineered uterus constructs, DNA quantification was carried out using the PicoGreen assay. In this dissertation, we utilized EnSpire Multimode Plate Reader (2300; PerkinElmer) to evaluate it.

3.5.1 Sample preparation

For DNA quantification, the cellular DNAs are required to be separated from the ECM components. To break down the tissue constructs, it is subjected to lyophilization followed by incubation with enzyme proteinases (i.e. papain) at 60 °C, so that the tough protein fibers are digested to free the DNA. In some cases

such as animal tissues, polytron homogenizer helps further to break down finely the tissue for evaluation.

3.5.2 DNA quantification

In order to quantify the DNA contents from the tissue sample, PicoGreen assay was carried out using the Quant-iT PicoGreen dsDNA kit (Invitrogen). The PicoGreen reagents conjugate to the double stranded DNA (dsDNA) in the sample so that it allows to detect up to 25pg/mL of dsDNA from the sample. This assay enables to distinguish any contaminants including RNA from the target dsDNA. The absolute values of DNA can be obtained quantitatively by comparing it to a standard curve.

3.6 Gene expression analysis

In order to determine cell behaviors in the organisms, it regulates its genetic expressions such as DNA, resulting in up-regulation or down-regulation. The gene expression consists of two main stages; transcription and translation. The DNA in the cell nucleus transcribes messenger RNA (mRNA) by enzyme RNA polymerase. Then, the mRNA is translated into protein synthesis by ribosomes. Hence, scientists focus on changes in such a certain mRNA in the cell because it indicates the effect of the gene expression on the cell behaviors. Hence, reverse transcription-polymerase chain reaction (rt-PCR) has been widely used to detect the mRNA expression quantitatively from the complementary DNA (cDNA) produced from RNA samples.

In this study, the RNA is extracted from the cell/tissue sample by using phenol-chloroform extraction method. For the RNA extraction, the sample is lysed with the TRIzol reagent. The TRIzol reagent involves phenol and enables to lyse the sample. The RNA inside the sample can be isolated from other DNA and protein components by addition of chloroform and isopropanol. This process refers to as RNA extraction.

After RNA extraction, the RNA is further purified by addition of DNase I. The DNase removes genome DNA left in the sample. The reverse transcription of RNA to cDNA is induced by utilizing a reverse transcriptase. A pair of designed primer targeting a specific gene is mixed to the cDNA sample, resulting in a significant amplification. In this study, we utilized StepOnePlus (Real-Time PCR system; Abi) to quantify the cDNA. This machine allows to undertake three fundamental steps for PCR, such as denaturation, annealing, and extension. During denaturing, it breaks the hydrogen bonding in the double stranded DNA by increase in the temperature to 90 °C, so that it allows for primers to access to the active sites of the denatured cDNA. By changing the temperature to 65 °C, the primers bind to the active sites while polymerase enzyme helps to elongate and anneal, forming two copies of double stranded DNA. By repeating this cycle 40 times, the cDNA can be significantly amplified and finally evaluated quantitatively.

Table 2 Uterine function related gene markers

Endometrial epithelial cell marker	Cytokearin 7 (KRT7) ⁸⁴ , Cytokeratin 8 (KRT8) ⁸⁵ , Cytokeratin 18 (KRT18) ⁸⁵
Endometrial stromal cell marker	Vimentin (Vim) ^{86,87} , Membrane metallo-endopeptidase (MME; CD10) ⁸⁸ , Thymocyte antigen (Thy-1; CD90) ⁸⁹
Smooth muscle cell marker	Alpha smooth muscle actin (Acta2) ⁹⁰ , Transgelin (SM22a) ⁹¹
Blood vessel marker	Platelet endothelial cell adhesion molecule (PECAM-1; CD31) ⁹² , Protein tyrosine phosphatase, receptor type, C (PTPRC; CD45) ⁹³
Hormone receptor marker	Estrogen receptor (ER) ⁹⁴ , Progesterone receptor(PR) ⁹⁵
Decidualization marker	Insulin-like growth factor binding protein 1 (IGFBP-1) ⁹⁶ , Prolactin ⁹⁷
Other markers related to uterine function	Integrin β 3 subunit (ITGB3) ⁹⁸ , B-cell lymphoma 2 (BCL-2) ⁹⁹ , Ki67 ⁹⁹
Other markers related to implantation of embryo	Heparin-binding EGF-like growth factor (HBEGF) ^{100,101} , Homeobox A10 (HOXA-10) ¹⁰²

4. Study. 1: Enhancement of smooth muscle cells in human endometrial stromal cells by mechanical stimuli for uterine regeneration

4.1 Purpose

The uterus allows implantation of the embryo/fetus and regulates its growth by supplying nutrients from the mother's body. Its wall consists of three layers made respectively of epithelial cells, stromal cells, and smooth muscle cells. Defects of the uterus, however, do not only cause infertility, but may also induce perinatal diseases such as premature birth¹⁰³. Moreover, irreversible loss of function in uterine smooth muscle cells and stromal cells caused by uterine fibroids and adenomyosis is often observed in the patients who have a reproductive age¹⁰⁴⁻¹⁰⁶. Congenital uterine defects, such as the Mayer-Rokitansky-Kuster-Hauser syndrome, or hysterectomy performed to remove malignant tumors lead to permanent infertility¹⁰⁷⁻¹⁰⁹. Therefore, new approaches will be required for those who are suffering from the defects of the uterus.

It is now widely known that mechanical stimuli applied to various cell types can trigger intracellular signaling events leading to physiological and pathological changes^{59,64,68,110}. The outer layer of uterine smooth muscle (myometrium) undergoes remodeling by hyperplasia and hypertrophy during pregnancy, its mechanism still remains unclear¹¹¹. Even in the case of infertility, the myometrium still shows spontaneous contractile activity¹¹², and this mechanical stimulus from the myometrium is believed to affect physiological functions of the endometrium, such as menstruation and pregnancy. Thus, mechanical stimuli in the uterus are regarded as a significant factor for its physiological function on a par with biochemical stimuli induced by estradiol and progesterone secreted during the menstrual cycle.

Although the role of mechanical stimuli in cell models has been highlighted, only limited studies are conducted for uterine cells. Most of those studies particularly focused on certain chemical factors in endometrial stromal cells (ESCs) in response to mechanical stimuli^{67,68,113}. We hereby aimed to find out that the effect of mechanical stretching on ESCs with regard to differentiation. Understanding of this mechanism in

the uterus is thought to contribute to reveal the differentiation mechanism of cells in the uterus. Furthermore, it is expected to apply into tissue engineering approaches leading to three-dimensional reconstruction of uterine tissue by utilizing bioreactors.

In this study, assuming that there is some mechano-physiological signaling connection between the endometrium and the myometrium, we focused on the endometrial stromal cells that are the major components of the endometrium. By utilizing the Flexcell tension system to apply cyclic strain onto human endometrial stromal cells (hESCs), we conducted an *in vitro* study to reveal the effects of mechanical stimuli (cyclic strain) on hESCs.

4.2 Materials and Methods

4.2.1 Isolation and culture of hESCs

Endometrial biopsies were obtained from 38~48-year-old female patients who had regular menstrual cycles. Fresh human endometrial stromal cells were isolated and cultured as previously reported³³⁻³⁵. The purity of cells was examined and identified by positive cellular staining for vimentin (stromal cell marker) while those cells were not stained by cytokeratin 18 (epithelial cell marker) or SMA (smooth muscle cell marker). This study was approved by the Institutional Review Board of the University of Tokyo, and each patient signed informed consent for sample collection. We cultured hESCs in DMEM/Ham's F12 (Sigma) supplemented with 2.5% charcoal-stripped FBS (Funakoshi) and 1% of Antibiotic-Antimycotic (GIBCO) in a humidified incubator at 37°C with 5% CO₂. Culture medium was changed every 3 or 4 days. For inhibitor tests, we used the adenylyl cyclase inhibitor SQ22538 (Cayman) and the protein kinase A (PKA) inhibitor H-89 (Cayman). SQ22538 (100 μM) and H-89 (10 μM) were added to the samples with culture medium while loading cyclic strain.

4.2.2 Uniaxial cyclic strain loading

In this study, we loaded cyclic strain using the Flexcell tension system (FX-4000™; Flexcell International Corporation) placed in a humidified incubator at 37°C with 5% CO₂. The Flexcell is computer-operated and applies its strain by vacuum. Since there exist no data regarding the effect of cyclic strain on differentiation changes of hESCs in previous studies, the parameters of cyclic strain, such as its intensity, frequency, or time, were optimized by myself. In this study, 15% uniaxial strain was applied at 0.1 Hz that exerted significant results. During application of the uniaxial cyclic strain, the culture medium was changed every 3 or 4 days. For control samples, hESCs were cultured in identical Flexcell plates but without strain.

4.2.3 rt-PCR

To measure mRNA expression in the different samples from the Flexcell system, we carried out reverse transcriptional PCR (rt-PCR). After finishing loading cyclic strain, the cells were rinsed with PBS and immediately collected with Trizol reagent (Invitrogen) before RNA extraction and cDNA synthesis using the ReverTra Ace qPCR RT Master Mix with gDNA Remover (Toyobo). *CD10* and *CD90* were used as endometrial stromal cell markers while *SM22a* and *ACTA2* are highly expressed in smooth muscle cells. Primer sequences and amplicon sizes are listed in the table below. Oxytocin receptor (*OXTR*) was also examined as representative of uterine smooth muscle cell marker while desmin (*DES*) and interleukin 6 (*IL6*) were utilized to distinguish its property compared to myofibroblast. Similarly, expressions of vascular smooth muscle cell markers were used, namely, angiopoietin 1 (*ANGPT1*) and receptor activity modifying protein 1 (*RAMP1*). Insulin like growth factor binding protein 1 (*IGFBP1*) was also examined as a decidualization marker in endometrial stromal cell. All genes were normalized to *RPL32* expression and further normalized to the control samples.

Table 3 Primer List

Gene	Forward primer	Reverse primer	Amplicon size (bp)
<i>RPL32</i>	GCCCAAGATCGTCAAAAAGA	GTCAATGCCTCTGGGTTT	98

<i>CD10</i>	TCCACTGGAGATCAGCCTTT	TATCGGGAAGTGGTCTCAGG	237
<i>CD90</i>	CTAGTGGACCAGAGCCTTCG	TGGAGTGCACACGTGTAGGT	235
<i>SM22a</i>	AGGTCTGGCTGAAGAATGGC	TTCAAAGAGGTCAACAGTCTGG	199
<i>ACTA2</i>	CTGAGCGTGGCTATTCCCTTC	TTCTCAAGGGAGGATGAGGA	133
<i>OXTR</i>	TTCTTCGTGCAGATGTGGAG	ACGAGTTCGTGGAAGAGGTG	149
<i>DES</i>	CTGAGCAAAGGGGTCTGAG	TGGCAGAGGGTCTCTGTCTT	135
<i>ANGPT1</i>	GAAGGGAACCGAGCCTATTC	GCTCTGTTTTCTGCTGTCC	108
<i>RAMP1</i>	CCTCACCCAGTTCAGGTAG	GAACCTGTCCACCTCTGCAT	157
<i>IGFBP1</i>	AGGCTCTCCATGTCACCAAC	CCTGTGCCTTGGCTAAACTC	90

4.2.4 Immunostaining

After 7 days of cyclic strain, hESCs were immediately fixed with 4% paraformaldehyde. The fixed samples were permeabilized with 0.2% Triton-X 100 in PBS for 3 min and washed with PBS 3times. Then non-specific binding was blocked with PBS containing 1% BSA before covering the cells with anti-SMa antibody (Abcam) at the dilution of 1/500 for 1 hour at room temperature or overnight at 4°C. After revealing the antibody using the DAB peroxidase substrate kit (Vector Laboratories), the samples were mounted on slide glass for visualization and storage.

4.2.5 Measurement of cell reorientation against cyclic strain

In order to measure the angle of cell orientation after applying cyclic strain for 7 days, we used a normal microscope image ($\times 5$). By using ImageJ, a line was drawn from the bottom of the cell to the top of the cell across its longest point. After drawing the line, we measured the angle of the line in ImageJ. The angles of the cells were measured up to 50 cells in one sample and then quantified.

4.2.6 Cyclic adenosine monophosphate (cAMP) measurement

The samples were collected and lyzed with 0.1 M HCl. After centrifugation at 1,000 g, the supernatant was decanted and stored at -80 °C until assay. Cyclic AMP concentrations were measured using the cyclic AMP EIA kit (Cayman) according to the manufacturer's instructions. The absorbance at 412 nm was measured with an EnSpire plate reader (PerkinElmer). The cAMP concentrations

were normalized to the DNA amounts quantified using the Quant-iT PicoGreen dsDNA Reagent and Kit (Invitrogen).

4.2.7 Cell contraction assay

After the samples were subjected to cyclic strain, they were trypsinized and resuspended in medium at 2.0×10^6 cells/ml. By using Collagen-based contraction assay kit (CELL BIOLABS, INC.), we prepared a collagen lattice with bovine Type I collagen at 3.0mg/ml. As shown in protocol of the kit, the collagen gel was polymerized with the samples and waited for two days in the incubator to develop stress against culture dish. Before the stress was released, oxytocin (10 nM) was added to promote its contractile activity like smooth muscle cells. At 7 days after releasing the stress from the sample, a surface area of the sample was measured for quantification.

4.2.8 Statistical analysis

The bars in the RT-PCR graphs represent the means \pm standard error of the mean. The statistical significance was assessed using Student's t-test. P-values below 0.05 were regarded as significant.

4.3 Results

4.3.1 Up-regulation of uterine smooth muscle cell markers in hESCs in response to uniaxial strain.

In this study, we used the Flexcell system to load 15% of uniaxial cyclic strain at 0.1 Hz to hESCs for up to 7 days. As shown in Fig 39, we then carried out rt-PCR to assess the gene expression changes in several stromal cell markers including *CD10* and *CD90* and uterine smooth muscle cell (SMC) markers such as *ACTA2* and *SM22a*. Cyclic strain slightly decreased endometrial stromal cell marker expression, (0.90-fold change for *CD10* and 0.86-fold change for *CD90*) but the changes were not significant. With regards to SMC markers, both smooth muscle cell markers were significantly up-regulated by cyclic strain (1.32-fold change

for *ACTA2*, $p < 0.005$; and 1.59-fold change for *SM22a*, $p < 0.05$). As well as the smooth muscle markers, 7 days of cyclic strain significantly raised mRNA expression of oxytocin receptor (2.13-fold change for *OXTR*, $p < 0.05$).

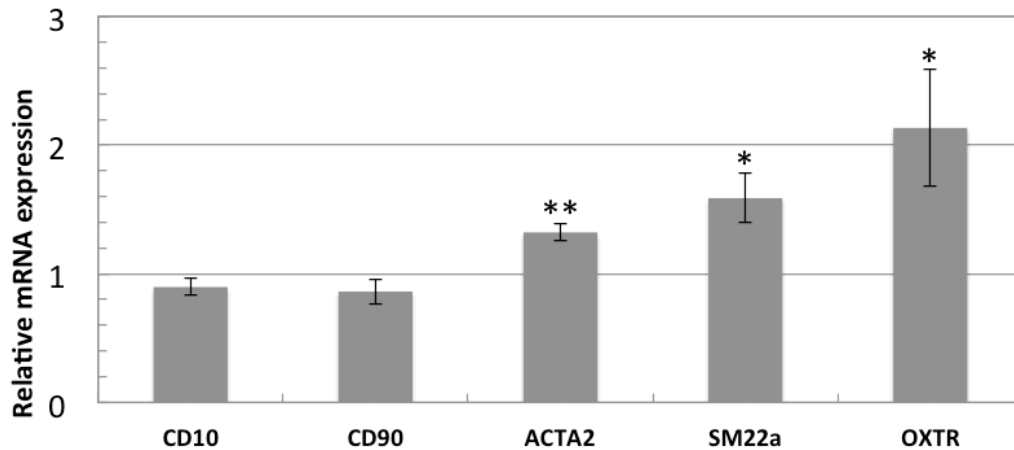


Figure 39 mRNA expressions of endometrial stromal cell markers and smooth muscle cell markers in hESCs after applying cyclic strain for 7 days measured by rt-PCR. (*CD10*, *CD90*, *ACTA2*, *SM22a*, and *OXTR*). Graphs show the fold change of mRNA expressions relative to *RPL32* mRNA normalized to the control mean (n=6). The bars represent the mean ± standard error (p-value was obtained from student's *t*-test; * $p < 0.05$, ** $p < 0.005$).

After applying cyclic strain for 7 days, immunostaining for smooth muscle actin (SMA) was carried out to visualize the morphologic changes in smooth muscle cell marker expression. Fig. 40 shows that SMA were randomly oriented in the control samples. On the other hand, after 7 days the strained cells reoriented perpendicularly to the direction of stretch and became elongated; furthermore, there was an increase in the staining intensity of SMA in the strained cells.

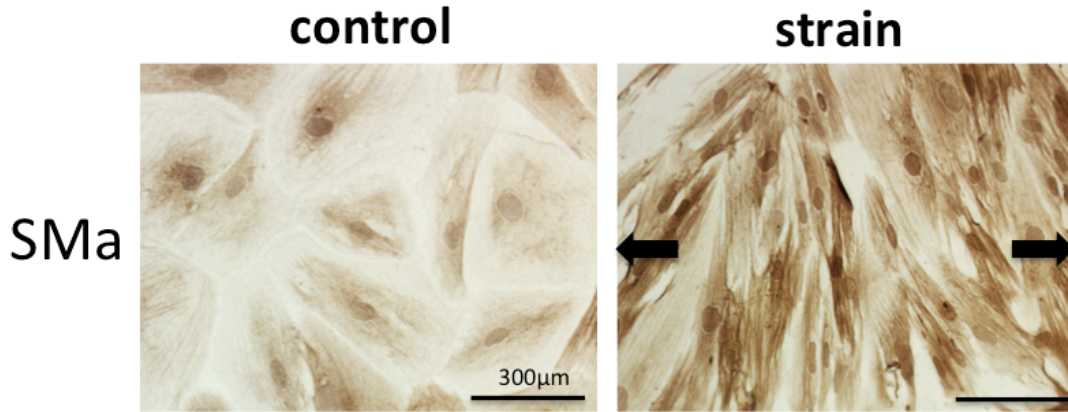


Figure 40 Smooth muscle actin (SMA) expressions by immunostaining in hESCs were represented after loading cyclic strain for 7 days. SMA for control sample (left). SMA for strained sample (right). The arrows and bars indicate the direction of cyclic strain and 300 μm , respectively. Magnification $\times 20$

Fig. 41 showed the up-regulation of desmin mRNA expression (1.63-fold change for *DES*, $p < 0.05$) while decreasing IL6 (0.68-fold change; $p < 0.05$) after applying cyclic strain. On the other hand, it decreased mRNA expressions of *ANGPT1* (0.73-fold change; $p = 0.12$) and *RAMP1* (0.50-fold change, $p < 0.005$) as well as a decidualization marker, *IGFBP1* (0.32-fold change for *IGFBP1*, $p < 0.05$).

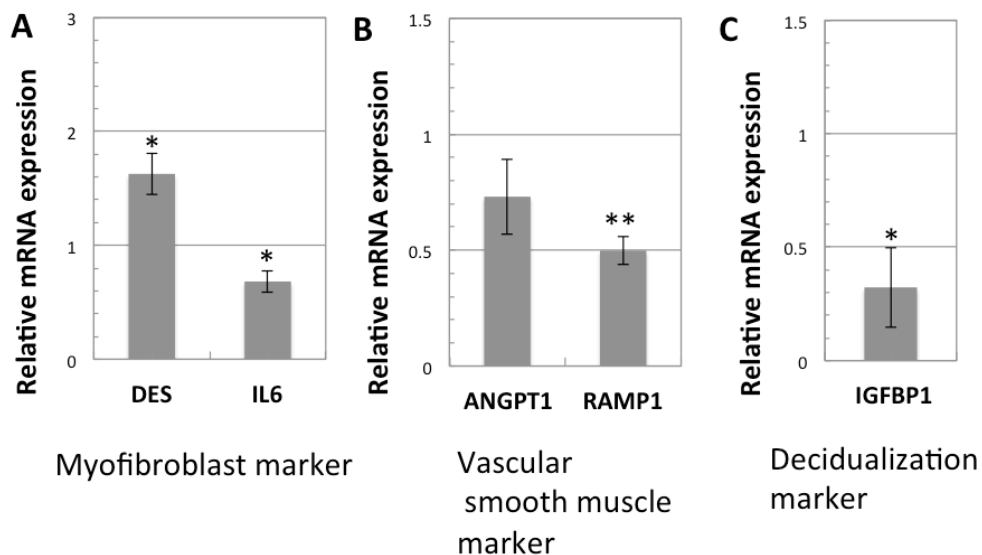


Figure 41 mRNA expressions in hESCs after applying cyclic strain for 7 days measured by rt-PCR. (A) *DES* and *OXTR*, (B) *ANGPT1* and *RAMP1*, and (C) *IGFBP1*. Graphs show the fold change of endometrial stromal cell markers and smooth muscle cell markers mRNA expression relative to *RPL32* mRNA

normalized to the control mean (n=6). The bars represent the mean \pm standard error (p-value was obtained from student's *t*-test; * $p < 0.05$, ** $p < 0.005$).

4.3.2. Reorientation of hESCs after applying 7 days of uniaxial cyclic strain

In order to quantify the reorientation of hESC after applying uniaxial cyclic strain for 7 days, we evaluated the angle of the cells. We utilized normal microscope images of control sample and strained sample as represented in Fig 42 (A) and (B), respectively. In Fig 42 (C) and (D), the mean angles of cells (or mean direction of elongation) in control and strained hESCs were 108° (SEM 69.1°) and 91.3° (SEM 33.6°), respectively. The mean angle of strained hESCs compared to that of control sample was significantly different with a p-value of 0.0002. Moreover, the standard deviation of the angle in the strained cells was much smaller than that of the control sample. It indicates the angle of the cells in the strained hESCs was much more uniform compared to the more random orientation of the control hESCs.

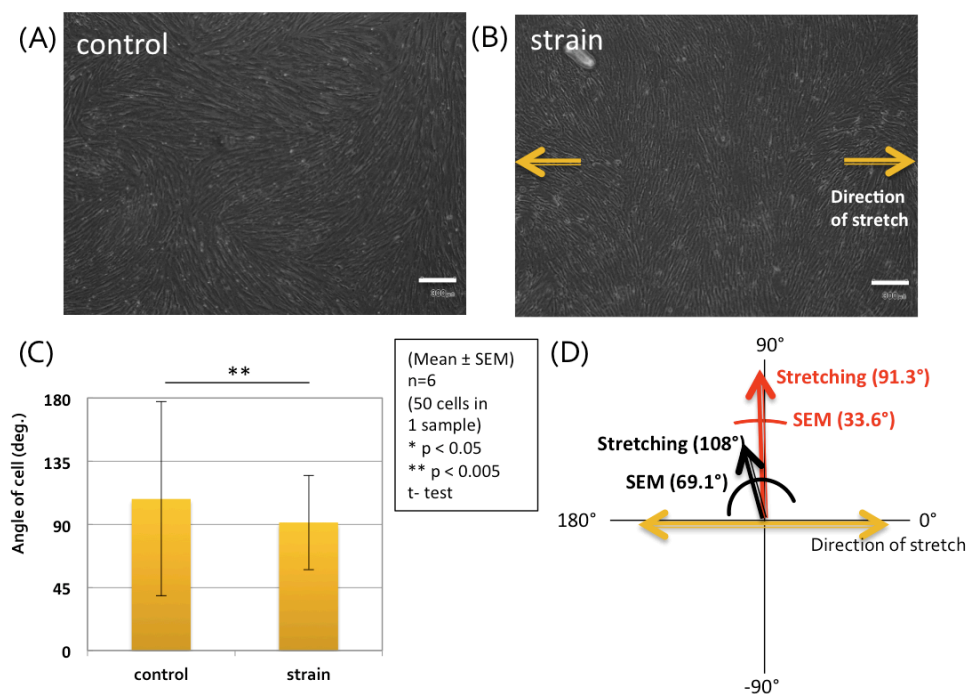


Figure 42 Microscope images of (A) control and (B) strained cells after applying 7 days of cyclic strain. (C) Quantification data of angle changes in cells. Graphs show the angle of cells (n=6, 300 cells in each group). The bars represent the mean \pm standard error (p-value was obtained from student's *t*-test; * $p < 0.05$, ** $p < 0.005$). (D) Schematic plot of the cell distribution.

4.3.3 Induction of cAMP production by cyclic strain in hESCs

To check the involvement of cAMP in the up-regulation of smooth muscle cell markers in hESCs against cyclic strain, we measured the production level of cAMP in the strained hESCs. Firstly, cAMP concentrations after 15 mins of cyclic strain were measured. Fig. 43 (A) shows a transient and significant up-regulation in cAMP production (1.75-fold change; $p < 0.005$) in as little as 15 mins. In addition, Fig. 43 (B) shows the levels of cAMP after 7 days of cyclic strain. There was a non-significant increase in cAMP production immediate after 7 days of strain (1.62-fold change; $p = 0.07$). Then, we performed 7 days of strain, followed by a 2-hour break for cAMP levels to stabilize, and followed by an extra 15 mins of cyclic strain. After such a strain regimen, cAMP concentration was significantly up-regulated (2.35-fold change; $p < 0.05$).

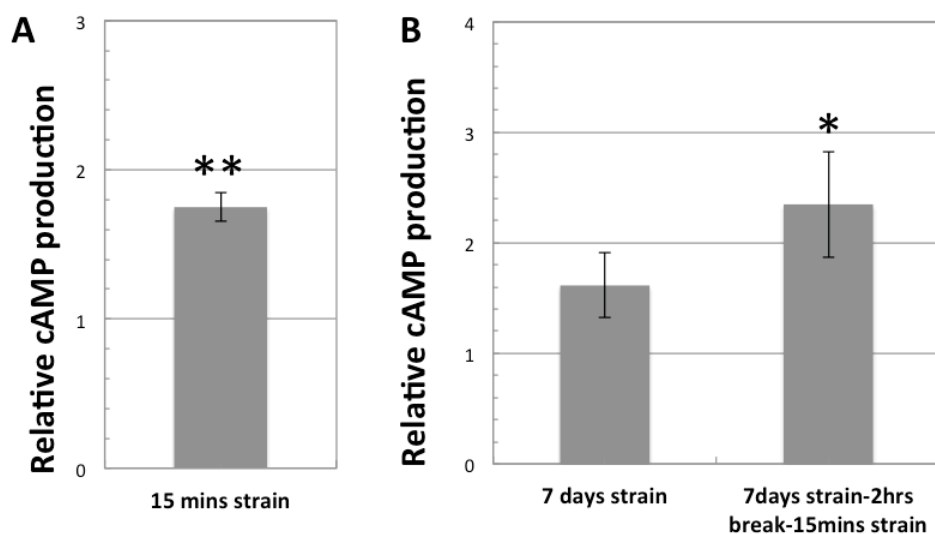


Figure 43 Relative cAMP production level measured by cyclic AMP EIA kit. A) Applying cyclic strain for 15 mins significantly up-regulated cAMP production in hESCs. B) cAMP levels were measured after 7 days of strain, followed by a 2-hour break for cAMP levels to stabilize, followed by an extra 15 mins of cyclic strain. 7 days of strain induced a non-significant increase in cAMP production while 2-hour break followed by an extra 15 mins significantly up-regulated. Graphs showed the fold change of cAMP production level relative to the amounts of DNA quantification and further normalized to the control mean. The bars represent the mean \pm standard error ($n=4$) (p -value was obtained from student's t -test; * $p < 0.05$, ** $p < 0.005$).

4.3.4 Inhibitor test using SQ22536 and H-89

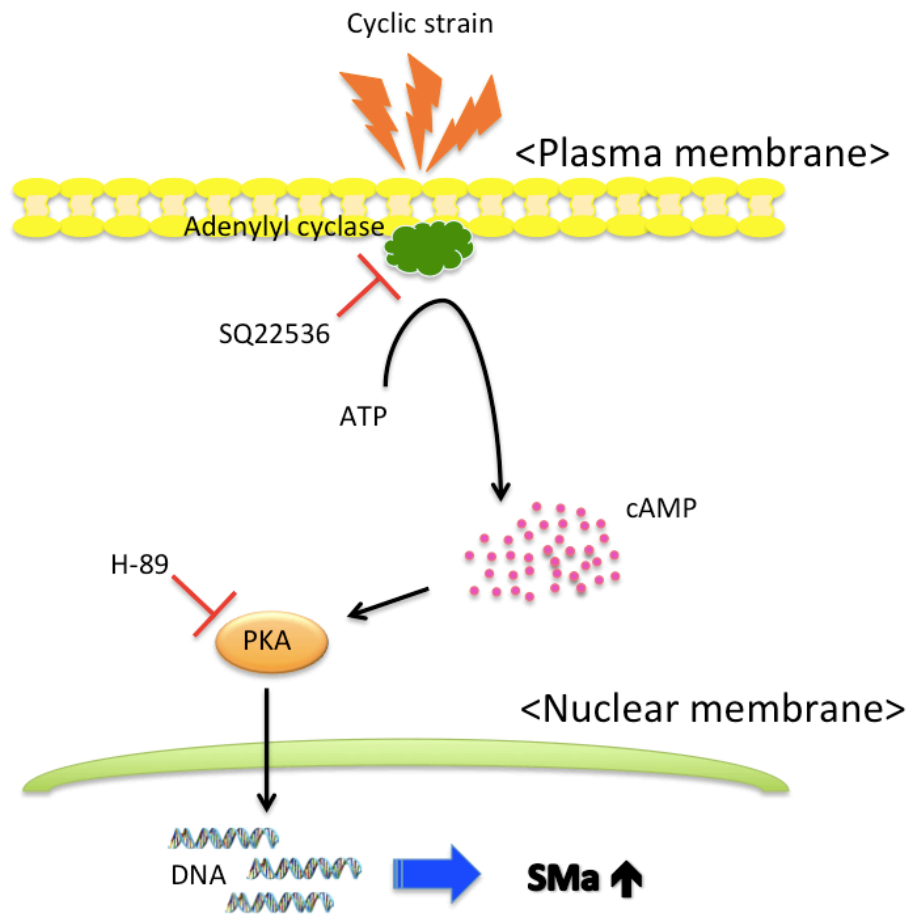


Figure 44 Schematic describing the signaling pathway in hESCs in response to cyclic strain. Adenylyl cyclase located on the inner side of the plasma membrane converts ATP to intracellular cAMP second messenger. Induced cAMP by cyclic strain promoted the SMa markers, which is directly regulated by adenylyl cyclase and PKA.

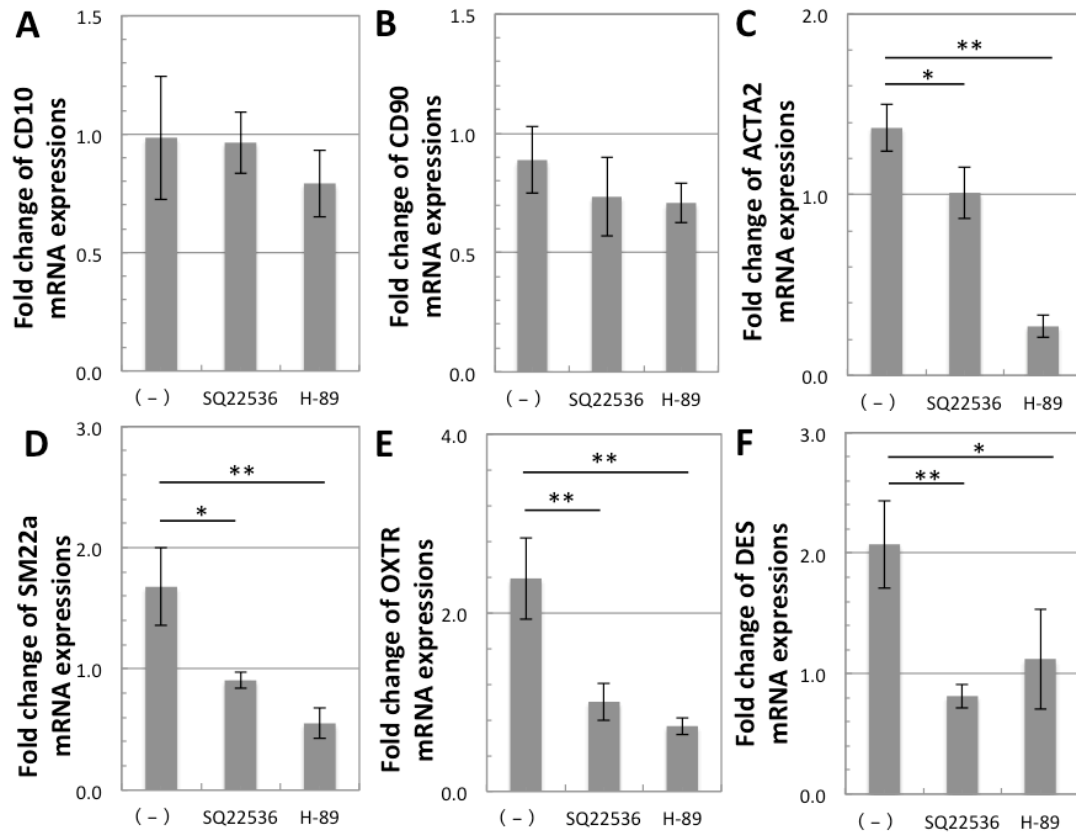


Figure 45 mRNA expressions of (A) *CD10*, (B) *CD90*, (C) *ACTA2*, (D) *SM22a*, (E) *OXTR*, and (F) *DES* in hESCs after applying cyclic strain with SQ22536 and H-89 inhibitor measured by rt-time PCR. All the mRNA expressions were normalized to the RPL32 expressions and further normalized to control values. Applying cyclic strain for 7 days non-significantly down-regulated both endometrial stromal cell markers while it up-regulated the smooth muscle cell markers. While non-significant down-regulations of *CD10* and *CD90* were remained by addition of SQ22536 and H-89 inhibitors, both SQ22536 and H-89 inhibitors successfully inhibited the up-regulation of both *ACTA2*, *SM22a*, *OXTR*, and *DES*. The bars represent the mean \pm standard error of fold changes between strained and control samples (n=4) (p-value was obtained from student's *t*-test; * p < 0.05).

To determine whether the cAMP signaling pathway was involved in the up-regulation of smooth muscle cell markers under strain, we stretched hESCs in the presence or absence of the adenylyl cyclase inhibitor SQ22536 or the PKA inhibitor H-89 as described in the schematic diagram, Fig 44. Fig. 45 represented fold-changes of mRNA expression obtained by rt-PCR for inhibitor tests. As in the previous experiment, cyclic strain did not significantly affect *CD10* or *CD90* expression in hESCs but significantly up-regulated *ACTA2* (1.37-fold change; p<0.05) and *SM22a* (1.68-fold change; p<0.05) expression. By adding SQ22536, the up-regulation of smooth muscle cell makers by cyclic strain was inhibited,

with a respectively 1.01 and 0.91-fold change in *ACTA2* and *SM22a* expression. Moreover, the use of H-89 also showed an inhibiting effect on both *ACTA2* (0.33-fold change) and *SM22a* (0.55-fold change) expression. In order to confirm the effect of inhibitors, we compare those fold changes of *ACTA2* after adding SQ22536 and H-89 normalized to negative control samples were 0.75-fold change ($p < 0.05$) and 0.26-fold change ($p < 0.005$), respectively, while those of *SM22a* after adding SQ22536 and H-89 were 0.57-fold change ($p < 0.05$) and 0.33-fold change ($p < 0.005$), respectively. As well as the smooth muscle cell markers, the up-regulation of both *OXTR* and *DES* mRNA expressions were inhibited by addition of SQ22536 and H-89. After addition of SQ22536, the inhibiting effects in *OXTR* (0.44-fold change; $p < 0.005$) and *DES* (0.47-fold change; $p < 0.005$) were significantly exerted while the inhibition effects by H-89 on *OXTR* and *DES* were 0.39-fold change ($p < 0.005$) and 0.51-fold change ($p < 0.05$), respectively. Hence, both SQ22536 and H-89 performed the inhibition for the up-regulation of smooth muscle cell markers under cyclic strain.

4.3.5 Effect of oxytocin on hESCs-mediated collagen I gel with regard to its contractile ability

To confirm if the strained hESC can behave like uterine smooth muscle cells (myometrium) in three-dimensional structure over cellular level, the cell contraction assay was carried out using collagen gel. Oxytocin was also added during the contractile assay since it is known to regulate the contractile movement of myometrium in the uterus. Before the stress against culture dish was released, Fig.45 (A)-(D) showed the samples mediated with collagen I gel in the presence or absence of Oxytocin (10 nM). The surface areas of the samples were measured and quantified after 7 days as shown in Fig.46 (E). The mean surface areas of the control samples with and without oxytocin were 54,051 and 42,179 square pixels, respectively. In the presence of oxytocin, the sample was contracted to the 22% of the negative control sample ($p = 0.39$). On the other hand, the strained samples showed a significant elevation in its contractile ability both in the absence of oxytocin (32% of the negative control; 36,898 square

pixels; $p=0.16$) and in the presence of oxytocin (49% of the negative control; 27,687 square pixels; $p<0.05$).

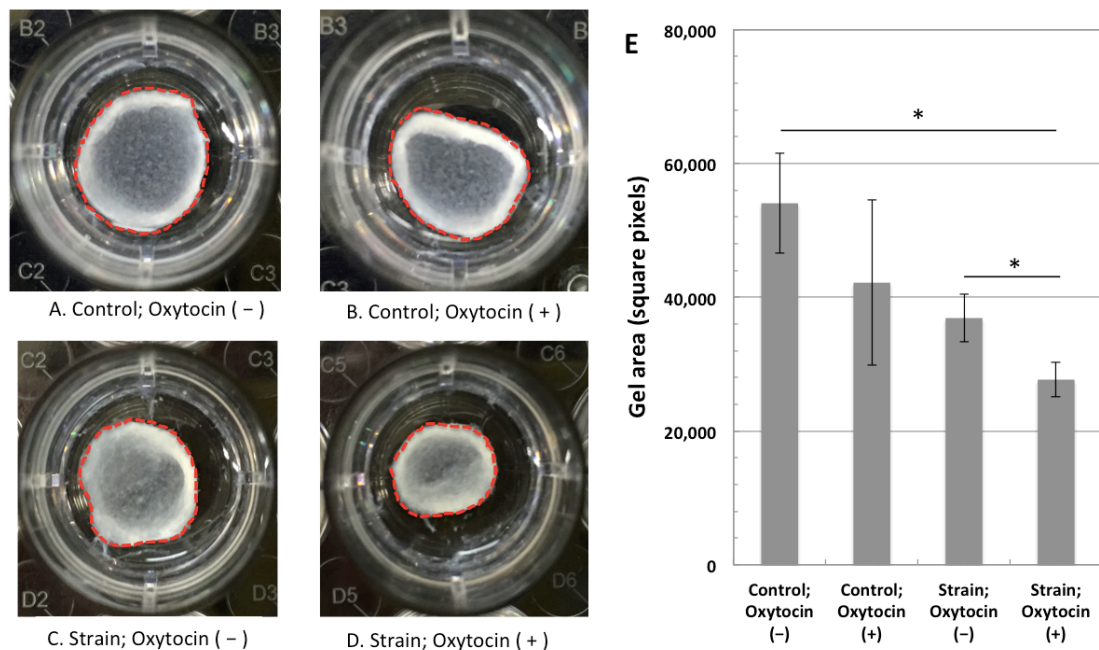


Figure 46 hESCs-mediated collagen I gel after 7 days in response to oxytocin (10nM). (A) control sample without oxytocin (B) control sample with oxytocin, (C) strained sample without oxytocin, and (D) strained sample with oxytocin. (E) The graph represented a quantification data of gel area in square pixels. The bars represent the mean \pm standard error of fold changes between strained and control samples ($n=4$) (* $p < 0.05$).

4.4 Discussion

Recently, tissue engineering approaches have been applied in the field of uterine regeneration by many researchers. Although allograft transplantation of the uterus can be performed, immune rejection, side effects induced by immunosuppressive agents, and a lack of donors make this treatment very difficult. Hence, uterus regeneration and the development of tissue engineered uterus using the patient's cells for autograft transplantation is currently more promising. Previous studies have reported that decellularized matrices, which retain the complex structure of native tissues and have extremely low immune rejection rates, can be utilized for various organs including uterus regeneration^{7,82,87,114,115}. Although those studies suggested the possibility of

using scaffolds for uterus regeneration, it still remains difficult to repopulate a decellularized matrix with cells, particularly with smooth muscle cells, which seem to repopulate with a relatively low efficiency compared to stromal or epithelial cells^{7,116}. Consequently, regenerating the smooth muscle cell layer of the uterus remains as an important challenge. On the other hand, mechanical stimuli have been highlighted as a significant factor in the field of tissue engineering. While many researchers have reported on the effects and roles of mechanical stimuli on various cell models, the studies on the uterus in response to mechanical stimuli are still limited. There have been only a few studies reporting the effect of mechanical stimuli on hESCs, particularly focusing on specific genes such as *IGFBP1* or interleukin-8 (*IL-8*) which is associated with inflammation^{67,68}. Hereby, we highlighted the role of mechanical stimuli onto hESC for regenerating the uterine smooth muscle layer.

Mechanical stimulus in this study was applied by using Flexcell system to load the cyclic strain. In the Flexcell system, the cells cultured on the PDMS membrane was pulled down by a vacuum pump, exerting strain force to the cells. In this study, we loaded 15% of uniaxial cyclic strain onto hESCs at 0.1 Hz for up to 7 days. The intensity and frequency of cyclic strain was determined based on the previous studies from harada and bulletti^{67,68}, while the period of cyclic strain was set to 7 days because we predicted to take a long time for hESC to have some changes with regard to differentiation. Most of the parameters used in the experiments were then optimized by myself while only significant data were included in this study.

Finally, we found that applying cyclic strain for 7 days significantly up-regulated the expressions of smooth muscle cell markers (*ACTA2* and *SM22a*), while slightly reducing the expression of endometrial stromal cell makers (*CD10* and *CD90*). The immunostaining results also represented an increase in the expression of SMA in strained samples, consistent with RT-PCR results. The immunostaining results and quantification data for changes of cell angles in the strained hESCs showed that cyclic strain induced the reorientation of the cells in the direction perpendicular to the strain axis.

In order to confirm that the up-regulation of smooth muscle cell indicates the changes into uterine smooth muscle-like cell, we confirmed the significant up-regulation in the mRNA expression of oxytocin receptor after loading cyclic strain for 7 days, which is strongly expressed in the myometrium¹¹⁷⁻¹¹⁹. On the other hand, we also checked that cyclic strain significantly down-regulated a decidualization marker, *IGFBP1*, which convinces that mechanical stimuli did not induce the decidualization of endometrial stromal cells. Then, we focused on its different features to myofibroblast. While there is a lack of desmin accumulated in myofibroblast, the expression of desmin is known to be relatively abundant in myometrium^{120,121}. Application of cyclic strain for 7 days significantly induced the expression of desmin, which also indicates the distinguished features to the myofibroblast. The down-regulation of *IL6* against cyclic strain also supports this because it showed a contrastive result while *IL6* production level is supposed to elevate in the myofibroblast¹²²⁻¹²⁴. On the other hand, an essential marker abundantly expressed in the vascular smooth muscle cells, *ANGPT1*, was reduced by cyclic strain¹²⁵⁻¹²⁸. As well as *ANGPT1*, *RAMP1* mRNA expression specific to vascular smooth muscle cells in uterine arteries was significantly down-regulated by loading cyclic strain, indicating that the smooth muscle like cell induced after loading cyclic strain was distinguished from vascular smooth muscle cells¹²⁹⁻¹³¹.

In this study, cAMP production assay was undertaken after loading strain in hESCs. cAMP is a second messenger produced from adenosine triphosphate (ATP) and is known to regulate endometrial stromal cells for decidualization during the menstrual cycle¹³². There is a report that addition of estradiol in uterine cells evoked increase in cAMP level, and cAMP pathway via adenylyl cyclase is involved in this mechanism¹³³. Moreover, cAMP treatment on bone marrow-derived MSC suggested a potential possibility as a source of endometrial stem/progenitor cells¹³⁴. Thus, cAMP has a significant regulatory role in uterus as well as other hormones such as estrogen and progesterone. Furthermore, cAMP is known to be transiently up-regulated by mechanical stimuli in other cell

models^{135,136}, so that we focused on the involvement of cAMP in response to cyclic strain.

Here we also report that cyclic strain up-regulated cAMP production in hESCs, implying that the cAMP signaling pathway may be involved in the up-regulation of SMC markers under stretch. Applying cyclic strain in as little as 15 mins induced the up-regulation of cAMP production in hESCs. After inducing differentiation of hESCs into smooth muscle cells under cyclic strain for 7 days, we also examined whether cAMP production was responsive to the strained hESCs for 7 days. Since cAMP production is usually transiently induced, cells strained for 7 days were subjected to a 2-hour break (static condition) to stabilize the level of cAMP, followed by 15 mins of cyclic strain to induce cAMP production. This resulted in a significant up-regulation of cAMP production, showing that stretch was able to induce cAMP production both before and after applying cyclic strain for 7 days.

In order to reveal the involvement of cAMP signaling pathway in the stretch-induced differentiation, we carried out inhibitor tests using the adenylyl cyclase inhibitor SQ22536 and the PKA inhibitor H-89, since adenylyl cyclase regulates cAMP production while PKA is known as cAMP-dependent protein kinase^{137,138}. As shown in Fig. 6, neither inhibitor affected *CD10* or *CD90* expression. They, however, exerted a strong inhibiting effect on up-regulations of SMC marker under stretch, suggesting that this phenomenon was directly regulated by adenylyl cyclase and PKA in the cAMP pathway.

As shown in Fig. 44, adenylyl cyclase is an enzyme located on the inner side of the plasma membrane and usually activated by G proteins. Activation of adenylyl cyclase under cyclic strain converts adenosine triphosphate (ATP) to cAMP, an intracellular second messenger. Consequently, cyclic strain induced cAMP production level. As a result of the inhibitor tests, the increase in intracellular cAMP level is shown to be essential for differentiation of hESCs into uterine smooth muscle cells.

The cell contraction assay using collagen gel was undertaken to prove its innate ability of contraction like SMCs. The strained samples for 7 days seemed to show the promoted contractile ability compared to the control samples. The enhanced contractile ability of hESC is known to minimize the defects in the endometrial wound and promote endometrial tissue repair *in vivo* ¹³⁹. Moreover, its contractile ability in the strained samples was significantly strengthened in the presence of oxytocin, indicating that the strained hESCs has a similar property to endometrial SMCs. Since the endometrium is exposed to dynamic condition induced by the myometrium, ESCs together with dynamic condition may contribute to the differentiation of SMCs in the uterus and become a source of SMCs *in vivo*. It further highlights an importance of dynamic condition for ESCs within uterus while ESCs are known to play a significant role in wound contraction for the self-repair of uterus. These results suggested that hESCs have a potential possibility in applications for three-dimensional uterine reconstruction particularly strengthening the myometrium.

In summary, we firstly reported that applying uniaxial cyclic strain significantly up-regulated the expression of smooth muscle cell markers as well as cAMP production. Together, the results show that strained hESCs became uterine smooth muscle-like cells, suggesting they may serve in the future as a possible cell source for regenerating endometrial SMCs. Furthermore, these findings may imply that contractile movements by the myometrium have a significant role in regulating endometrial stromal cell differentiation into uterine smooth muscle cells *in vivo*, though further studies *in vivo* will be needed to clarify this phenomenon. The application of cyclic strain to endometrial stromal cells may therefore be a promising strategy for tissue engineered uterus.

5. Study 2: Reconstruction and evaluation of scaffold-free tissue for partial uterine regeneration in murine model

5.1 Purpose

The uterus refers to a womb that is an essential organ to allow embryo/fetus to grow inside the mother's body. The wall of uterus consists of three layers; epithelial cell layer (inner), endometrial stromal cell layers (middle), and smooth muscle layer (outer). Recently, the rate of uterine disease has been tremendously increased. Endometrial disorders such as Asherman's syndrome is known to cause infertility when malformed endometrium defects become severe by adhesions or fibrosis occurred in the endometrium. Moreover, when those uterine diseases including gynecological cancer become severe, most of the patients are subjected to hysterectomy that refers to a removal of uterus with the defects or malignant tumors. This surgical procedure, however, results in permanent infertility from the patient. Therefore, many researchers have attempted reconstructions of uterus for the patients who are suffered from the defects or loss of the uterus.

Tissue engineering approaches have been widely discussed to regenerate organs in various cell/tissue models. In the tissue engineering, scaffolds are often recruited to support three-dimensional cell growth as well as using biochemical or mechanical factors to promote its regenerating effect^{59,78,140,141}. The scaffolds, however, have complex criteria to encounter its clinical needs and applications according to properties of organs in terms of biodegradability, biocompatibility, porosity, etc¹⁴². While those scaffolds are often made of natural or synthetic polymer, our group first attempted the use of decellularized matrix fabricated by SDS or high hydrostatic pressure for uterine regeneration^{7,116}. Although those scaffolds involving decellularized matrices are known to play a key role in the tissue engineering for various organs, those materials may induce foreign body rejections or prevent any physiological interaction between embryo and uterus

wall when implantation occurs during the pregnancy. On the other hand, the scaffold-free tissues (SFT) including cell sheet engineering have become a new strategy in the field of tissue engineering for the last decade. It exerts such an advantage of using no scaffold or any material that may induce a negative interaction with donor cells.

In this study, we attempted to develop a novel method to reconstruct a thicker engineered tissue constructs using rat endometrial stromal cells (rESCs) particularly for transplantation experiment, compared to the conventional method to fabricate cell sheets using thermo responsive culture dish. Moreover, the aim of this study was to utilize this SFT for partial uterine regeneration and further to reveal the regenerative mechanism in the endometrium.

The SFT was reconstructed by using the rESCs and first evaluated its *in vitro* application with rat embryo for its uterine function. The rESC SFT was transplanted into uterine horns of 9 week-old female Sprague Dawley rat (SD rat) for certain periods. The SFT transplanted was then evaluated by histological analysis and immunohistochemistry assay. In order to transplant the SFT, we also established a new defect model using SD rat for murine model. Although there are few studies reporting on mechanism of uterine regeneration¹¹⁶, those studies use the artificial materials. In this study, since the transplanted SFT only consists of cells, we hypothesized that the unknown native regenerative mechanism can be revealed by introducing this SFT that does not contain any materials.

5.2 Method

5.2.1 Isolation and culture of rESCs

In this study, we dissect and harvest uterine horns from 9 week-old female GFP Sprague Dawley (SD) rat (CLEA Japan). The uterine horns are gently sliced off pieces of the uterine tissues on a culture dish filled up with PBS. After transferring the minced uterine tissues into DMEM/F12 medium containing

collagenase (0.42% w/v; Worthinton) and DNase (0.02% w/v; Roche), it was incubated at 37°C for 30 minutes. The incubated tissues were filtered through a 100µm cell strainer to remove tissue debris as well as glandular parts, followed by centrifuging at 2,150rpm for 5 minutes at 10°C. The supernatant was discarded and resuspended it with DMEM/F12 medium, followed by filtering through a 40µm cell strainer to remove myometrium. Then, they are transferred to a culture dish and incubated for 30 minutes. During this incubation time, the stromal cells were attached onto the dish while the epithelial cells are not capable of attaching. After 30 minutes, the old medium containing the epithelial cells was removed, followed by replacing it with fresh medium. The culture medium is changed every 3 – 4 days and passage cells when reaching 70 – 80 % confluent.

5.2.2 Collecting embryo

We collected rat embryo from female SD rats (CLEA Japan). The female rat was regularly subjected to vagina smear to check their menstrual cycles. When the menstrual cycle of the female rat became proestrus phase, the female rat was mated overnight. Once the mating was confirmed, the female rat was sacrificed 4 days after mating. The uterine horns are isolated from the rat and flushed with PBS inside the horns. The flushed PBS usually contained 6-20 rat embryos. The embryos were cultured with KSOM culture medium (Merck Millipore).

5.2.3 Fabrication of scaffold free tissue (SFT) using rESCs

We utilized rat endometrial stromal cells (rESCs) isolated from GFP SD rats. When the cells became 70 – 80% confluent, we trypsinized them from the culture dish. The cells at 1.0×10^5 cells/ml were transferred into a 5mm cloning ring that is placed on a gas permeable dish, as known as Lumox dish (94.6077.410; SARSTEDT). After the monolayer was tightly formed inside the ring on the lumox dish, we resuspended the rESCs with culture medium at a density of 2.5×10^6 cells/ml into the cloning ring. After 3 hours of incubation, the

cloning ring was gently removed, forming a single layer of SFT in a disc shape. The single layer of SFT was incubated for another 2 days. Then, this process was repeated until stacking up to three layers so that it resulted in the reconstruction of hESC SFT as described in Fig. 47. The rESC SFT was collected by physically scrapping prior to *in vivo* transplantation experiment.

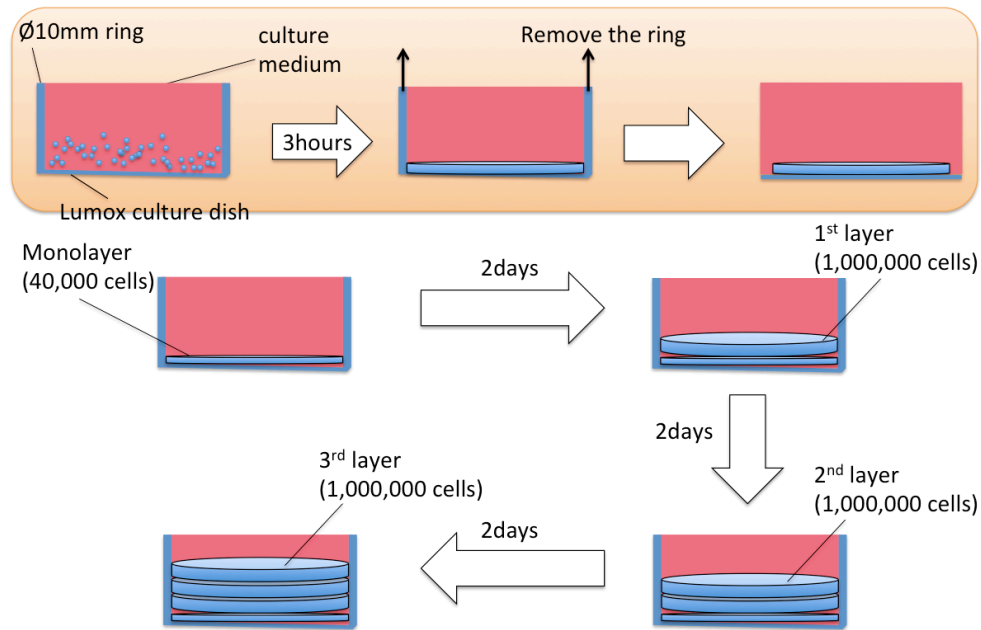


Figure 47 Schematic diagram of scaffold-free tissue constructs

5.2.4 Cocultivation of embryo on SFT

The embryos collected from SD rats were incubated for 1 day in a humidified incubator at 37°C with 5% CO₂. In order to evaluate the development process of embryo in terms of its early implantation, we checked two key events of embryo during early implantation; hatching and attachment. The hatching refers to a removal of outer glycoprotein layer (zona pellucida) in embryo, which is an essential event occurred prior to attachment process on the endometrium. The presence of zona pellucida with the embryo was confirmed at 24 hours for hatching process. After 24 hours of incubating embryos, the embryos were gently flushed with PBS several times. If the embryos were kept in the same position, the embryos were regarded as attached one^{143,144}.

5.2.5 Transplantation of SFT

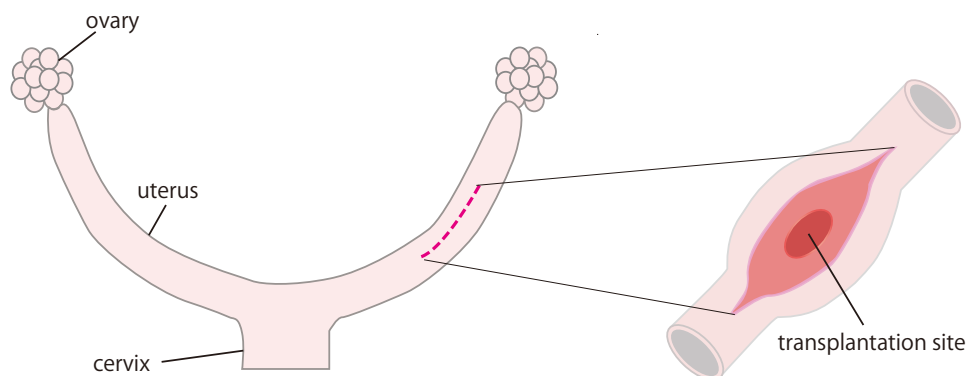
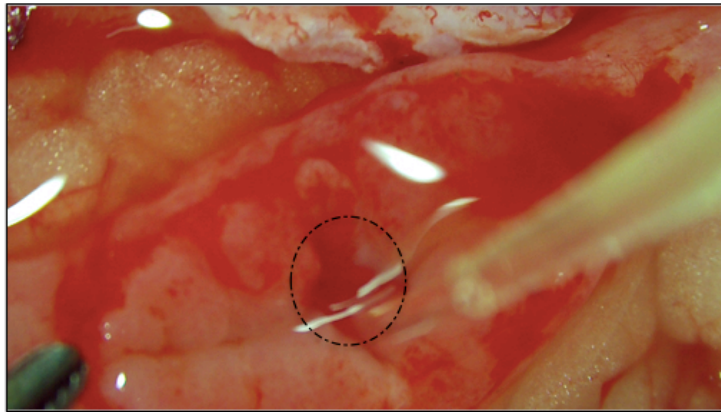


Figure 48 Schematic diagram of rat uterus and transplantation site in the uterine horn.

The rESC SFT reconstructed was then transplanted in a female 9 week-old SD rat. The female rat was anesthetized by isoflurane (503578; Pfizer), and the uterine horn was dissected to access the lumen of uterine horn as shown in Fig 48. In order to prepare for a defect model, the lumen of uterine horn was picked up by pincers, followed by incising endometrium (both endometrial epithelial and stromal layers) above myometrium. The defect model is made as shown in Fig. 49 (A). Fig. 49 (B) showed that the rESC SFT placed at the defected site. Then, the dissected uterine horn with the SFT or defect model was gently sutured and covered with an adhesion barrier seprafilm (Kaken) to prevent adhesion between the scarred uterine horn and any other organs during healing. The period of transplantation varies from 3 days to 2 weeks. After certain times of recovery, the rats were sacrificed, and then its biopsy were isolated and processed for histological assay.

(A) Defect model



(B) SFT transplanted

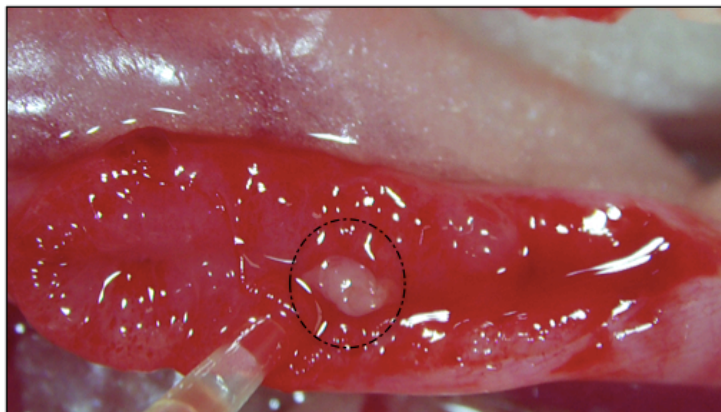


Figure 49 (A) The defect model for partial uterine defects in SD rat (B) Transplantation of SFT in the defect.

5.2.6 Immunostaining

The biopsies were washed by PBS once and fixed in the 10% neutral buffered formalin solution overnight. The fixed samples were then put in 30% sucrose for 2 hours or overnight, followed by O.C.T compound for 2 hours. After O.C.T compounds were embedded entirely inside the tissue samples, the samples were subjected to snap-freezing to make frozen blocks. By utilizing cryostat, the frozen blocks were cut in a thickness of 5 μm for staining.

For the immunostaining, the samples were heated in 10mM sodium citrate at 60°C for 1 hour to retrieve antigens in the fixed samples. In this study, several

primary antibodies were utilized to stain cytokeratin 18 (krt18; Abcam) for epithelial cells, vimentin (vim; Abcam) for stromal cells, smooth muscle alpha actin (α -SMA; Abcam), and ki67 (Abcam) for proliferating cells. After the sample was incubated with primary antibodies in PBST solution with 1% BSA for 1 hour, the secondary antibody (Envision+ System – HRP Labelled Polymer Anti-Rabbit; DAKO) was added and incubated in room temperature for 1 hour. For chromogenic detection of the antibodies, it is treated with 3,3' Diaminobenzidine (DAB) and counterstained by hematoxylin (Mayer's hamatoxylin; Sigma-aldrich).

5.3 Results

5.3.1 Need for a monolayer formed underneath the scaffold-free tissue

The conventional method fabricating the scaffold-free tissue with bovine chondrocytes was not applicable in rESCs. In this study, we first attempted to form a monolayer by seeding rESCs at a cell density of 1.0×10^5 cells/ml in a glass ring with a 5 mm inner diameter. On top of the rESC monolayer, the SFT was formed. Then, we performed a comparative experiment in the presence or absence of this rESCs monolayer formed underneath the scaffold-free tissues in Fig. 50. For the sample without the monolayer, a single layer of rESCs at a cell density of 2.5×10^6 cells/ml was not tightly attached onto the lumox dish immediate after removing the cloning ring (3 hours after seeding the cells inside the ring). As a result, the tissue became fully shrank 24 hours later. On the other hand, the single layer with the monolayer formed underneath attached tightly onto the lumox dish immediate after removing the ring and further retained its shape for next 24 hours without any detachment or shrinkage.

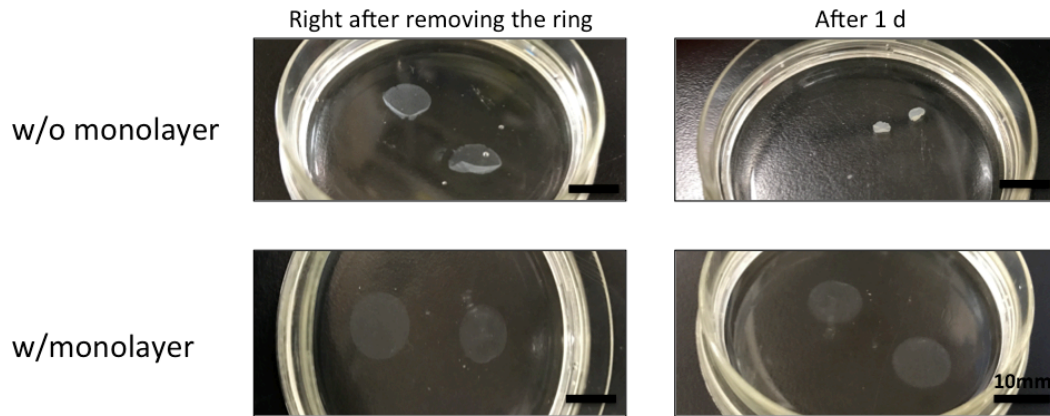


Figure 50 Need of monolayer formed under the scaffold-free tissue

5.3.2 Reconstruction and evaluation of SFT using rESC

The monolayer was incubated for 2 days in a humidified incubator at 37°C with 5% CO₂. After the monolayer was tightly formed inside the ring on the lumox dish, we resuspended the rESCs with culture medium at a density of 2.5×10⁶ cells/ml, and then transferred into the cloning ring at 400µl/ring after aspirating the old medium left. After 3 hours of incubation, the cloning ring was removed gently, and the tissues were further incubated with the culture medium for 2 days. After 2 days, we set a new sterilized cloning ring on top of the single layer, and then stacked another layer by cell suspension at a density of 2.5×10⁶ cells/ml with fresh culture medium in the same way for the first layer. We repeated this process until stacking three layers together, and the scaffold-free tissue with three layers was incubated for 2 days and ready to use for experiments.

The SFT reconstructed by GFP rESCs was examined by staining. Images of hematoxylin and eosin (HE) staining and toluidine blue (TB) staining in Fig. 51 represented that the cells were tightly formed in a disc shape with 100 – 120 µm thickness. Immunostaining images using collagen 1 (Col1) for type I collagen and vimentin (Vim) for stromal cell showed that the type I collagen and stromal cell markers were entirely detected inside and surface of the SFT. We established the method to fabricate the SFT using rat endometrial stromal cells.

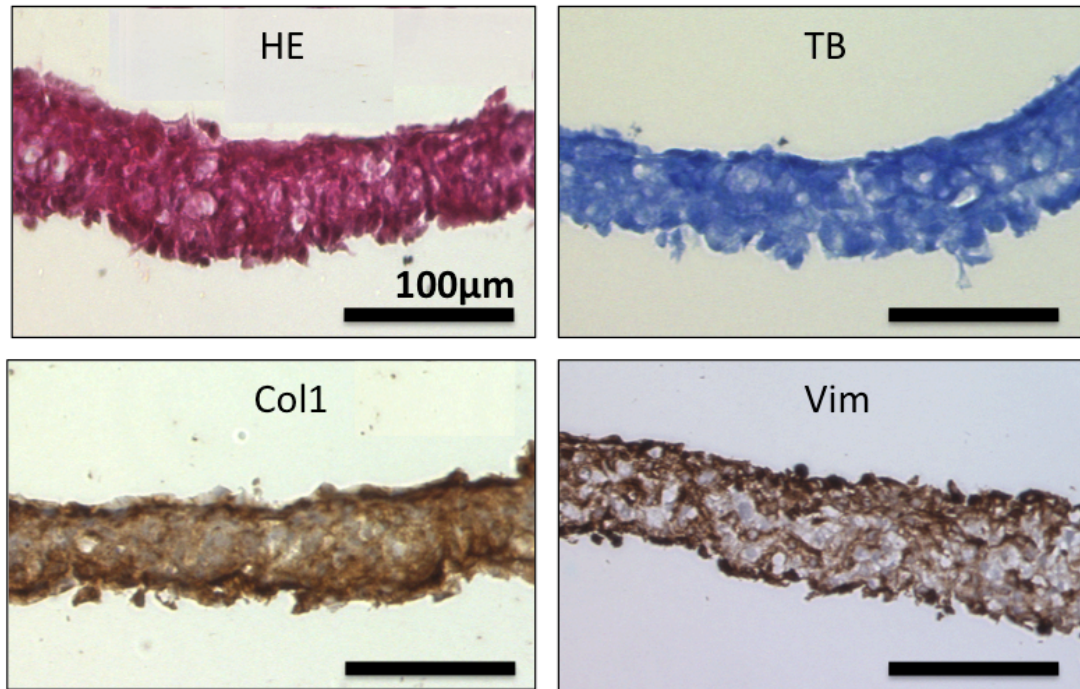


Figure 51 Staining images of rESC SFT

5.3.3 Rat embryo incubation on rESC SFT *in vitro*

In order to evaluate its *in vitro* capability as uterus, we cocultured rat embryos onto the rESC SFT for 1 day and evaluated them with regard to its hatching and attachment on the SFT. Most of rat embryo collected was set to late morula or blastocyst stage in this study. In Fig. 52, the embryos were incubated on lumox culture dish, rESC monolayer, or rESC SFT. After 1 day of incubation, the embryos inside the zona pellucida were died or degenerated in Fig. 53 (A). On the other hand, Fig. 53 (B) represented that most of the embryos cocultured on the SFT were developed and hatched. Table 4 represented the statistical data regarding early implantation of embryo on the SFT after 24 hours of incubation, with 10 replicates. In terms of hatching, only 1 out of 23 embryos (4.3%) occurred on the gas permeable culture dish while culturing embryos on rESC monolayer and rESC SFT exerted hatching at 54% and 68%, respectively. For attachment of rat embryo, there was no attached embryo onto both culture dish (0/23) and monolayer (0/13). On the other hand, the SFT exerted attachment for 5 out of 22 embryos (23%).

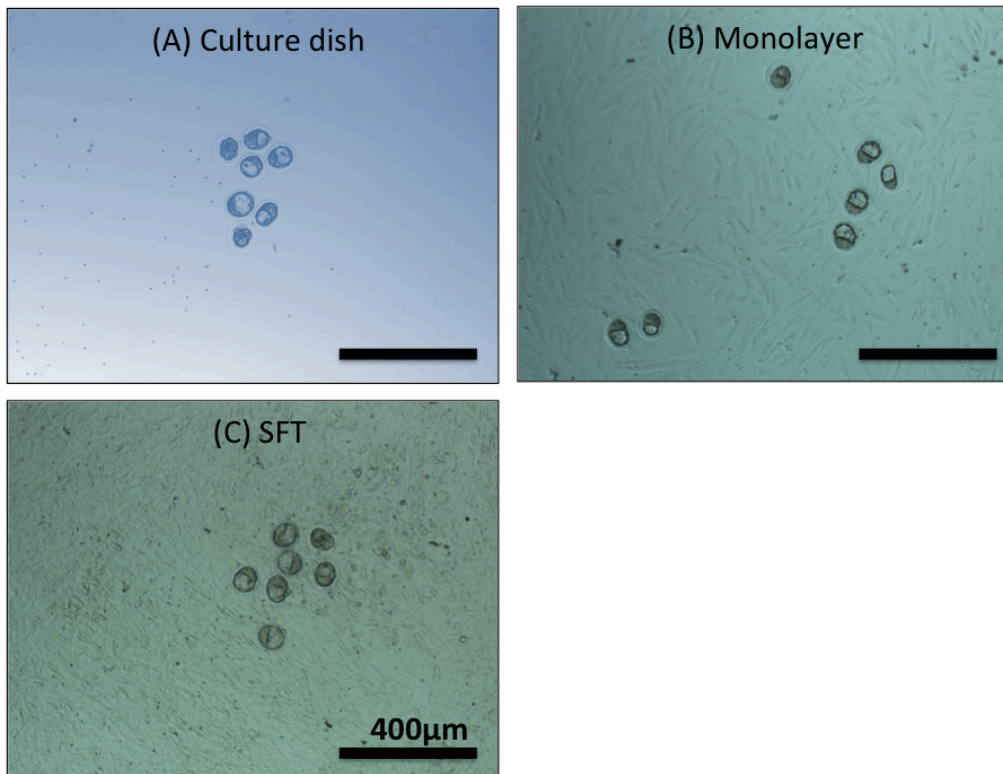


Figure 52 Coculturing rat embryo on (A) gas permeable culture dish, (B) rESC monolayer, or (C) rESC SFT at 0 day (immediate after starting incubation)

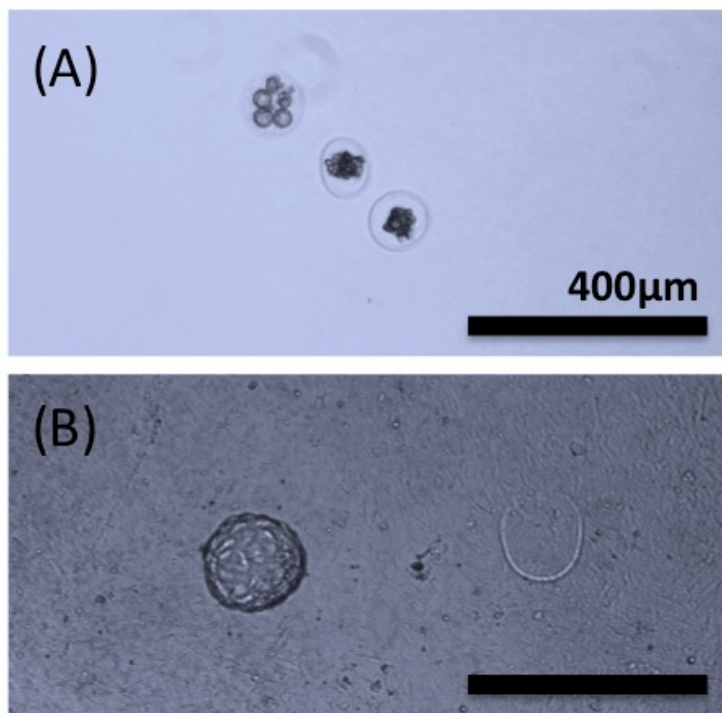


Figure 53 Coculturing rat embryo on (A) gas permeable culture dish or (B) rESC SFT for 1 day

Table 4 Evaluation for incubation of rat embryo on culture dish, rESC monolayer, or rESC SFT for 1 day (10 replicates)

	Hatching	Attachment
Culture dish	1/23 (4.3%)	0/23 (0%)
Monolayer	7/13 (54%)	0/13 (0%)
SFT	15/22 (68%)	5/22 (23%)

5.3.4 Establishing a defect model for partial uterine regeneration

To transplant the rESC SFT into SD rats, we made a defect model that had a partial defect in the inner layer of endometrium including epithelial cell layer and endometrial stromal cell layer above myometrium (smooth muscle layer). By using the medical pincers, the defect was successfully made up to endometrial stromal cell layer in the uterine lumen. We collected the sample immediate after making the defect inside the lumen of rat uterus and carried out immunostaining. As shown in vimentin and smooth muscle actin staining results in Fig. 54, the defect was successfully made right above the myometrium. The endometrial epithelial and stromal layers were removed by pincers as targeted.

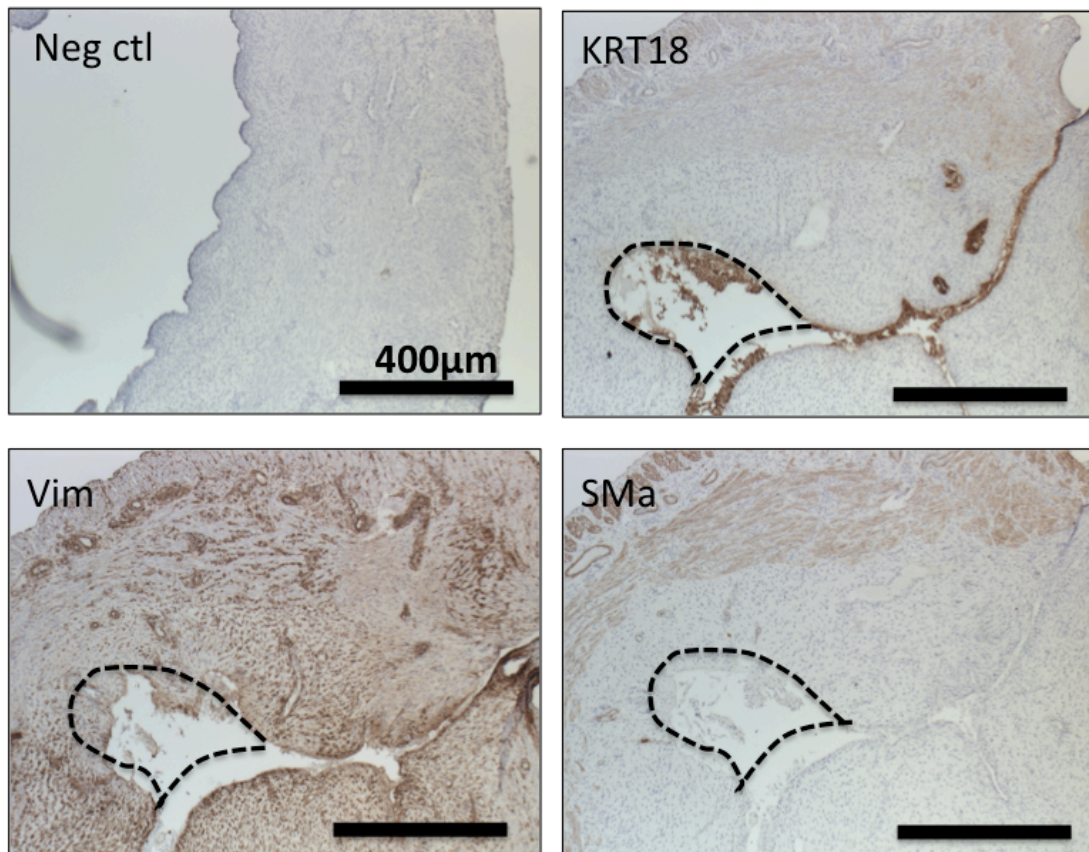


Figure 54 Defect model for partial uterine regeneration immediate after making the defect inside rat uterine lumen. Each image is a representative from at least 2 independent experiments

After the defect model was made, the dissected uterine horn was sutured without transplanting any artificial materials or SFT. The rat was allowed to recover for 3 days and sacrificed for histological assay. In Fig. 55, the uterine horns had swelling as well as inflammation due to the defects made 3 days ago. The immunostaining results in Fig. 56 showed that the defect still remained after 3 days of recovery. Although the epithelial cell layer seemed to start covering the defect parts in the lumen of uterus, the defects was still remained missing up to right above smooth muscle layer in the uterus.



Figure 55 Rat uterine horns 3 days after making defects inside the lumen of uterus

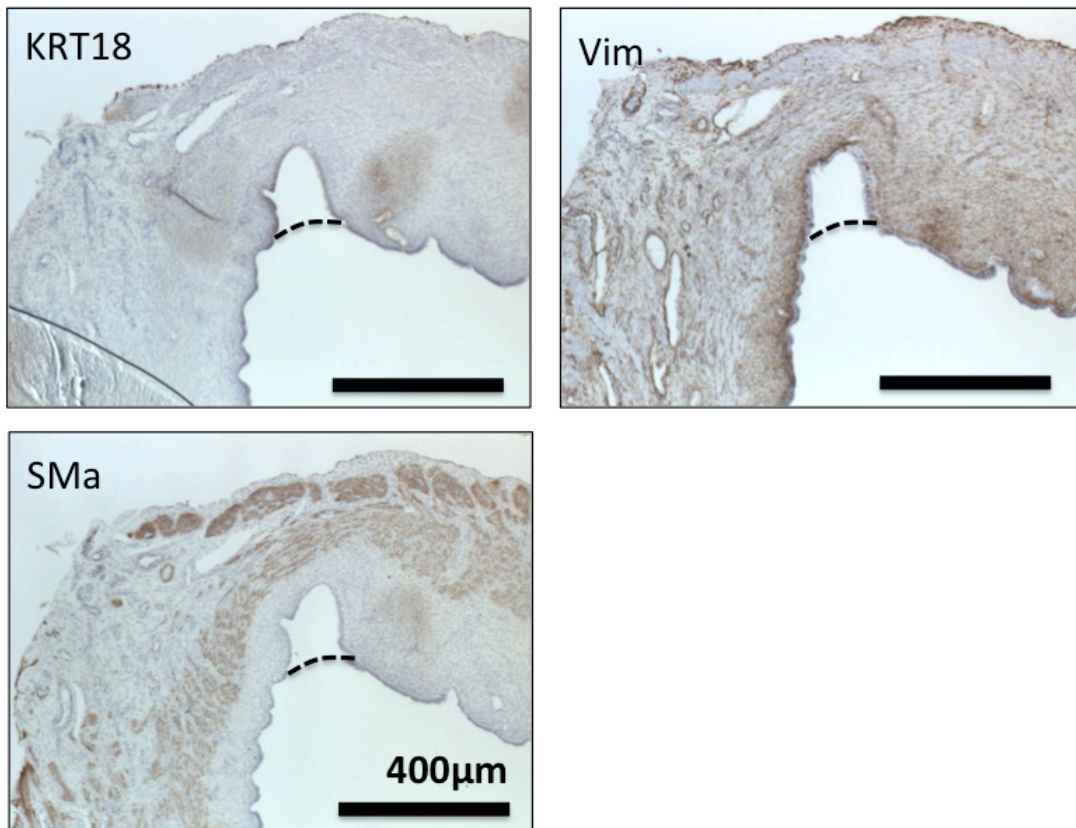


Figure 56 Staining images of defect model for partial uterine regeneration 3 days after making the defect inside rat uterine lumen. Each image is a representative from at least 2 independent experiments.

5.3.5 Transplantation of rESC SFT into the defect model

We transplanted the SFT reconstructed by rESC at the site where the defect was made. The transplanted rat was then recovered for 24 hours (1 day). The rat was sacrificed by excessive dosage of isoflurane and the uterine horns were collected in Fig. 57. The uterine horns after 1 day of transplantation were swollen and still remained a severe scar with bloods at the sutured place. The GFP image in Fig. 58 allowed to confirm that the SFT is placed inside the uterine horn.

Immunostaining for Cytokeratin 18 (KRT18), epithelial cell marker, represented that the epithelial cells from the donor tissue started to cover the SFT in as little as 1 day. The stromal cell marker of vimentin was strongly expressed in the SFT, compared to the native tissue. The proliferation marker, Ki67, was also entirely detected inside the SFT as well as the native tissue. Although all the staining results showed that the SFT was not completely integrated into the native tissue, it was partially attached to the native tissue.

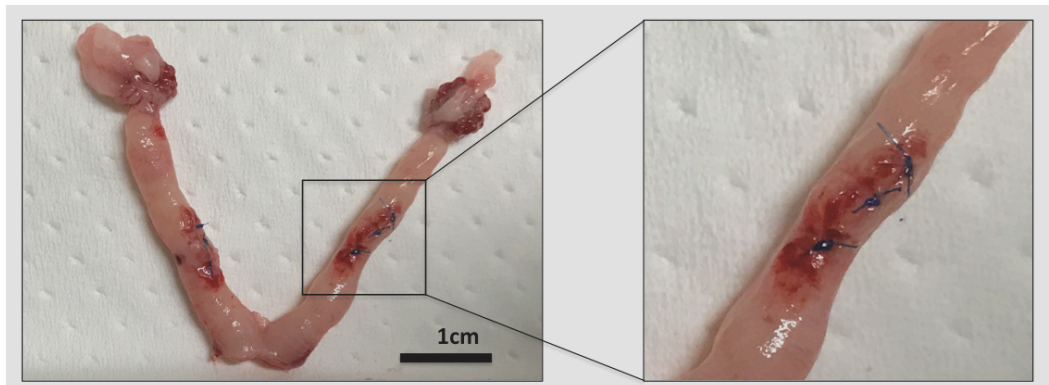


Figure 57 Rat uterine horns 1 day after transplanting rESC SFT

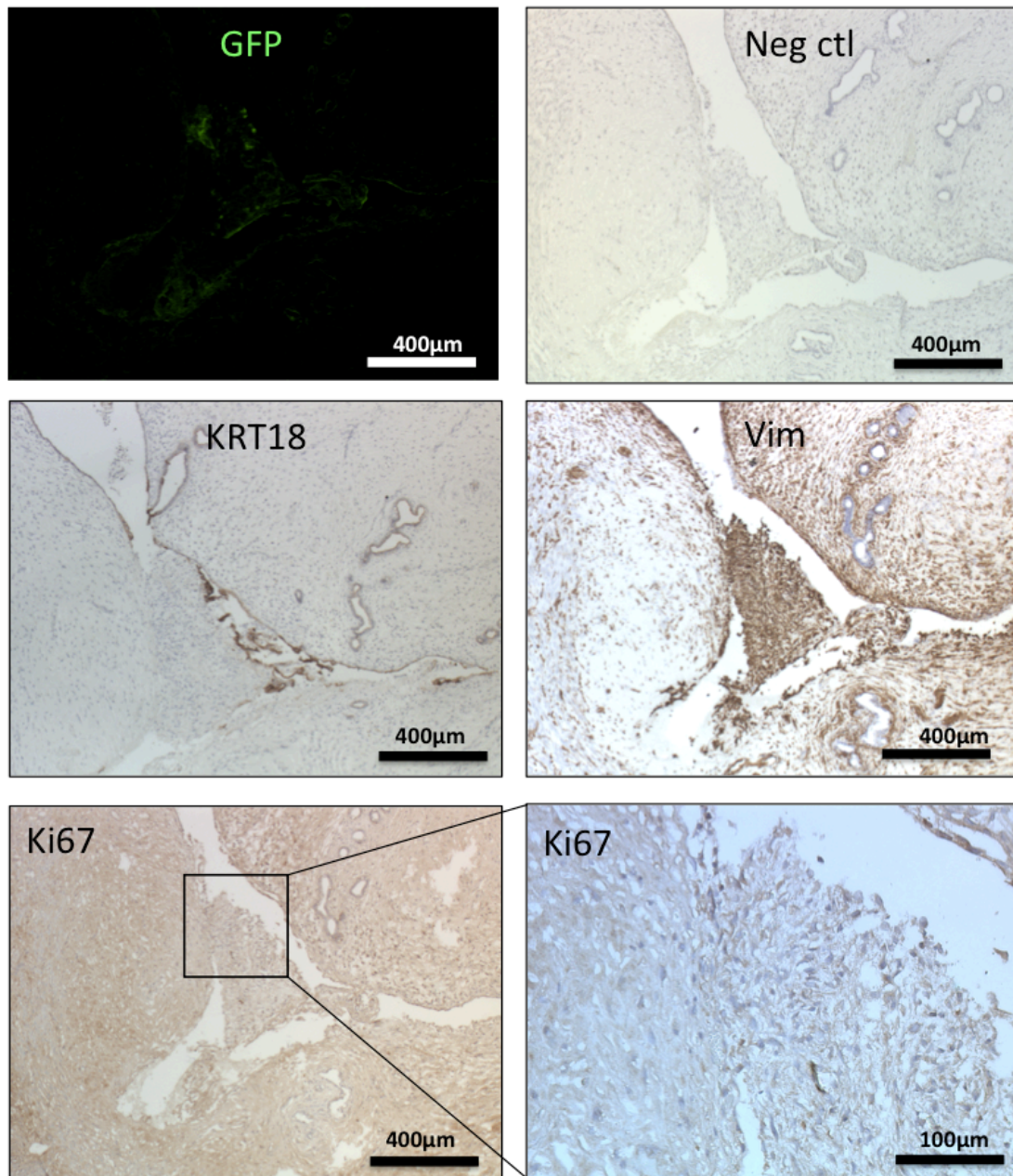


Figure 58 Staining images of uterus 1 day after transplanting rESC SFT into SD rat. Each image is a representative from at least 2 independent experiments

Then, we carried out 3 days of transplantation experiment. After 3 days of recovery transplanting the SFT, the uterine horns were collected in Fig 59. As well as 1 day of transplantation, the uterine horns had swelling. The scar sutured seemed to remain, but the blood was less compared to the 1 day transplantation model. In Fig. 60, the GFP image clearly indicated the SFT embedded inside the native tissue. The immunostaining image for KRT18 showed that the epithelial cells were completely covered the SFT. The stromal cell marker (Vim) detected

strongly corresponded to the location where a bright GFP was detected. Similarly, the SFT after 3 days of transplantation showed a relatively greater intensity of proliferation marker (Ki67) inside the SFT than the native tissue. We can observed that the SFT was successfully placed inside and combined to the native tissue after 3 days.

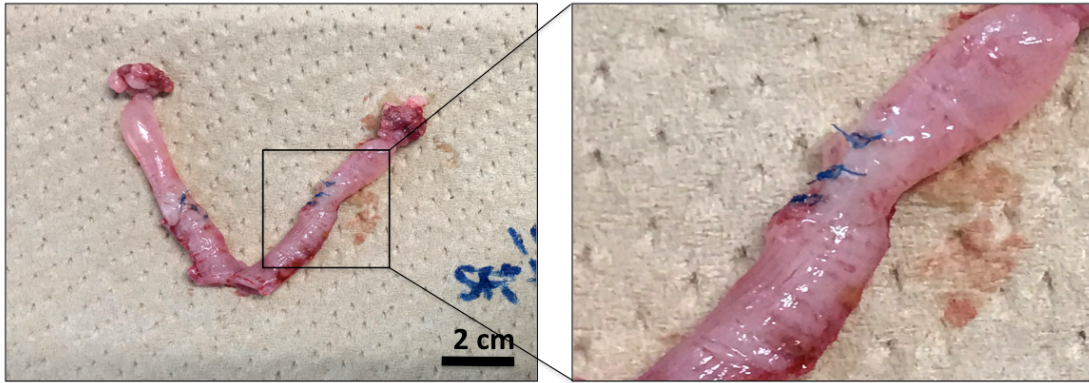


Figure 59 Rat uterine horns 3 days after transplanting rESC SFT

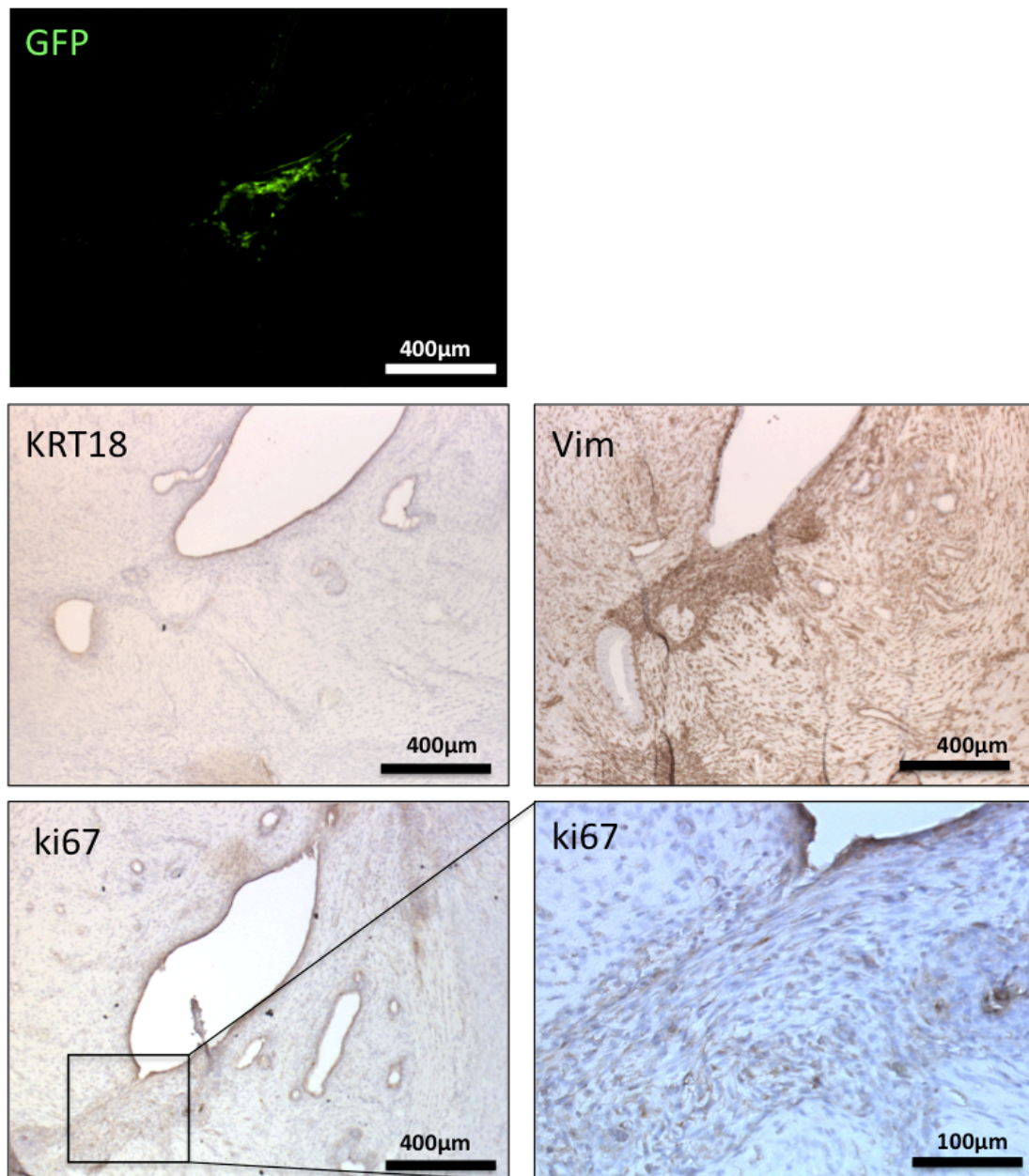


Figure 60 Staining images of uterus 3 days after transplanting rESC SFT into SD rat. Each image is a representative from at least 3 independent experiments

The appearance of uterine horns after 1 week of transplantation was similar to that of 1 or 3 days transplantation. The uterine horns still had a swelling, but the scar sutured seemed to recover. In Fig 62, the GFP was detected inside the uterus while the stromal cell marker was also strongly expressed at the same location, indicating the SFT was successfully transplanted. KRT18 was expressed around the lumen of uterus including where the SFT was placed. The proliferation

marker was also detected inside the SFT and around the border where vimentin or GFP was expressed.

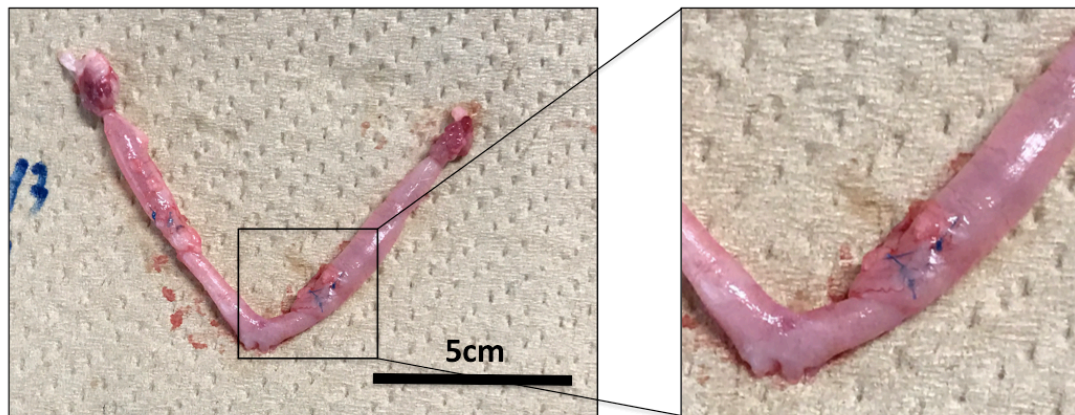


Figure 61 Rat uterine horns 7 days after transplanting rESC SFT

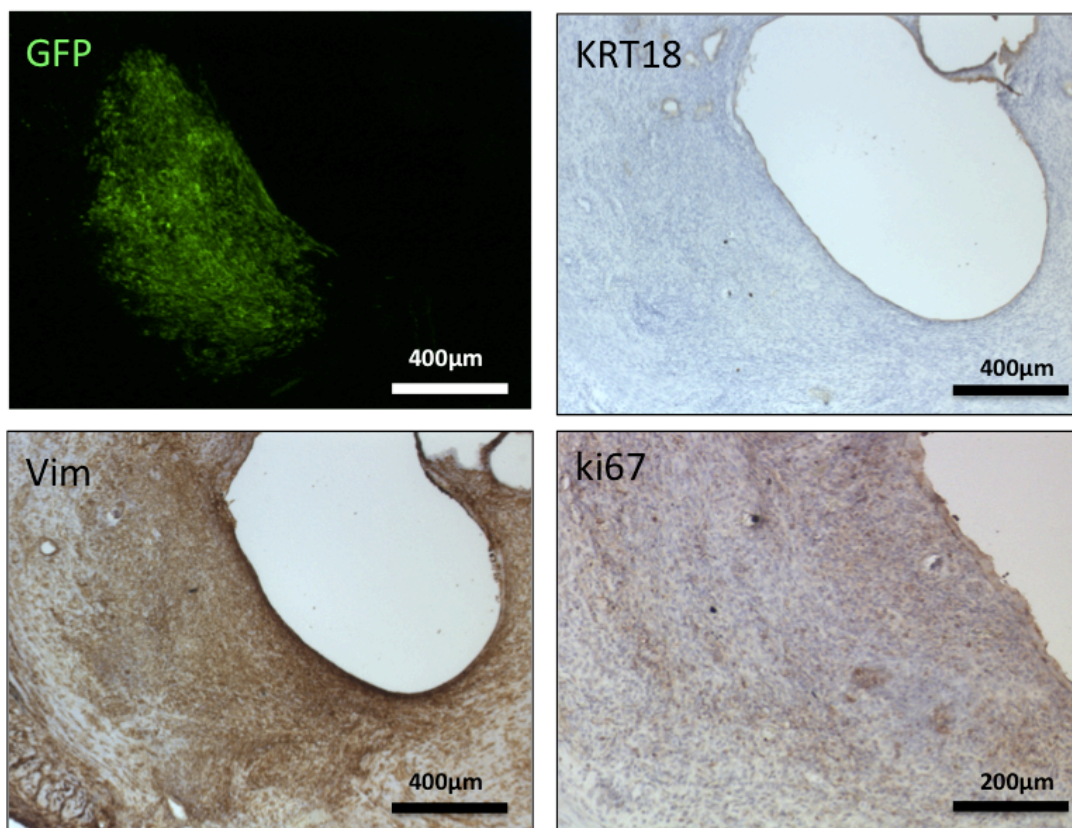


Figure 62 Staining images of uterus 7 days after transplanting rESC SFT into SD rat. Each image is a representative from at least 2 independent experiments

For the 14 days of recovery after transplanting the SFT, Fig. 63 represented that the uterine horns did not have any swelling. The sutured scar was completely

recovered. The appearance of transplanted uterus was similar to that of native rat uterus. From the results of staining image in Fig 64, the expression of GFP was widely spread around the stromal layer of uterus. The epithelial cell and stromal cell markers were expressed at the location where GFP detected in the endometrium.

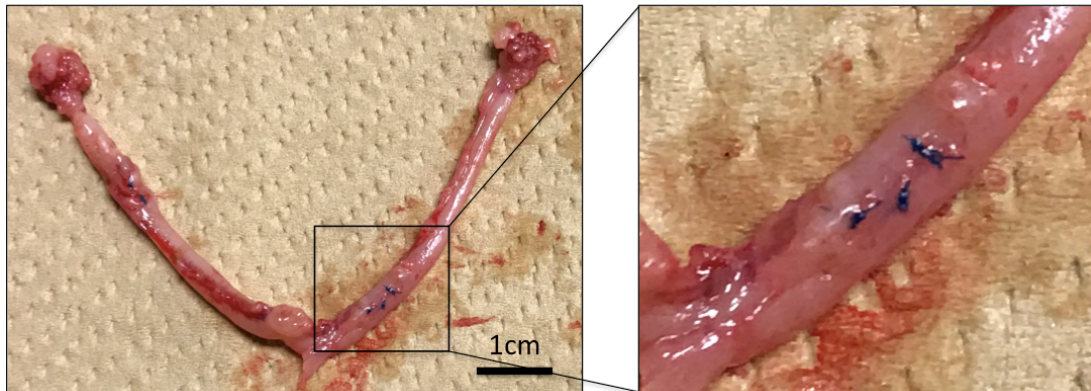


Figure 63 Rat uterine horns 14 days after transplanting rESC SFT

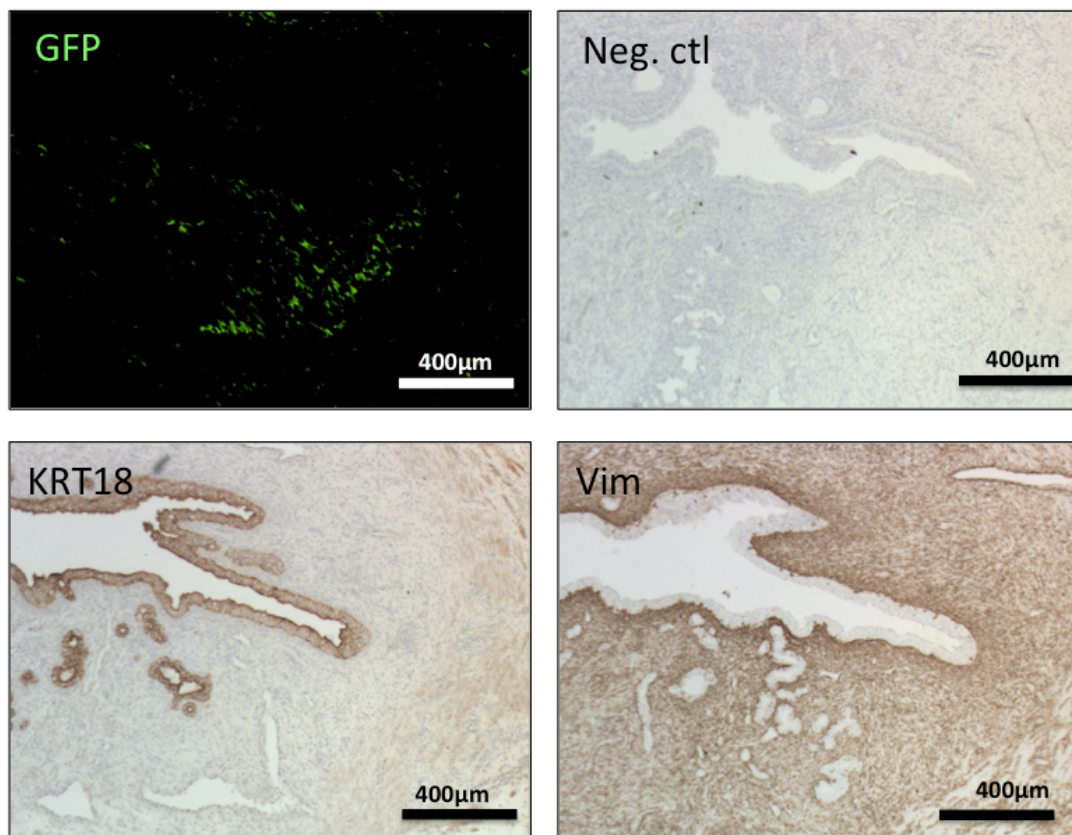


Figure 64 Staining images of uterus 14 days after transplanting rESC SFT into SD rat. Each image is a representative from at least 2 independent experiments

5.4 Discussion

For regenerative medicine, the tissue engineering approaches have been widely applied in various cell or tissue models for several decades. While diverse methods have been developed and attempted for the regenerative medicine, studies on uterine tissue engineering are relatively limited as contrasted to other organs. As the number of severe uterine diseases increases, the only available treatment for most of the cases is the hysterectomy that causes the permanent infertility. Therefore, the uterine regeneration by tissue engineering approaches has been demanded.

In order to accomplish uterine regeneration for the patients who are suffering from partial or total defects of uterus, we have developed our novel method to reconstruct the scaffold-free tissue (SFT) using endometrial stromal cells. To fabricate the thicker tissue engineering constructs, we utilized the monolayer formed by ESC, which was embedded underneath the tissue to hold it and prevent from shrinkage immediate and about 1 day after removing the cloning ring. By using this method, we successfully reconstructed the scaffold-free tissue (SFT) with about 100 – 120 μm of thickness, which was greater than that of the conventional cell sheet model (about 25 μm)¹⁴⁵. From the results of staining, it was tightly formed by cells with type I collagen and vimentin positive.

Our novel method using the combination of the monolayer fabricated underneath the SFT did not recruit a thermo-responsive culture dish while typical cell sheet engineered constructs requires it. Moreover, the SFT reconstructed exerts enough mechanical properties to be applicable for *in vivo* model since it can be detached physically by scraping from the culture dish. This simple cost-friendly method can be applicable for other cell types that have a strong cell-cell interaction force.

The rESC SFT was first evaluated *in vitro* by introducing rat embryo collected from SD rat. In order to check the uterine function of rESC SFT particularly in early implantation, we cocultured rat embryo either on the normal culture dish, rESC monolayer, or rESC SFT. With regard to hatching and attachment ratio of embryo, the SFT provided a superior environment for embryo to induce hatching which is an necessary step for implantation of the embryo in the uterus. Moreover, the attachment of the embryo was occurred only on the SFT after 1 day of incubation. It implies the potential usage of SFT for *in vitro* application to incubate embryo in a health condition and also to mimic the situation when the embryo attaches onto the endometrium *in vivo*. The further study for the SFT as *in vitro* model needs to be carried out.

In addition to the *in vitro* evaluation, we performed the *in vivo* study by transplanting this rESC SFT into SD rats. To evaluate the SFT *in vivo*, we first established a defect model by removing the endometrium partially. In the defect model, it remained loss of the endometrium even after 3 days of recovery time as much as the initial defect made. On the other hand, the recruitment of the SFT made the defect recover immediately by covering the defect and integrating into the native tissue. Hence, the SFT played a role to regenerate immediately compared to the natural healing, reducing the further risk to induce uterine disease such as Asherman syndrome. Asherman syndrome refers to the attachment and/or development of fibrosis from the defects in uterine lumen. When this syndrome becomes severe, it results in permanent infertility. In order to prevent such a syndrome, the SFT can be used to cover the defect in the uterine lumen, further promoting the partial uterine regeneration.

By using time-dependent transplantation experiment, we also figured out the mechanism of the uterine regeneration using the rESC SFT. By transplanting the SFT for 1 day, we observed that the native epithelial cells started to cover the SFT. However, the SFT was not settled down and partially attached to the native tissue. After the epithelial cells covered the SFT, the integration of the SFT into the native tissue was occurred in as little as 3 days of recovery. By recovering for 1 week, the SFT was completely combined to the native tissue, so that the

endometrial stromal cells consisting of SFT began to spread around the tissue as confirmed by immunostaining for Vimentin and Ki67. As a result of GFP image for the 2 weeks transplantation, the SFT had been widely spread around the endometrium in the native tissue, so that the initial appearance of SFT, a huge aggregation of vimentin, was not observed. The endometrium, however, formed a nice and natural morphology of uterus without any swelling or inflammation shown.

Although the SFT was successfully combined to the native uterus tissues in SD rat without any inflammation after 2 weeks of transplantation, the transplanted uterus needs to be examined functionally. After a certain time of transplanting the SFT, the pregnancy test by mating will be required to confirm that the transplanted uterus is capable of pregnancy. Despite the fact that there still remains some issues to be confirmed by additional experiments in the future, the SFT successfully suggested its potential possibility *in vivo* for the partial uterine regeneration.

6. Study 3: Novel *in vitro* application of scaffold-free tissue using human endometrial stromal cells for early implantation of embryo

6.1 Purpose

We developed the engineered tissue construct, named as scaffold-free tissue (SFT), by using a novel method as discussed in the previous study. The SFT with rat endometrial stromal cells was successfully fabricated and exerted its uterine function *in vitro* that enables to coculture rat embryo by providing a superior condition in terms of its hatching and attachment. Since the uterus has a unique and significant role to pregnant, any artificial materials have a potential risk to disturb any biochemical or physiological interaction between the uterus (mother) and embryo (baby) during implantation or development of the embryo, so that the use of SFT has a great advantage in the uterus studies *in vitro* and *in vivo*.

By using the SFT, many studies have been conducted to regenerate various organs such as heart, cornea, cartilage, skeletal muscle, esophagus, etc^{64,146-149}. While only limited reports on the SFT using rat endometrial cells are available for uterine tissue engineering, there are no reports on reconstruction of the SFT using human endometrial stromal cells (hESCs) that is the major components of the human endometrium. One of the most difficulties to fabricate the SFT with hESC is its strong cell-cell interaction force in hESCs, making it difficult to retain in three-dimensional disc shape as demanded. By conducting the reconstruction of SFT with hESC, it enables to lead to the clinical studies.

In this study, we developed a novel method to fabricate a scaffold-free tissue with hESCs. After reconstructing the hESCs SFT, we conducted the histological, immunohistochemical, and genetic assay. Moreover, we evaluated its function as uterus *in vitro* by incubating rat embryos on the hESC SFT. By using this model,

we also conducted a detailed study in the novel application of hESC SFT to facilitate the growth of embryo *in vitro*.

6.2 Materials and Methods

6.2.1 Isolation and culture of hESCs

Fresh human endometrial stromal cells (hESCs) were isolated and cultured from uterine biopsies as reported previously³³⁻³⁵. All the biopsies were obtained from 38 – 48-year-old female patients with regular menstrual cycles. The hESCs were cultured in DMEM/Ham's F12 (Sigma) consisting of 2.5% charcoal-stripped fetal bovine serum (Funakoshi) and 1% of Antibiotic-Antimycotic (GIBCO) in a humidified incubator at 37°C with 5% CO₂. We changed cell culture medium every 3 – 4 days and carried out passage when the cells become 80 – 90% confluent.

6.2.2 Scaffold-free tissue constructs

The hESC were subcultured and resuspended with DMEM/Ham's F12 medium consisting of 2.5% charcoal-stripped fetal bovine serum (Funakoshi) and 1% of Antibiotic-Antimycotic (GIBCO), at a density of 1.0×10^5 cells/ml. In order to form a monolayer, the cell suspension was transferred into glass cloning rings (Asahi glass) with a 10 mm inner diameter at 400 μ l/ring, placed on a gas permeable lumox dish (Sarstedt). The monolayer was incubated for 2 days in a humidified incubator at 37°C with 5% CO₂. After the monolayer was tightly formed inside the ring on the lumox dish, we resuspended the hESCs with culture medium containing Y27632 (10 μ M) at a density of 2.5×10^6 cells/ml, and then transferred into the cloning ring at 400 μ l/ring after aspirating the old medium left. After 3 hours of incubation, the cloning ring was removed gently, and the tissues were further incubated with the culture medium containing Y27632 for 2 days. After 2 days, we set a new sterilized cloning ring on top of the single layer, and then stacked another layer by cell suspension at a density of 2.5×10^6 cells/ml with fresh culture medium containing Y27632 in the same way for the first layer. We

repeated this process until stacking three layers together, and the scaffold-free tissue with three layers was incubated for 2 days and ready to use for experiments.

6.2.3 Actin staining

The hESCs were washed with PBS once, and fixed with 4% paraformaldehyde for 15 minutes. The fixed sample were washed with PBS again and permeabilized by 0.2% Triton-X for 3 minutes. After washing with PBS, 100 nM Actin-stain™ 555 phalloidin (Cytoskeleton, Inc.) was added and incubated for 30 minutes at room temperature in the dark condition. Lastly, the sample was counterstained with DAPI for 5 minutes and covered with mount media (VectorShield) on a slide glass for visualization and storage.

6.2.4 Histological analysis

The SFT with hESCs was collected and washed with PBS once. Then, the SFT was transferred into the 10 % neutral buffer formalin (Wako) for fixation. In this study, all the samples were embedded in O.C.T compound (Sakura Tissue TEK) and stored as the frozen block. The samples were then sectioned at a 5µm thickness and stained with hematoxylin and eosin (HE staining).

6.2.5 Immunohistochemical staining

For immunohistochemical staining, the sections was firstly heated with 10mM citrate buffer at 60 – 80 °C for 60 minutes. After treated with 3% hydrogen peroxide (Wako) in methoanol (Wako) for 10 minutes, the non-specific bindings were blocked with blocking solution (Dako) for 1 hour at room temperature inside a humidifying chamber. Then, the samples were covered with anti-collagen I antibody (Abcam) and anti-vimentin antibody (Abcam) at the dilution of 1/500 for 1 hour at room temperature or overnight at 4°C. After washing the

primary antibody with 0.1% TBST, the secondary antibody (Dako) was added to reveal the antibodies for 1 hour at room temperature, followed by DAB peroxidase substrate kit (Nichirei) for visualization. Then, the sample was finally stained with hematoxylin (Sigma).

6.2.6 rt-PCR

Reverse transcription PCR (rt-PCR) was performed to investigate any changes in gene expression in the hESCs. After completing the experiment, the cells were immediately dissolved in 1 ml of Trizol reagent (Invitrogen). The RNA in the sample was extracted by adding 0.2 ml of Chloroform into the sample and then centrifuged at 12,000 g for 15 minutes. After separating the aqueous phase with RNA, 0.5 ml of isopropanol was added and incubated for 10 minutes, and then centrifuged for 10 minutes at 12,000 g again. The precipitates were subjected to cDNA synthesis by using the ReverTra Ace qPCR RT Master Mix with gDNA Remover (Toyobo). All the human primers sequences were designed and ordered from Integrated DNA Technologies (IDT) as shown in Table. 5.

As an endometrial stromal cell marker, we utilized *CD10* and *CD90*. The uterine hormone receptors, estrogen receptor (*ER*) and progesterone receptor (*PR*), were investigated to check any changes in the level of gene expressions. We also utilized homeobox A10 (*HOXA10*), heparin-binding EGF-like growth factor (*HBEGF*), and integrin subunit beta 3 (*ITGB3*) that are known to play a significant role with regard to implantation of embryo. Insulin like growth factor binding protein 5 (*IGFBP5*) was also examined as a decidualization marker in the hESCs. The gene expression of cyclooxygenase (*COX2*), also referred as prostaglandin-endoperoxide synthase (*PTGS*), was also checked since it is expressed in the endometrium where the blastocyst attaches. To confirm the involvement of *LIF-STAT3* pathway during blastocyst attachment on the SFT in this study, the gene expressions changes in leukemia inhibitory factor (*LIF*) and signal transducer and activator of transcription 3 (*STAT3*) were examined. All genes were normalized to Ribosomal protein L32 (*RPL32*) expression and further normalized to the control samples.

Table 5 Primer List

Gene	Forward primer	Reverse primer	Amplicon size (bp)
<i>RPL32</i>	GCCCAAGATCGTCAAAAAGA	GTCAATGCCTCTGGGTTT	98
<i>CD10</i>	TCCACTGGAGATCAGCCTTT	TATCGGGAAGTGGTCTCAGG	237
<i>CD90</i>	CTAGTGGACCAGAGCCTTCG	TGGAGTGCACACGTGTAGGT	235
<i>ER</i>	TGGAGATCTTCGACATGCTG	TCCAGAGACTTCAGGGTGCT	145
<i>PR</i>	GTCAGTGGGCAGATGCTGTA	AGCCCTTCCAAAGGAATTGT	194
<i>HOXA10</i>	CCTTCCGAGAGCAGCAA	CCTTCTCCAGCTCCAGTGTC	145
<i>HBEGF</i>	TGGGGCTTCTCATGTTTAGG	CCCCTCTGCAGTCTGAAATC	179
<i>ITGB3</i>	ATGGGGACACCTGTGAGAAG	AACGGTTGCAGGTATTTTCG	120
<i>IGFBP5</i>	TGCACCTGAGATGAGACAGG	GAATCCTTTGCGGTCACAAT	136
<i>IGFBP1</i>	CTGCCAAACTGCAACAAGAA	TATCTGGCAGTTGGGGTCTC	153
<i>COX2</i>	CCGGACAGGATTCTATGGAG	GTGCACTGTGTTTGGAGTGG	91
<i>LIF</i>	GAACCAGATCAGGAGCCAAC	GTCCAGGTTGTTGGGGAAC	103
<i>STAT3</i>	GACCAGGCAGAAGATGCAG	CCTCGTCCGTGAGAGTTTTC	131

6.2.7 Collecting embryo

We utilized 9 weeks old female Sprague Dawley rats (CLEA Japan). The number of rats sacrificed for collecting embryo was 10 in this study. Ad libitum access was allowed for the rats to have food and water. The rats were also caged in an environmentally controlled room with alternating 12 h light/dark cycles. The estrous cycle of the rats were regularly checked by vaginal smear, and mating was carried out with a male Sprague Dawley rat (CLEA Japan). At 5 days after mating, the female rat was sacrificed by using an overdose of isoflurane (Pfizer). Two uterine horns were harvested from the rat and subjected to PBS flushing through a cavity of the uterine horn on a culture dish. 6 – 18 embryos were collected from a rat.

6.2.8 Embryos coculturing on SFT

Embryos were cocultured on culture dish, monolayer or SFT with KSOM medium (Merck Millipore) (10 replicates). After 24 hours of incubation in a humidified incubator at 37°C with 5% CO₂, the embryos were observed if development, hatching, and attachment occurs. The development of the embryo was evaluated and recorded

by change in embryo stage (fertilized egg, 2-cell stage, 4-cell stage, 8-cell stage, 16-cell stage, morula, or blastocyst) and its size change. The hatching was confirmed by existence of zona pellucida in the embryo as previous study. After 24 hours of incubation, the embryos were subjected to flushing with PBS for several times and considered as attached one if the embryo remained at the same position.

6.2.9 Applying cyclic strain on the SFT

In this study, we loaded cyclic strain using the Flexcell tension system (FX-4000™; Flexcell International Corporation) placed in a humidified incubator at 37°C with 5% CO₂. The hESC SFT or monolayer was reconstructed on the Flexcell plate. 15% of cyclic strain at 0.1 Hz was applied for 24 hours in this study. For control samples, hESCs were cultured in identical Flexcell plates but without strain.

6.2.10 Statistical analysis

The bars in the rt-PCR graphs represent the means \pm standard error of the mean. A student's t-test and ANOVA test were performed to evaluate its statistical significance. P-values of 0.05 or less were assumed significant.

6.3 Results

6.3.1 Utilization of Y27632 to fabricate the scaffold-free tissue

When making a single layer of SFT using hESCs, we observed partial shrinkages of the tissue after 1 – 2 days due to its strong cell-cell interaction force in hESCs. In order to prevent the shrinkages, we introduced a Rho-associated protein kinase (ROCK) inhibitor, Y27632. The 10 μ M of Y27632 was added into the culture medium while reconstructing the singly layer of hESCs. By addition of Y27632, it prevented the partial shrinkages and retained its shape for 2 days or longer without any changes.

We also carried out the actin immunofluorescence staining to observe changes in actin cytoskeleton inside the hESCs after treating with Y27632. While the hESCs in the absence of Y27632 exerted tightly packed bundle of actin filaments (red) in Fig. 65, the sample under the treatment of Y27632 had relatively less packed actin filaments where the similar numbers of DAPI (blue), nucleus, were observed in both samples. Hence, the results implied that addition of Y27632 reduced the actin filaments in hESCs.

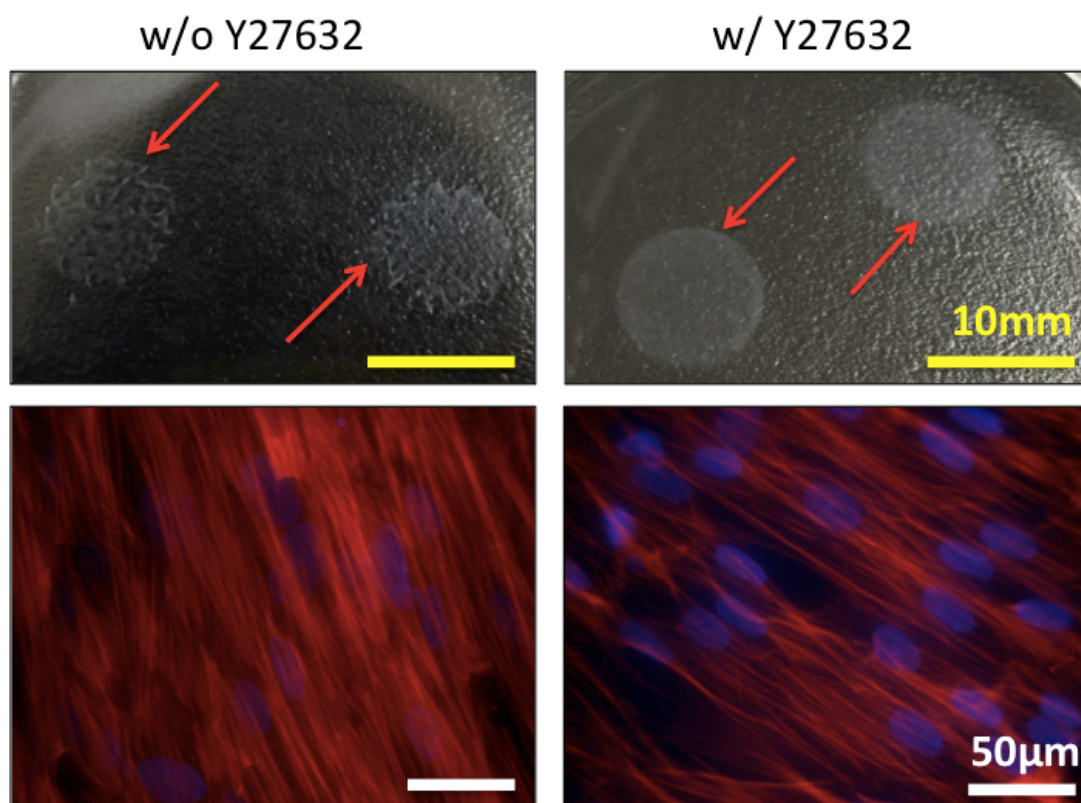


Figure 65 Significant role of Y27632 during fabrication of the scaffold-free tissue

6.3.2 Gene expression changes in hESCs after treating with Y27632

To check any negative effect by addition of Y27632 into the hESCs, we assessed rt-PCR after treating Y27632 to the hESCs for 7 days (n=4). Fig. 66 showed that the relative mRNA expressions of endometrial stromal cell markers, *CD10* and *CD90*, were 1.20-fold change (p=0.46) and 1.46-fold change (p=0.22), respectively. We also evaluated important uterine hormone receptors, *ER* (1.66-

fold change; $p=0.22$) and *PR* (1.18-fold change; $p=0.27$). The relative mRNA expressions of *HOXA10*, *HBEGF*, and *ITGB3* were 1.49-fold change ($p=0.26$), 0.80-fold change ($p=0.16$), and 1.32-fold change ($p=0.24$). The relative mRNA expression of decidualization marker, *ITGFB5*, was 0.85-fold change ($p=0.25$).

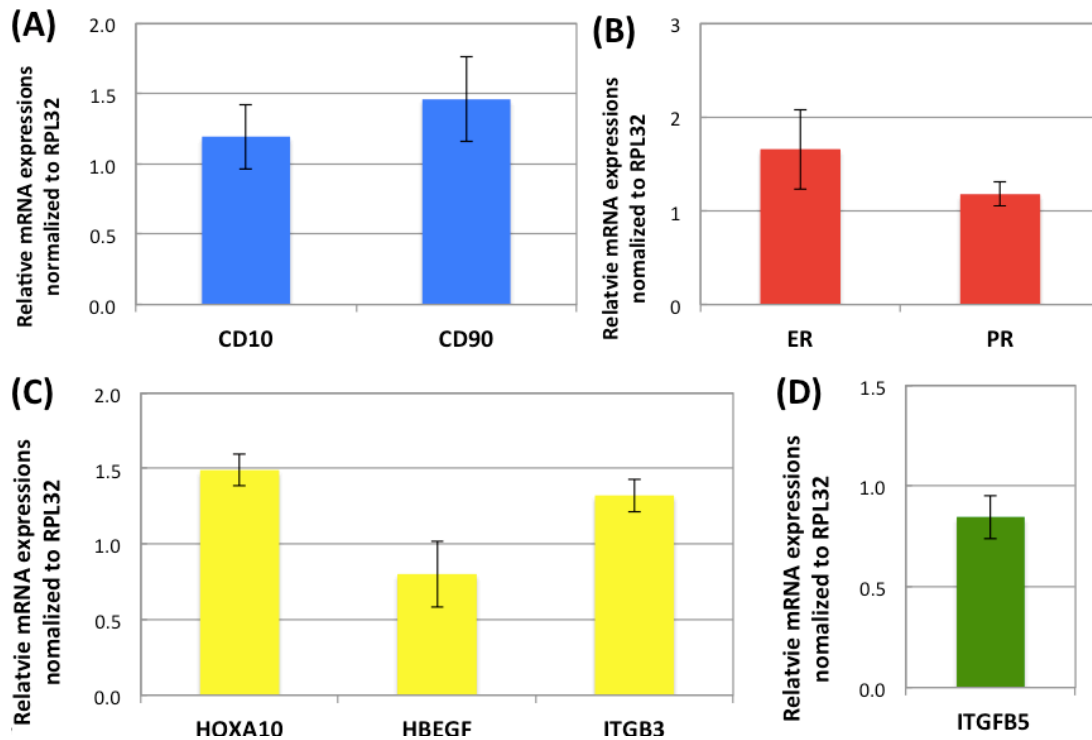


Figure 66 mRNA expressions of (A) *CD10* and *CD90*, (B) *ER* and *PR*, (C) *HOXA10*, *HBEGF*, and *ITGB3*, and (D) *ITGFB5* in hESCs after treating with Y27632 for 7 days measured by rt-PCR. All the mRNA expressions were normalized to the RPL32 expressions and further normalized to control values. The bars represent the mean \pm standard error of fold changes between strained and control samples ($n=4$) (p -value was obtained from student's t -test; * $p < 0.05$).

6.3.3 Histological assay and immunochemistry staining

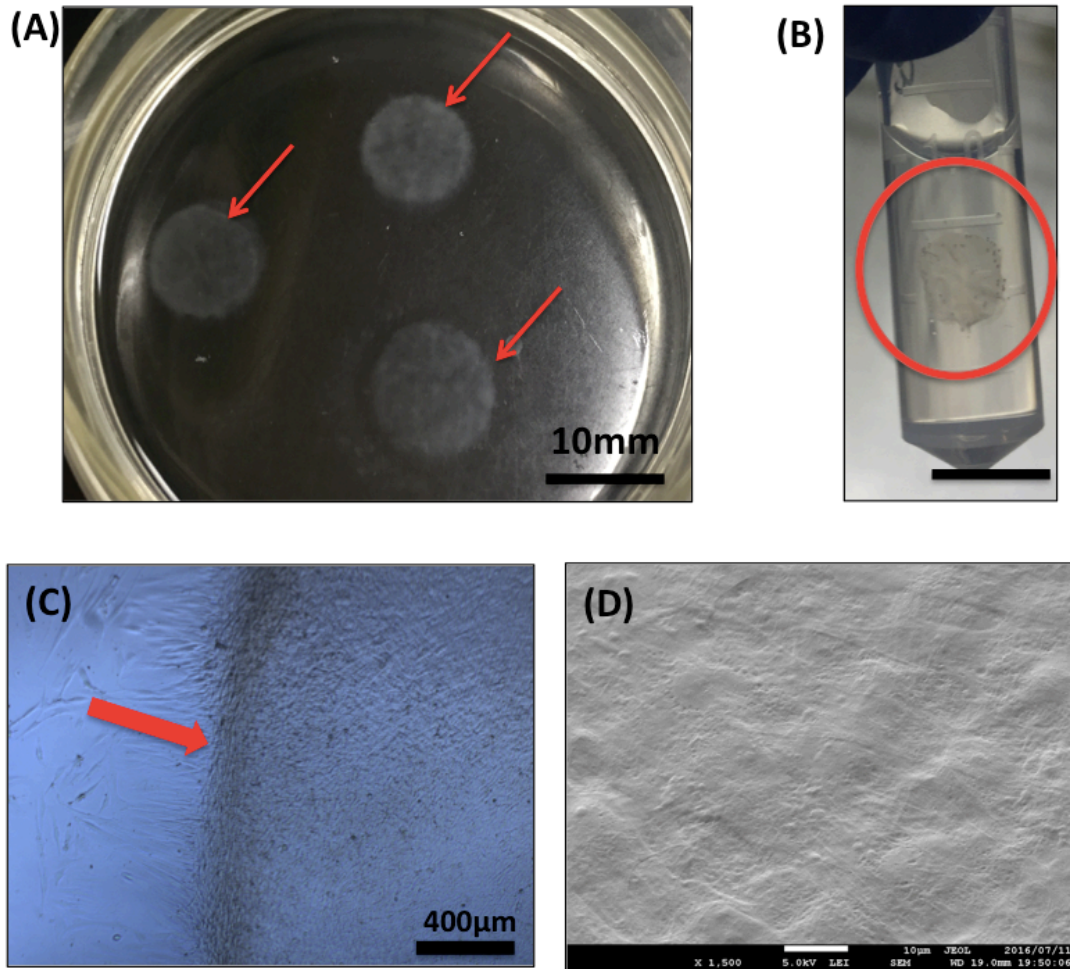


Figure 67 (A) Reconstruction of scaffold-free tissue (SFT) using human endometrial stromal cells (hESC) with three layers, (B) The hESC SFT collected in the PBS, (C) Microscope image of border of the SFT (x5), and (D) SEM image of the surface in the hESC SFT (×1,500).

By utilizing monolayer embedded underneath the SFT and Y27632, the hESC SFT with 3 layers is successfully fabricated. As shown in Fig. 67 (A) and (B), the hESC SFT reconstructed can be collected in PBS or formalin for *in vitro* or *in vivo* experiment as well as further evaluation. As shown in Fig. 66 (D), the SEM image shows a tight and smooth surface of the cell sheet. Then, we implemented the histological staining, hematoxylin and eosin (HE), to stain nucleus and cytoplasm in the samples. The HE staining in Fig. 68 represented that there was no vacant area among the layers of the SFT that indicates cell death and tightly conjugated each other. A thickness of the SFT was about 100 – 125 µm. Moreover, the immunostaining results showed that type I collagen (coll1) and vimentin (vim) were entirely detected and expressed in the SFT.

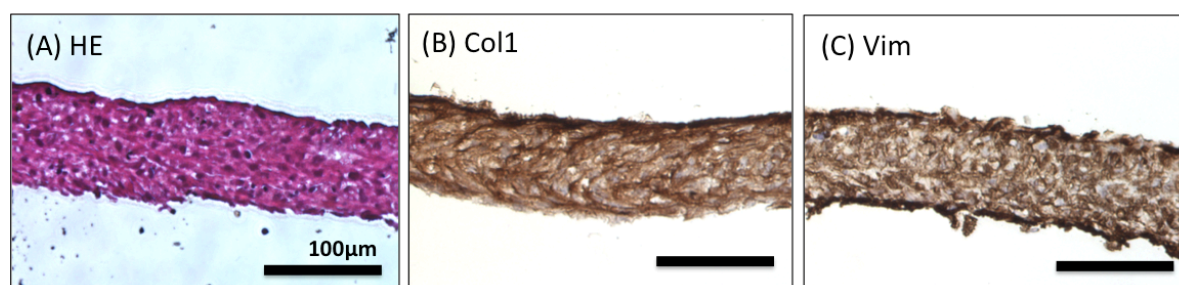


Figure 68 Staining image of cross section in hESC SFT (A) hematoxylin and eosin (HE) staining, (B) type I collagen (Col1), and (C) vimentin (Vim).

6.3.4 Incubating rat embryo on hESC SFT for 24 hour

After successfully reconstructing the SFT using the hESCs, we collected rat embryos from 9 weeks old female Sprague Dawley (SD) rat. To examine *in vitro* uterine function of SFT as uterus, we cocultured the rat embryo for 1 day on the hESC SFT. As control groups, we also cocultured embryos on lumox culture dish and monolayer formed by hESCs. In this study, we evaluated three significant processes of the embryo that usually occur during early implantation in the uterus; development, hatching and attachment. As shown in Table 6, the hatching ratio, removal of zona pellucida in the embryo, was greatly enhanced by coculturing on the SFT (75%) compared to that on the culture dish (12%) or the monolayer (50%). With regard to the development of embryo, the SFT and monolayer showed a greater ratio of 97% and 84%, respectively, while only 38% of embryo developed on the culture dish. Lastly, the ratio of attachment by embryo showed that coculturing the rat embryo on the hESC SFT remarkably increased its ratio up to 25% while few embryos attached onto both control (0%) and monolayer (1%).

Table 6 Evaluation of rat embryo cultured on lumox dish, hESC monolayer, or hESC SFT (10 replicates).

	Development	Hatching	Attachment
Control (dish)	11/29 (38%)	3/25 (12%)	0/29 (0%)

Monolayer	18/21 (84%)	10/20 (50%)	2/21 (1%)
SFT	31/32 (97%)	24/32 (75%)	8/32 (25%)

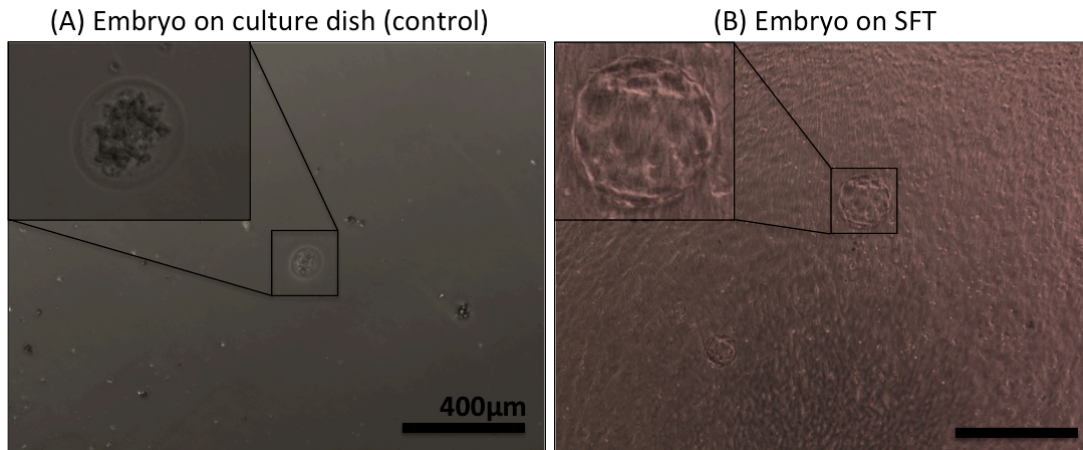


Figure 69 Coculturing rat embryo for 24 hours on (A) culture dish and (B) hESC SFT

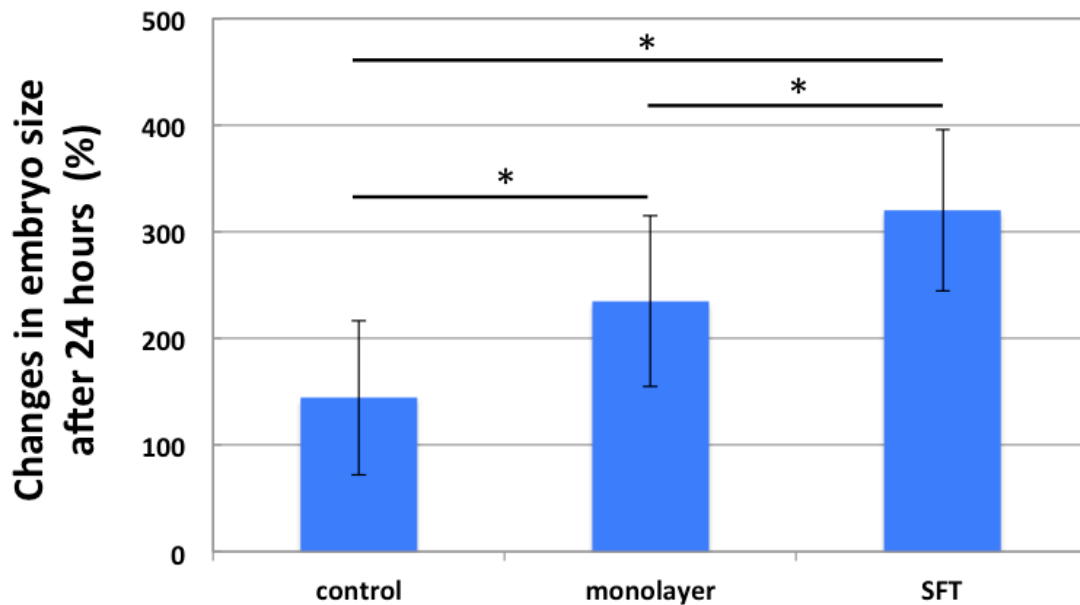


Figure 70 Changes in rat embryo size after 24 hours of incubation on culture dish, monolayer, or SFT. The graph represented a quantification data of area changes in embryo size. The bars represent the mean \pm standard deviation of area changes (n=20) (p-value was obtained from ANOVA test; * p < 0.05, ** p<0.005).

For the development of embryo, we also quantified the area changes in embryo size by measuring the size of embryo before and after incubation in Fig. 70.

Depending on the condition of embryo collected (e.g. the stage of embryo), many of the embryos inside the zona pellucida cultured on the lumox culture dish degenerated or died. By coculturing the embryo on the SFT, the embryos became enlarged quickly compared to that on the culture dish or monolayer. The mean value of size changes incubated on the culture dish and hESC monolayer were 144.5% and 234.6%, respectively. On the other hand, the mean value of size changes when the embryos were cocultured on the SFT became 308.5%. By culturing the rat embryos on the SFT, most of those became a superior size without degeneration or death compared to the control groups.

Although the period of incubation was set to 24 hours to evaluate the early implantation in this study, we also cocultured the rat embryo on hESC SFT for 2 days. After 2 days of longer incubation, most of hatched embryo did implement the attachment on the SFT. Fig 71 showed the rat embryo attached on the hESC SFT after 2 days of incubation.

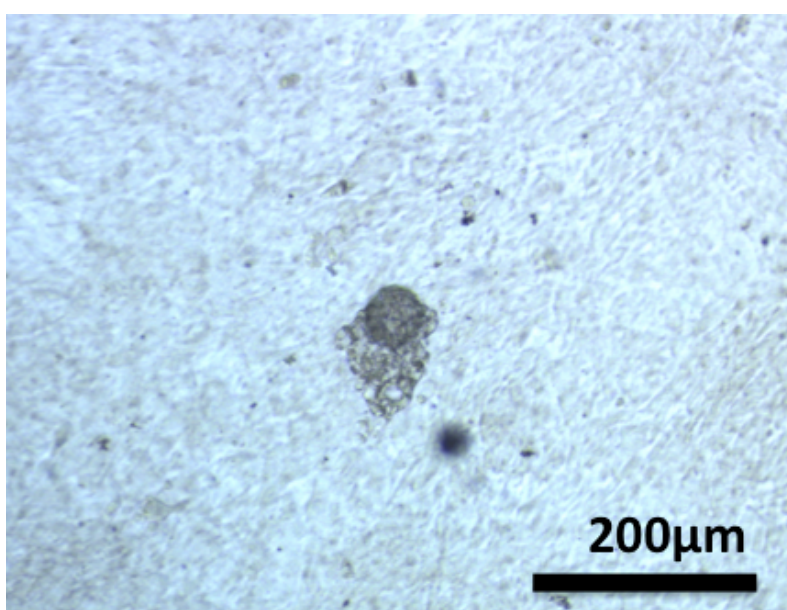


Figure 71 Attachment of rat embryo onto the hESC SFT after 2 days of incubation

In Fig 72, the rat embryos were observed while they are incubated on the hESC SFT for up to 96 hours. After 48 hours incubation, the hatched embryo was covered by surrounding cells of the SFT. At 96 hours, the embryo was fully embedded inside the SFT.

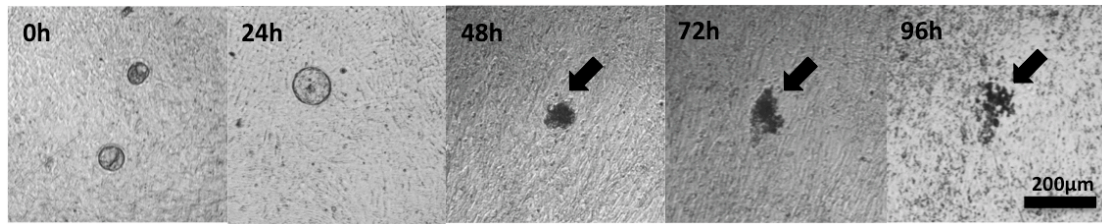


Figure 72 Incubation of rat embryo on the hESC SFT up to 96 hours

6.3.5 Gene expression changes between hESC monolayer and SFT

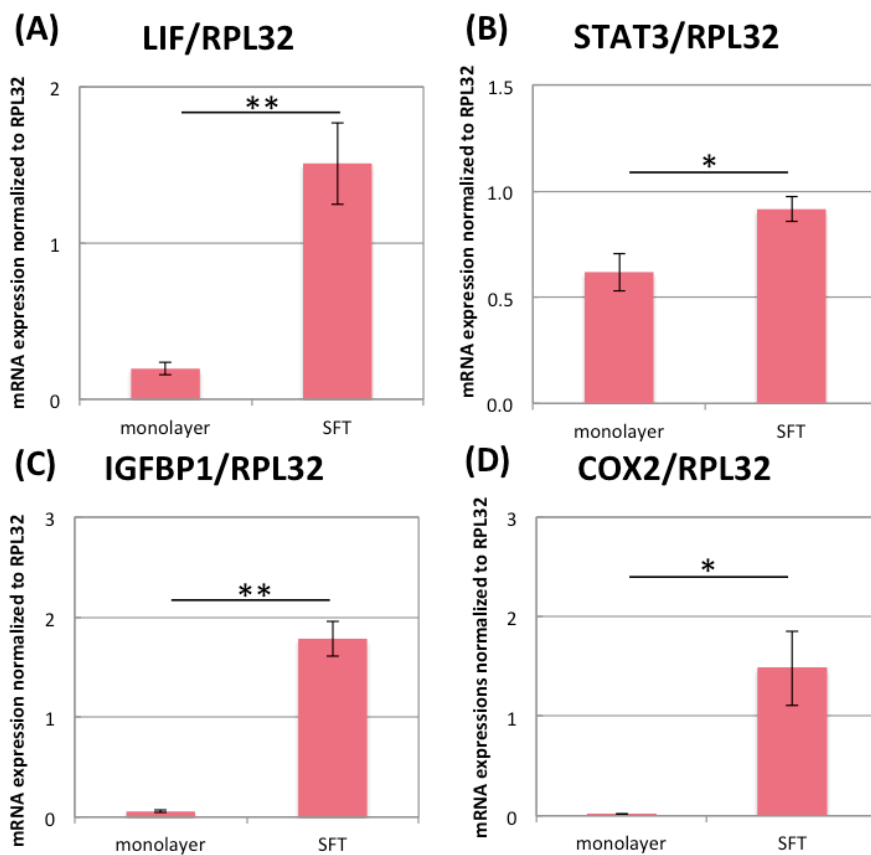


Figure 73 mRNA expressions of (A) LIF, (B) STAT3, (C) IGFBP1, and (D) COX2 in hESC monolayer and SFT measured by rt-PCR. All the mRNA expressions were normalized to the RPL32 expressions. The bars represent the mean \pm standard error (n=6) (p-value was obtained from student's *t*-test; * $p < 0.05$, ** $p < 0.005$)

In order to compare any changes in gene expression of hESC in the form of monolayer or SFT, rt-PCR was carried out. Fig 73 showed that it significantly up-regulated mRNA expressions of (A) *LIF* (7.7-fold change; $p < 0.005$) and (B) *STAT3* (1.5-fold change; $p < 0.05$). Moreover, the hESC in the form of SFT showed greater

mRNA expressions than monolayer condition in *IGFBP1* (32-fold change; $p < 0.005$) and *COX2* (106-fold change; $p < 0.05$).

6.3.6 Applying cyclic strain in hESC monolayer and SFT

In order to compare gene expression changes in hESC monolayer and SFT against cyclic strain, we applied 15% of cyclic strain at 0.1Hz for 24 hours on the hESC SFT. The rt-PCR results in Fig. 74 showed that applying cyclic strain did not induce any significant gene expression changes in the hESC in the form of monolayer. On the other hand, as shown in Fig. 75, it up-regulated some gene expressions in the hESC SFT, such as *STAT3* (1.62-fold change; $p < 0.05$), *IGFBP1* (1.65-fold change; $p = 0.20$), *HOXA10* (1.84-fold change; $p < 0.005$), *HBEGF* (1.72-fold change; $p < 0.05$), and *ITBG3* (2.25-fold change; $p < 0.05$)

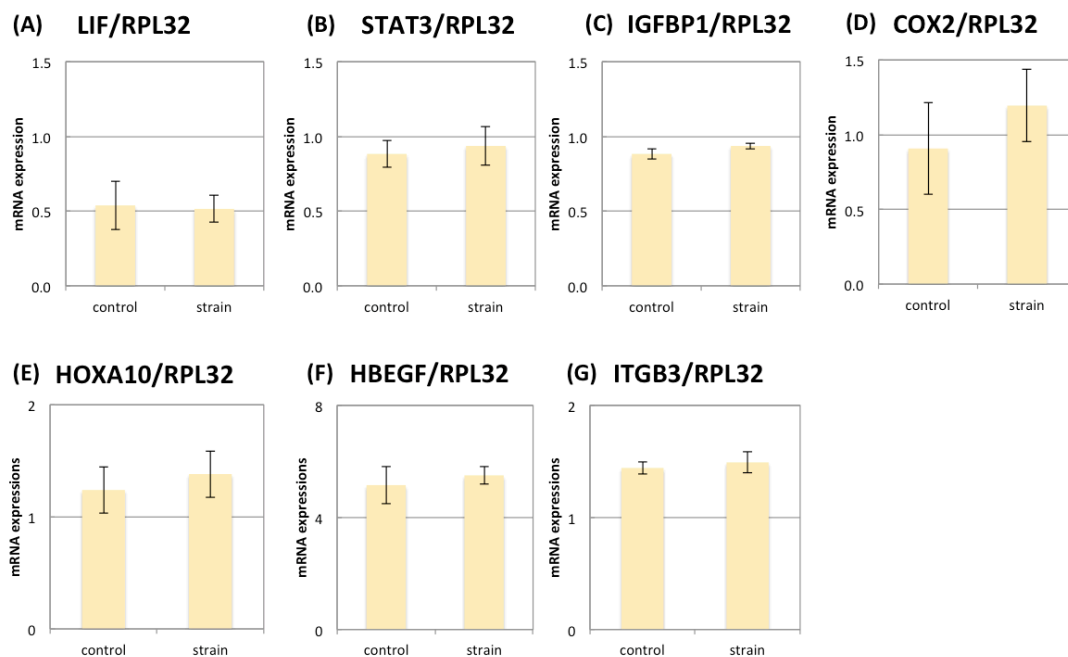


Figure 74 mRNA expressions of (A) LIF, (B) STAT3, (C) IGFBP1, (D) COX2, (E) HOXA10, (F) HBEGF, and (G) ITGB3 in hESC monolayer after applying cyclic strain for 24 hours examined by rt-PCR. All the mRNA expressions were normalized to the RPL32 expressions. The bars represent the mean \pm standard error ($n=3$) (p -value was obtained from student's t -test; * $p < 0.05$, ** $p < 0.005$)

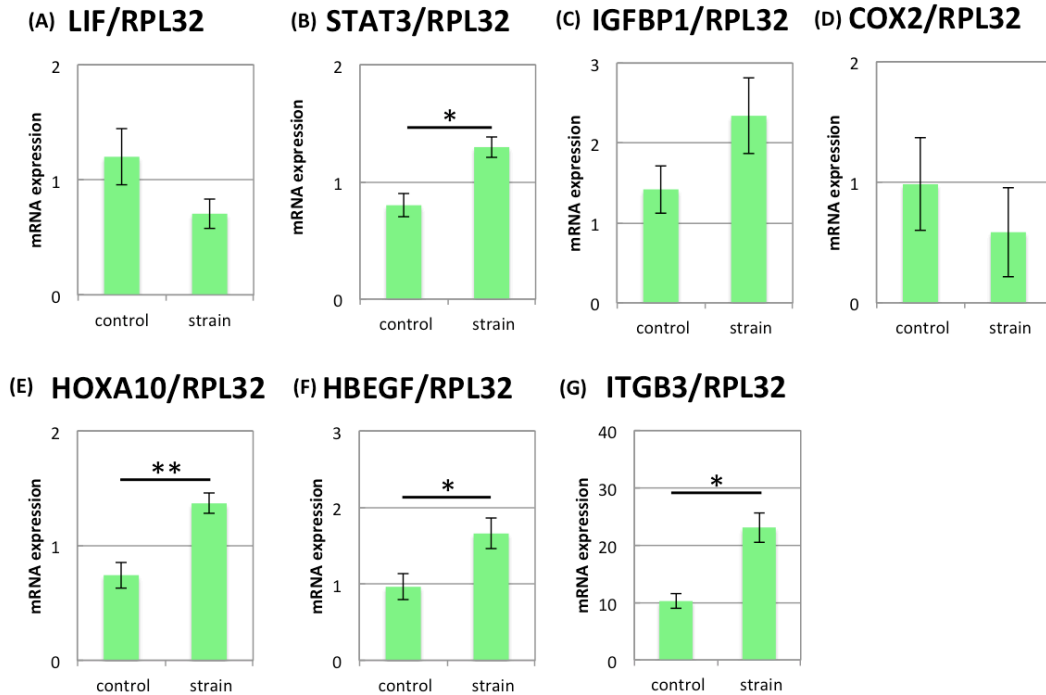


Figure 75 mRNA expressions of (A) LIF, (B) STAT3, (C) IGFBP1, (D) COX2, (E) HOXA10, (F) HBEGF, and (G) ITGB3 in hESC SFT after applying cyclic strain for 24 hours examined by rt-PCR. All the mRNA expressions were normalized to the RPL32 expressions. The bars represent the mean \pm standard error (n=5) (p-value was obtained from student's *t*-test; * p < 0.05, ** p < 0.005)

6.4 Discussion

In the previous study, we have successfully fabricated the SFT using rat endometrial stromal cells. To apply this method for human endometrial stromal cells (hESCs), we optimized this method because the hESC has a different cell size as well as its cell-cell interaction force. Although retaining its shape by using the monolayer, the tissue again started to shrink partially after 1 day because of its strong cell-cell interaction force. In order to weaken this cell-cell interaction force in the hESCs, we introduced the use of ROCK inhibitor while fabricating the SFT by reduction of the actin cytoskeletons. As a result, the SFT no longer showed the shrinkage and retained its shape for a longer period.

By stacking this tissue up to three layers, the hESC SFT was formed in a thickness of about 100 – 125 μ m and entirely expressed type I collagen as well as

endometrial stromal cell marker (vimentin). There was no vacant space shown in the cross section of SFT that indicates the cell death. The SFT reconstructed in this study became thicker engineered tissue constructs as the previous study. We also carried out to stack them over four layers or to increase cell density per a single layer of the SFT, but it was not able to retain its shape or found out cell death inside the SFT induced by lacks of oxygen or nutrients due to its excessive thickness.

The ROCK inhibitor, Y27632, was often recruited in many studies of embryonic stem cells with regard to its differentiation, proliferation and survival¹⁵⁰⁻¹⁵². Moreover, it has been widely known that the Y27623 inhibits the actin polymerization¹⁵³. The reduction of actin filaments in the hESCs under the treatment of Y27632 correspond to Grewal's study representing that Y27632 on hESCs disrupted actin stress fibers and induced a loss of vinculin localization to focal adhesion¹⁵⁴. There is a report that Y27632 strongly blocked the contractility of human endometriotic stromal cells mediated by a three dimensional collagen gel model¹⁵⁵. Therefore, the usage of Y27632 has been convinced by various cell and tissue models including endometrial stromal cells.

As a result of rt-PCR, treating Y27632 for 7 days into the hESCs did not induce any significant genetic changes. In particular, it did not show any negative effects on the endometrial cell markers or various markers that are related to uterine functions including hormone receptors, implantation of embryo, or decidualization marker. Hence, the treatment of Y27632 only reduced its cell-cell interaction force efficiently and did not affect significantly with regard to its uterine functions as long as we can confirmed in the change in genetic assay.

In order to exert its uterine function *in vitro*, we implemented the experiment coculturing rat embryos onto the hESC SFT. The results represented that the hESC SFT can provide a superior environment *in vitro* for the embryo compared to lumox culture dish or monolayer formed by hESCs. Both hatching and development ratio of embryo was highly promoted by about 50 percent compared to the culture dish. One hypothesis of this phenomenon was that the

hatching or development is known to occur by lytic factors, such as plasminogen, secreted from the endometrium¹⁵⁶⁻¹⁵⁸. Since the SFT contained a greater number of endometrial stromal cells compared to the monolayer or culture dish in a certain area, it resulted in the greater amount of lytic factors secreted from the SFT. This could raise the ratios of hatching and development of the embryos in the hESC SFT. With regard to development and attachment of the embryo, the similar reason could be also applied. It is known that the hatching is a prior and essential process for embryo to undertake the attachment process during early implantation, so that the greater ratio of hatching induced by the SFT resulted in the remarkable promotion of attachment ratio. While few embryos were attached on the culture dish (0%) and monolayer (1%), the attachment rate on the SFT (25%) was remarkably enhanced. The results altogether imply the potential usage of SFT as an *in vitro* incubator for embryo in the future.

In this study, we only incubated the rat embryo only for 24 hours, but the results with regard to attachment ratio of the embryo can be promoted if the incubation time becomes longer such as 48 hours. Further study will be needed to check the status of the embryo after the SFT fully covers the attached embryo at 72 – 96 hours. Moreover, it will be interesting to reveal how long the embryo can survive or develop inside the SFT. It, however, may require a better system of oxygen and nutrients supplies for the longer condition (7 days or longer) to examine for further development of the embryo or penetration of the embryo into the SFT. This model was suitable to evaluate the uterine function in terms of early implantation.

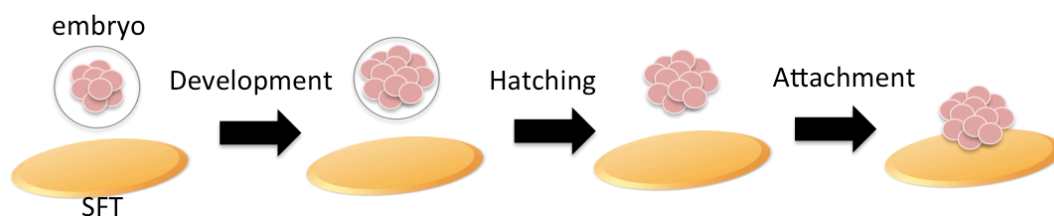


Figure 76 Schematic diagram of embryo cocultured on the SFT

During IVF, the zygotes/embryos are to incubate on a culture dish for 2 – 6 days for their developments, but death or degeneration of embryos are often occurred in this period. Since the SFT can keep them in a healthy condition and further accelerate the embryo development, introduction of SFT during IVF will be a time- and cost-effective strategy. On the other hand, in order to induce hatching of embryo, the assisted hatching is often performed mechanically or chemically. It, however, sometimes damages the zygote inside the zona pellucida. By coculturing the embryo on the SFT during IVF, we can also induce the hatching, so that it will result in promotion of embryo attachment onto the endometrium.

In addition to the increased lytic factors mentioned above, the three-dimensional culture provided by the SFT may play a key role for the promoted rate of early implantation of the embryo. As a result of rt-PCR to compare gene expressions of hESC monolayer and SFT, we found out that hESC in the form of SFT showed the greater increase in specific gene expressions that are known to highly regulate during blastocyst attachment. While Leukemia inhibitory factor (*LIF*) is known to be a downstream target of estrogen and essential for uterine receptivity as well as implantation, it binds to glycoprotein 130 (*GP130*) and LIF receptor (*LIFR*), resulting in further activation of signal transducer and activator of transcription (*STAT3*)^{159,160}. *IGFBP1* is a decidualization marker that is necessary step prior to implantation, while cyclooxygenase 2 (*COX2*), also known as prostaglandin-endoperoxide synthase (*PTGS*), is highly expressed in the regions where blastocyst attaches^{132,160-162}. We first reported that those genes were highly expressed when the hESC was formed in the three-dimensional structure of SFT compared to two-dimensional structure of monolayer. The up-regulations of those genes in hESC SFT were also thought to contribute to the promotion of early implantation events for embryo. The further study, however, will be required to confirm direction involvements of those genes by utilizing a knockout mouse.

In addition to the greater gene expressions related to uterine function markers in the SFT compared to the monolayer model, the SFT also exerted a greater response against cyclic strain. While there was no significant change observed

after applying 24 hours of cyclic strain in the hESC monolayer, it significantly up-regulated several gene expressions (*STAT3*, *HOXA10*, *HBEGF*, and *ITGB3*) that are known to be crucial for uterine functions and blastocyst attachment when hESCs were reconstructed in the form of three-dimensional structure, SFT. The three-dimensional structure of hESCs seems to involve a potential possibility for wide applications *in vitro*, but its detailed effects or mechanisms in the SFT still remains unclear. The further study will be required.

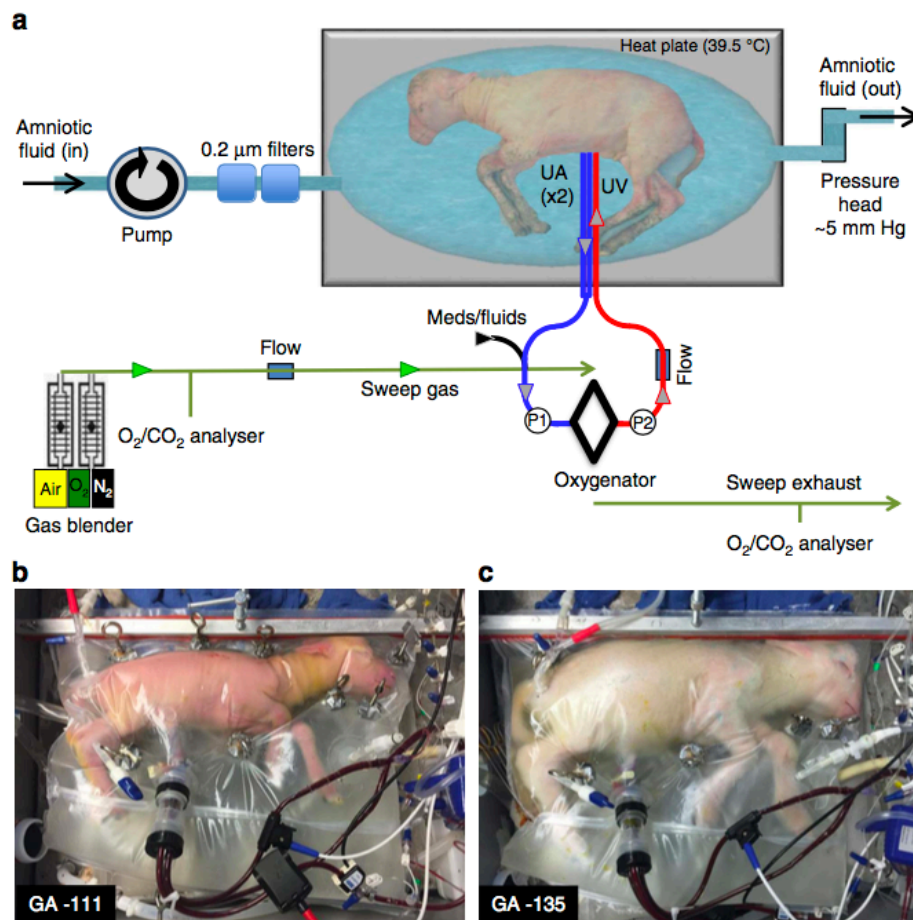


Figure 77 The extra-uterine system for premature lamb model¹⁶³

While we propose the SFT as novel embryo incubator as mentioned above, a recent study by Partridge's group in Fig. 75 reported a great performance of an external uterine system to support the premature lamb¹⁶³. This artificial womb can raise the infant into the plastic bag filled with an amniotic fluid like the placenta for up to 28 days by circulating the gas and oxygen from a pumpless oxygenator circuit. While this system is capable of supporting the development

of the premature infant that is already pre-developed up to a certain level *in vivo*, our model can support early stage of the embryo development *in vitro*. This may be interesting by combining those two concepts, resulting in the innovating total external uterine system to support embryo/fetus development for the patients who are suffering the infertility due to the loss of uterus.

While our *in vitro* study showed its superior function for embryo with regard to early implantation, *in vivo* study will be required in the future. Although the risk of foreign body rejection is expected to be very low compared to scaffold-based tissues, its regenerating process is still unknown. The pregnancy test also needs to be carried out to confirm whether or not the animal after transplanting the SFT can give a birth with normal development and numbers of babies. It, however, has a potential possibility to apply into uterine regeneration for partial defects clinically in a short period of time since it does not utilize any materials as contrasted to the scaffold-based tissues.

In conclusion, we successfully reconstructed the hESC SFT using monolayer embedded underneath the SFT as well as ROCK inhibitor. It also exerted an embryo-friendly place *in vitro* for embryo with regard to early implantation, one of the most significant uterine functions, so that this implies a possible potential as a new concept of *in vitro* incubator for embryo during *in vitro* fertilization.

7. Conclusion

7.1 Summary of Studies

The uterus refers to the essential organ to raise the embryo and fetus inside the mother until giving birth. While many studies have been carried out to regenerate various organs by tissue engineering approaches, the number of studies for uterine regeneration is still limited. On the other hand, the application of mechanical stimuli in tissue engineering has been highlighted due to its important role to modulate the differentiation of various cell models. In this study, we attempted to elucidate the effect of cyclic strain onto endometrial stromal cells. Furthermore, we successfully developed a tissue engineered construct using endometrial stromal cells for *in vitro* and *in vivo* application.

In the first study of this dissertation, we studied the effect of cyclic strain on the human endometrial stromal cells (hESCs). We first find out a new finding that applying cyclic strain onto hESCs for 7 days significantly up-regulated uterine smooth muscle cell (SMC) markers. The up-regulation of SMC markers in hESCs in response to cyclic strain was accompanied with increase in the cAMP production level. Moreover, we revealed that this phenomenon in hESCs in response to cyclic strain was occurred via cAMP signaling pathway. The change in hESCs against mechanical stimuli may imply the further possibility of hESCs as new cell source for uterine regeneration particularly in the outer layer of uterus that mainly consists of smooth muscle layer (myometrium).

In the second study, we attempted to develop a new model using rat endometrial stromal cells for uterine regeneration. By using the novel method, we successfully reconstructed the engineered tissue constructs named scaffold-free tissue (SFT). The reconstructed SFT *in vitro* was transplanted to 9 weeks old female SD rats. Since the rESC SFT did not contain any artificial materials, it was regarded as a great *in vivo* model to reveal the uterine regenerative mechanism. Throughout the time-dependent transplantation experiment, we found out that the epithelial cells from the native tissue started covering the SFT. It was integrated into the endometrium in as little as 3 days after transplantation. The

SFT transplanted after 14 days showed complete regeneration and was spread out entirely in the endometrium without any inflammation. In this study, we suggested the potential possibility of the SFT using endometrial stromal cells for uterine regeneration.

The last study involves the reconstruction of SFT using hESCs as well as the detailed study of *in vitro* application for embryo. While hESC contains such a strong cell-cell interaction force that makes difficult to retain its shape in a certain three-dimensional structure, we established a novel method to fabricate the tissue-engineered constructs using ROCK inhibitor without other mediator such as artificial materials or scaffolds. This three-dimensional disc shape of tissue-engineered constructs using hESCs refers to scaffold-free tissue (SFT) that provided a superior environment *in vitro* for rat embryo to induce its early implantation of the embryo in terms of development, hatching, and attachment. As compared to the monolayer condition of hESC, the hESC SFT had a great increase in specific gene expressions (i.g. *IGFBP1*, *COX2*, *LIF*, and *STAT3*) that are known to highly secrete *in vivo* during blastocyst implantation. Furthermore, while hESC in the form of 2D monolayer had no change in response to cyclic strain, it significantly up-regulated the gene expressions related to uterine functions and blastocyst attachment (i.g. *STAT3*, *HBEGF*, *HOX10*, and *ITGB3*) when hESCs are reconstructed in the form of 3D SFT. We first highlighted the significance role for the use of hESC in the form of three-dimensional structure as a new *in vitro* model.

7.2 Concluding Remarks

In this dissertation, we elucidated the effect of mechanical stimuli on the endometrial stromal cells for uterine tissue engineering. Moreover, a new model for tissue engineered constructs has developed using endometrial stromal cells (ESCs). The data combined delivered new insights for the usefulness of mechanical stimuli as well as tissue engineered constructs in order to fulfill uterine regeneration with the tissue engineering approaches.

Particularly, newly *in vitro* and *in vivo* strategies of the tissue engineered constructs, scaffold-free tissue, will be expected to solve the current issues facing women who are suffered from the infertility. As exerting a superior environment for embryo, the scaffold-free tissue reconstructed by endometrial stromal cells can be utilized as new concept of an incubator for embryo during *in vitro* fertilization to retain the health condition of embryo or to accelerate development of embryo. In addition, coculturing embryo on the SFT can provide the three dimensional situation mimicking the situation that the embryo attaches onto the endometrium during early implantation in pregnancy, compared to the conventional experimental model using monolayer of ESCs. By using this three-dimensional SFT model, it can also utilized as *in vitro* model to reveal the molecular mechanism in order to find out key factors to regulate early implantation during pregnancy. This finding will be a breakthrough to contribute to a fundamental treatment of any deficiency in any of those essential genes during early implantation of the embryo.

Lastly, the SFT can be utilized to develop a uterine implantation patch. The concept of uterine implantation patch is to implant the SFT as well as the embryo *in vitro*. By coculturing embryo onto the SFT until the embryo become attached within 1 – 2 days, the SFT with the embryo attached can be transplanted altogether to the endometrium. The conventional method of IVF waits for the embryo to attach onto the endometrium *in vivo*, so that it results in very low rate of success pregnancy rate due to the low implantation rate of the embryo. Hereby, our proposal makes the embryo to attach the SFT *in vitro* prior to transplantation. After the attachment of embryo onto the SFT is confirmed, the SFT as well as embryo attached will be transplanted to the endometrium. This new concept of uterine implantation patch will be expected to overcome the low success rate of pregnancy, further playing a role to overcome the female infertility.

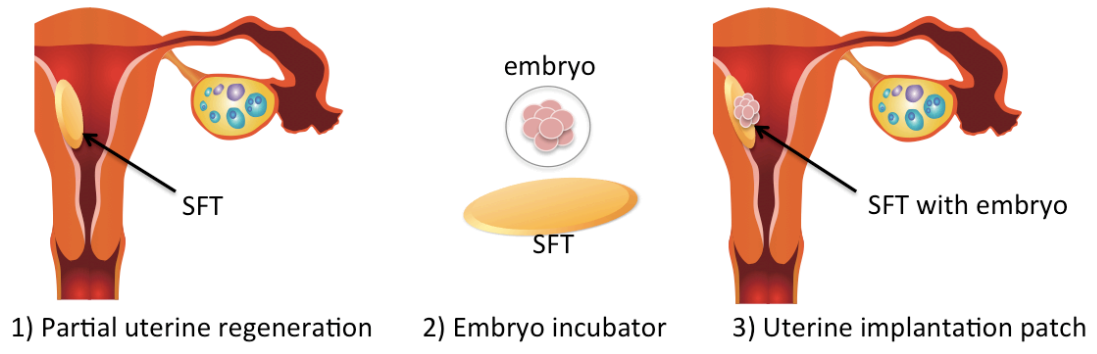


Figure 78 Applications of the scaffold-free tissue using endometrial stromal cells.

8. Future Work

8.1 Elucidation of mechanosensors in endometrial stromal cells and application of bioreactor for total uterine regeneration

Although we found out that the enhancement of smooth muscle cells in human endometrial stromal cells was modulated through cAMP signaling pathway by applying cyclic strain for 7 days, the effect of cyclic strain in the short period remains still unknown. Particularly, revealing mechanosensors in endometrial stromal cells will be key targets, so that we can achieve detailed understandings in response to mechanical stimuli. By understanding the mechano-sensor, we will further promote it chemically by addition of growth factors. On the basis of the understanding those mechano-sensing in the cell level, it will allow us to apply for designing a bioreactor in order to apply the efficient mechanical stimuli into the tissue levels. The recruitment of bioreactor is believed to be essential and enable to apply mechanical stimuli involving cyclic strain, shear force, or hydrostatic pressure for blood or nutrients supply to the entire tissue. By utilizing the bioreactor, the total uterine regeneration could be achieved in the next one or two decades.

8.2 Verification of specific genes involving early implantation of embryo using scaffold-free tissue

In this dissertation, as a result of rt-PCR, specific gene expressions (*IGFBP1*, *COX2*, *LIF*, and *STAT3*) in endometrial stromal cells were greatly up-regulated in the form of scaffold-free tissue when compared to the form of two dimensional structure of monolayer. Those genes are known to highly relate to uterine receptivity or blastocyst implantation¹⁶⁰. However, this dissertation did not figure out any direct interaction for the involvement of those genes for the SFT that exerted a superior environment for embryo. In the further study, application of knockout mouse or genetically modified mouse will be useful to reveal the involvement of those genes. After reconstruction of scaffold-free tissue using

cells harvested from the knockout mouse with deficiency of a certain gene, the embryo could be cocultured on the SFT *in vitro* as we carried out in this dissertation. Furthermore, microarray assay will allow thousands of genes monitored in the SFT in order to check relative changes in genetic expressions compared to the monolayer sample, so that it allows to understand which genes are modulated in the form of the three dimensional structure. This will further find out new candidates for the involvement of specific genes.

8.3 Scale-up of scaffold-free tissue for total uterine regeneration

The major limitation of utilizing the SFT *in vivo* was due to its weak mechanical property. The current SFT reconstructed by endometrial stromal cells had a thickness of about 100 – 120 μm . The current model is more suitable for the partial uterine regeneration, for example, after removal of cancer or tumor in the endometrium. Although transplanting the SFT is available for a post-surgery treatment to prevent further uterine diseases such as Asherman syndrome, the scale up of SFT is required for the total uterine regeneration. In order to reconstruct a thicker SFT with greater mechanical properties, application of mechanical stimuli such as cyclic strain or rotational culture will be considered for the future study¹⁶⁴.

References

1. Edwards, R. G., Steptoe, P. C. & Purdy, J. M. ESTABLISHING FULL-TERM HUMAN PREGNANCIES USING CLEAVING EMBRYOS GROWN IN VITRO. *BJOG: An International Journal of Obstetrics & Gynaecology* **87**, 737–756 (1980).
2. Steer, C. V., Mills, C. L., Tan, S. L., Campbell, S. & Edwards, R. G. SHORT COMMUNICATION: The cumulative embryo score: a predictive embryo scoring technique to select the optimal number of embryos to transfer in an in-vitro fertilization and embryo transfer programme. *Hum. Reprod.* **7**, 117–119 (1992).
3. Edwards, R. G. IVF, IVM, natural cycle IVF, minimal stimulation IVF – time for a rethink. *Reproductive BioMedicine Online* **15**, 106–119 (2007).
4. Edwards, R. G. Human implantation: the last barrier in assisted reproduction technologies? *Reproductive BioMedicine Online* **13**, 887–904 (2006).
5. Das, S., Blake, D., Farquhar, C. & Seif, M. M. W. Assisted hatching on assisted conception (IVF and ICSI). *Cochrane Database Syst Rev* **72**, CD001894 (2009).
6. Cohen, J., Alikani, M., Trowbridge, J. & Rosenwaks, Z. Implantation enhancement by selective assisted hatching using zona drilling of human embryos with poor prognosis. *Hum. Reprod.* **7**, 685–691 (1992).
7. Santoso, E. G. *et al.* Application of detergents or high hydrostatic pressure as decellularization processes in uterine tissues and their subsequent effects on in vivo uterine regeneration in murine models. *PLoS ONE* **9**, e103201 (2014).
8. Coroleu, B. *et al.* The influence of the depth of embryo replacement into the uterine cavity on implantation rates after IVF: a controlled, ultrasound-guided study. *Hum. Reprod.* **17**, 341–346 (2002).
9. Lintsen, A. M. E. *et al.* Effects of subfertility cause, smoking and body weight on the success rate of IVF. *Hum. Reprod.* **20**, 1867–1875 (2005).
10. Osol, G. & Mandala, M. Maternal Uterine Vascular Remodeling During Pregnancy. *Physiology* **24**, 58–71 (2009).

11. Weaker, F. J. & Herbert, D. C. Netter's Essential Histology by William K. Ovalle and Patrick C. Nahirney. *Clin Anat* **22**, 398–398 (2009).
12. Jost, A. HORMONAL FACTORS IN THE DEVELOPMENT OF THE FETUS. *Cold Spring Harb Symp Quant Biol* **19**, 167–181 (1954).
13. Wilhelm, D., Palmer, S. & Koopman, P. Sex Determination and Gonadal Development in Mammals. *Physiol. Rev.* **87**, 1–28 (2007).
14. LESSEY, B. A. *et al.* Immunohistochemical Analysis of Human Uterine Estrogen and Progesterone Receptors Throughout the Menstrual Cycle*. *The Journal of Clinical Endocrinology & Metabolism* **67**, 334–340 (1988).
15. Essentials of Anatomy and Physiology. (2014).
16. Popovici, R. M., Kao, L.-C. & Giudice, L. C. Discovery of New Inducible Genes in in vitro Decidualized Human Endometrial Stromal Cells Using Microarray Technology. *Endocrinology* (2013).
doi:10.1210/endo.2000.141.issue-9;pageGroup:string:Publication
17. Groothuis, P. G., Dassen, H. H. N. M., Romano, A. & Punyadeera, C. Estrogen and the endometrium: lessons learned from gene expression profiling in rodents and human. *Hum. Reprod. Update* **13**, 405–417 (2007).
18. Friberg, E., Mantzoros, C. S. & Wolk, A. Diabetes and Risk of Endometrial Cancer: A Population-Based Prospective Cohort Study. *Cancer Epidemiol Biomarkers Prev* **16**, 276–280 (2007).
19. Dubeau, L. The cell of origin of ovarian epithelial tumours. *The Lancet Oncology* **9**, 1191–1197 (2008).
20. Stewart, B. Wild, C.P. (eds.), International Agency for Research on Cancer, WHO. World Cancer Report 2014. (2014).
21. Bergeron, C., Amant, F. & Ferenczy, A. Pathology and physiopathology of adenomyosis. *Best Practice & Research Clinical Obstetrics & Gynaecology* **20**, 511–521 (2006).
22. Maheshwari, A., Gurunath, S., Fatima, F. & Bhattacharya, S. Adenomyosis and subfertility: a systematic review of prevalence, diagnosis, treatment and fertility outcomes. *Hum. Reprod. Update* **18**, 374–392 (2012).
23. Harada, T. *et al.* The Impact of Adenomyosis on Women's Fertility. *Obstetrical & Gynecological Survey* **71**, 557–568 (2016).

24. Capella-Allouc, S., Morsad, F. & Rongières-Bertrand, C. Hysteroscopic treatment of severe Asherman's syndrome and subsequent fertility. *Human ...* (1999).
25. Yu, D., Wong, Y.-M., Cheong, Y., Xia, E. & Li, T.-C. Asherman syndrome—one century later. *Fertil Steril* **89**, 759–779 (2008).
26. Tur-Kaspa, I., Jeelani, R. & Doraiswamy, P. M. Preimplantation genetic diagnosis for inherited neurological disorders. *Nature Publishing Group* **10**, 417–424 (2014).
27. Hurst, B. S., Tucker, K. E., Awoniyi, C. A. & Schlaff, W. D. Assisted hatching does not enhance IVF success in good-prognosis patients. *J. Assist. Reprod. Genet.* **15**, 62–64 (1998).
28. Lanzendorf, S. E., Nehchiri, F., Mayer, J. F., Oehninger, S. & Muasher, S. J. A prospective, randomized double-blind study for the evaluation of assisted hatching in patients with advanced maternal age. *Hum. Reprod.* **13**, 409–413 (1998).
29. Hellebaut, S., De Sutter, P. & Dozortsev, D. Does assisted hatching improve implantation rates after in vitro fertilization or intracytoplasmic sperm injection in all patients? A prospective randomized study. *Journal of assisted ...* (1996).
30. Schieve, L. A. *et al.* Does assisted hatching pose a risk for monozygotic twinning in pregnancies conceived through in vitro fertilization? *Fertil Steril* **74**, 288–294 (2000).
31. Carney, S. K., Das, S., Blake, D. & Farquhar, C. Assisted hatching on assisted conception (in vitro fertilisation (IVF) and intracytoplasmic sperm injection (ICSI)) - Cochrane Database of Systematic Reviews - Carney - Wiley Online Library. *The Cochrane ...* (2012).
32. Wang, E.-H., Wang, A.-C., Wang, B.-S. & Li, B. Outcomes of vitrified-warmed cleavage-stage embryo hatching after in vitro laser-assisted zona pellucida thinning in patients. *Biomed Rep* **5**, 376–382 (2016).
33. Koga, K. *et al.* Demonstration of angiogenin in human endometrium and its enhanced expression in endometrial tissues in the secretory phase and the decidua. *The Journal of Clinical Endocrinology & Metabolism* **86**, 5609–5614 (2001).

34. Taguchi, A. *et al.* Resveratrol Enhances Apoptosis in Endometriotic Stromal Cells. *Am. J. Reprod. Immunol.* **75**, 486–492 (2016).
35. Hirota, Y. *et al.* Possible implication of midkine in the development of endometriosis. *Hum. Reprod.* **20**, 1084–1089 (2005).
36. Gil-Sanchis, C. *et al.* Contribution of different bone marrow-derived cell types in endometrial regeneration using an irradiated murine model. *Fertil Steril* **103**, 1596–605.e1 (2015).
37. Zhang, W.-B. *et al.* A study in vitro on differentiation of bone marrow mesenchymal stem cells into endometrial epithelial cells in mice. *Eur. J. Obstet. Gynecol. Reprod. Biol.* **160**, 185–190 (2012).
38. Du, H. & Taylor, H. S. Contribution of bone marrow-derived stem cells to endometrium and endometriosis. *Stem Cells* **25**, 2082–2086 (2007).
39. Djouad, F., Bouffi, C., Ghannam, S., Noël, D. & Jorgensen, C. Mesenchymal stem cells: innovative therapeutic tools for rheumatic diseases. *Nat Rev Rheumatol* **5**, 392–399 (2009).
40. Caplan, A. I. Adult mesenchymal stem cells for tissue engineering versus regenerative medicine. *J. Cell. Physiol.* **213**, 341–347 (2007).
41. Ito, K. & Suda, T. Metabolic requirements for the maintenance of self-renewing stem cells. *Nat. Rev. Mol. Cell Biol.* **15**, 243–256 (2014).
42. Liu, J. *et al.* Hydrostatic pressures promote initial osteodifferentiation with ERK1/2 not p38 MAPK signaling involved. *J. Cell. Biochem.* **107**, 224–232 (2009).
43. Huang, C.-Y. C., Reuben, P. M. & Cheung, H. S. Temporal expression patterns and corresponding protein inductions of early responsive genes in rabbit bone marrow-derived mesenchymal stem cells under cyclic compressive loading. *Stem Cells* **23**, 1113–1121 (2005).
44. Engler, A. J., Sen, S., Sweeney, H. L. & Discher, D. E. Matrix elasticity directs stem cell lineage specification. *Cell* **126**, 677–689 (2006).
45. Seo, C. H., Furukawa, K., Montagne, K., Jeong, H. & Ushida, T. The effect of substrate microtopography on focal adhesion maturation and actin organization via the RhoA/ROCK pathway. *Biomaterials* **32**, 9568–9575 (2011).
46. Seo, C. H., Jeong, H., Furukawa, K. S., Suzuki, Y. & Ushida, T. The switching

- of focal adhesion maturation sites and actin filament activation for MSCs by topography of well-defined micropatterned surfaces. *Biomaterials* **34**, 1764–1771 (2013).
47. Wu, A. T. H. *et al.* Enhancing osteogenic differentiation of MC3T3-E1 cells by immobilizing inorganic polyphosphate onto hyaluronic acid hydrogel. *Biomacromolecules* **16**, 166–173 (2015).
 48. Démartheau, O. *et al.* Dynamic compression of cartilage constructs engineered from expanded human articular chondrocytes. *Biochemical and Biophysical Research Communications* **310**, 580–588 (2003).
 49. Kisiday, J. D., Jin, M., DiMicco, M. A., Kurz, B. & Grodzinsky, A. J. Effects of dynamic compressive loading on chondrocyte biosynthesis in self-assembling peptide scaffolds. *J Biomech* **37**, 595–604 (2004).
 50. Connor, C. J. O., Case, N. & Guilak, F. Mechanical regulation of chondrogenesis. *Stem Cell Research & Therapy* **4**, 1–1 (2013).
 51. Ng, K. W. *et al.* Duty Cycle of Deformational Loading Influences the Growth of Engineered Articular Cartilage. *Cel. Mol. Bioeng.* **2**, 386–394 (2009).
 52. Bian, L., Zhai, D. Y., Zhang, E. C., Mauck, R. L. & Burdick, J. A. Dynamic compressive loading enhances cartilage matrix synthesis and distribution and suppresses hypertrophy in hMSC-laden hyaluronic acid hydrogels. *Tissue Engineering Part A* **18**, 715–724 (2012).
 53. Dewey, C. F., Bussolari, S. R., Gimbrone, M. A. & Davies, P. F. The dynamic response of vascular endothelial cells to fluid shear stress. *J Biomech Eng* **103**, 177–185 (1981).
 54. Dan, P., Velot, É., Decot, V. & Menu, P. The role of mechanical stimuli in the vascular differentiation of mesenchymal stem cells. *J Cell Sci* **128**, 2415–2422 (2015).
 55. Ando, J. & Yamamoto, K. Vascular mechanobiology: endothelial cell responses to fluid shear stress. *Circ. J.* **73**, 1983–1992 (2009).
 56. Fitzgerald, J. B., Jin, M. & Grodzinsky, A. J. Shear and compression differentially regulate clusters of functionally related temporal transcription patterns in cartilage tissue. *J. Biol. Chem.* **281**, 24095–24103 (2006).

57. Silberman, M. *et al.* Shear stress-induced transcriptional regulation via hybrid promoters as a potential tool for promoting angiogenesis. *Angiogenesis* **12**, 231–242 (2009).
58. Du, D., Furukawa, K. S. & Ushida, T. 3D culture of osteoblast-like cells by unidirectional or oscillatory flow for bone tissue engineering. *Biotechnology and Bioengineering* **102**, 1670–1678 (2009).
59. Kim, J., Montagne, K., Ushida, T. & Furukawa, K. Enhanced chondrogenesis with upregulation of PKR using a novel hydrostatic pressure bioreactor. *Biosci. Biotechnol. Biochem.* **79**, 239–241 (2015).
60. Wagner, D. R. *et al.* Hydrostatic Pressure Enhances Chondrogenic Differentiation of Human Bone Marrow Stromal Cells in Osteochondrogenic Medium. *Annals of Biomedical Engineering* **36**, 813–820 (2008).
61. Elder, B. D. & Athanasiou, K. A. Hydrostatic Pressure in Articular Cartilage Tissue Engineering: From Chondrocytes to Tissue Regeneration. *Tissue Engineering* **15**, 1–12 (2009).
62. Kawanishi, M. *et al.* Redifferentiation of Dedifferentiated Bovine Articular Chondrocytes Enhanced by Cyclic Hydrostatic Pressure Under a Gas-Controlled System. <http://dx.doi.org/10.1089/ten.2006.0176> **13**, 957–964 (2007).
63. Kawanishi, M. *et al.* Redifferentiation of Dedifferentiated Bovine Articular Chondrocytes Enhanced by Cyclic Hydrostatic Pressure Under a Gas-Controlled System. *Tissue Engineering* **13**, 957–964 (2007).
64. Ting, M. S. Y. W., Montagne, D. K., Nishimura, M. Y., Ushida, P. T. & FURUKAWA, D. K. Modulation of the effect of transforming growth factor- β 3 by low-intensity pulsed ultrasound on scaffold-free dedifferentiated articular bovine chondrocyte tissues. <http://dx.doi.org/10.1089/ten.TEC.2014.0428> (2015).
doi:10.1089/ten.TEC.2014.0428
65. Kurpinski, K., Park, J., Thakar, R. G. & Li, S. Regulation of vascular smooth muscle cells and mesenchymal stem cells by mechanical strain. *Mol Cell Biomech* **3**, 21–34 (2006).
66. Collins, N. T. *et al.* Cyclic strain-mediated regulation of vascular

- endothelial occludin and ZO-1: influence on intercellular tight junction assembly and function. *Arterioscler. Thromb. Vasc. Biol.* **26**, 62–68 (2006).
67. Harada, M. Mechanical stretch upregulates IGFBP-1 secretion from decidualized endometrial stromal cells. *AJP: Endocrinology and Metabolism* **290**, E268–E272 (2005).
 68. Harada, M. *et al.* Mechanical Stretch Stimulates Interleukin-8 Production in Endometrial Stromal Cells: Possible Implications in Endometrium-Related Events. *The Journal of Clinical Endocrinology & Metabolism* **90**, 1144–1148 (2005).
 69. Grigg, P. Biophysical studies of mechanoreceptors. *J Appl Physiol* **60**, 1107–1115 (1986).
 70. Coste, B. *et al.* Piezo1 and Piezo2 Are Essential Components of Distinct Mechanically Activated Cation Channels. *Science* **330**, 55–60 (2010).
 71. Kim, S. E., Coste, B., Chadha, A., Cook, B. & Patapoutian, A. The role of Drosophila Piezo in mechanical nociception. *Nature* **483**, 209–212 (2012).
 72. Bae, C., Sachs, F. & Gottlieb, P. A. The mechanosensitive ion channel Piezo1 is inhibited by the peptide GsMTx4. *Biochemistry* **50**, 6295–6300 (2011).
 73. Calebiro, D., Nikolaev, V. O., Persani, L. & Lohse, M. J. Signaling by internalized G-protein-coupled receptors. *Trends in Pharmacological Sciences* **31**, 221–228 (2010).
 74. Chachisvilis, M., Zhang, Y.-L. & Frangos, J. A. G protein-coupled receptors sense fluid shear stress in endothelial cells. *Proceedings of the National Academy of Sciences* **103**, 15463–15468 (2006).
 75. Liedert, A., Claes, L. & Ignatius, A. in *Mechanosensitive Ion Channels* **1**, 253–265 (Springer Netherlands, 2008).
 76. Montagne, K., Uchiyama, H., Furukawa, K. S. & Ushida, T. Hydrostatic pressure decreases membrane fluidity and lipid desaturase expression in chondrocyte progenitor cells. *J Biomech* **47**, 354–359 (2014).
 77. Shenoy, V. B., Wang, H. & Wang, X. A chemo-mechanical free-energy-based approach to model durotaxis and extracellular stiffness-dependent contraction and polarization of cells. *Interface Focus* **6**, 20150067 (2016).

78. Martin, I., Wendt, D. & Heberer, M. The role of bioreactors in tissue engineering. *Trends in Biotechnology* **22**, 80–86 (2004).
79. Langer, R. *et al.* Tissue Engineering: Biomedical Applications. <http://dx.doi.org/10.1089/ten.1995.1.151> (2007).
doi:10.1089/ten.1995.1.151
80. GILBERT, T., SELLARO, T. & BADYLAK, S. Decellularization of tissues and organs. *Biomaterials* (2006). doi:10.1016/j.biomaterials.2006.02.014
81. Kawasaki, T. *et al.* Novel detergent for whole organ tissue engineering. *J. Biomed. Mater. Res.* **103**, 3364–3373 (2015).
82. Song, J. J. *et al.* Regeneration and experimental orthotopic transplantation of a bioengineered kidney. *Nature Medicine* **19**, 646–651 (2013).
83. Funamoto, S. *et al.* The use of high-hydrostatic pressure treatment to decellularize blood vessels. *Biomaterials* **31**, 3590–3595 (2010).
84. Chu, P., Wu, E. & Weiss, L. M. Cytokeratin 7 and Cytokeratin 20 Expression in Epithelial Neoplasms: A Survey of 435 Cases. *Modern Pathology* **13**, 962–972 (2000).
85. Wonodirekso, S., Hadisaputra, W., Affandi, B., Siregar, B. & Rogers, P. A. Cytokeratin 8, 18 and 19 in endometrial epithelium of Norplant and norethisterone enanthate injectable progestogen contraceptive users. *Hum. Reprod.* **11 Suppl 2**, 144–149 (1996).
86. Glasser, S. R. & Julian, J. Intermediate filament protein as a marker of uterine stromal cell decidualization. *Biology of Reproduction* **35**, 463–474 (1986).
87. Miyazaki, K. & Maruyama, T. Partial regeneration and reconstruction of the rat uterus through recellularization of a decellularized uterine matrix. *Biomaterials* **35**, 8791–8800 (2014).
88. Toki, T., Shimizu, M., Takagi, Y., Ashida, T. & Konishi, I. CD10 is a marker for normal and neoplastic endometrial stromal cells. *Int. J. Gynecol. Pathol.* **21**, 41–47 (2002).
89. Schwab, K. E., Hutchinson, P. & Gargett, C. E. Identification of surface markers for prospective isolation of human endometrial stromal colony-forming cells. *Hum. Reprod.* **23**, 934–943 (2008).

90. Fitzgibbon, J., Morrison, J. J., Smith, T. J. & O'Brien, M. Modulation of human uterine smooth muscle cell collagen contractility by thrombin, Y-27632, TNF alpha and indomethacin. *Reproductive Biology and Endocrinology* 2009 7:1 7, 2 (2009).
91. Li, L., Miano, J. M., Cserjesi, P. & Olson, E. N. SM22 alpha, a marker of adult smooth muscle, is expressed in multiple myogenic lineages during embryogenesis. *Circ. Res.* **78**, 188–195 (1996).
92. Pusztaszeri, M. P., Seelentag, W. & Bosman, F. T. Immunohistochemical expression of endothelial markers CD31, CD34, von Willebrand factor, and Fli-1 in normal human tissues. *J. Histochem. Cytochem.* **54**, 385–395 (2006).
93. Yoder, M. C. Human Endothelial Progenitor Cells. *Cold Spring Harb Perspect Med* **2**, a006692–a006692 (2012).
94. Weihua, Z. *et al.* Estrogen receptor (ER) beta, a modulator of ERalpha in the uterus. *Proceedings of the National Academy of Sciences* **97**, 5936–5941 (2000).
95. Lessey, B. A. *et al.* Endometrial progesterone receptors and markers of uterine receptivity in the window of implantation. *Fertil Steril* **65**, 477–483 (1996).
96. Fowler, D. J., Nicolaides, K. H. & Miell, J. P. Insulin-like growth factor binding protein-1 (IGFBP-1): a multifunctional role in the human female reproductive tract. *Hum. Reprod. Update* **6**, 495–504 (2000).
97. Telgmann, R. & Gellersen, B. Marker genes of decidualization: activation of the decidual prolactin gene. *Hum. Reprod. Update* **4**, 472–479 (1998).
98. Bazer, F. W. *et al.* Uterine biology in pigs and sheep. *Journal of Animal Science and Biotechnology* 2012 3:1 **3**, 23 (2012).
99. Classen-Linke, I. *et al.* Marker molecules of human endometrial differentiation can be hormonally regulated under in-vitro conditions as in-vivo. *Hum. Reprod. Update* **4**, 539–549 (1998).
100. Lim, H. J. & Dey, S. K. HB-EGF: A unique mediator of embryo-uterine interactions during implantation. *Experimental Cell Research* **315**, 619–626 (2009).
101. Das, S. K. *et al.* Heparin-binding EGF-like growth factor gene is induced in

- the mouse uterus temporally by the blastocyst solely at the site of its apposition: a possible ligand for interaction with blastocyst EGF-receptor in implantation. *Development* **120**, 1071–1083 (1994).
102. Varayoud, J. *et al.* Neonatal exposure to bisphenol A alters rat uterine implantation-associated gene expression and reduces the number of implantation sites. *Endocrinology* **152**, 1101–1111 (2011).
 103. Barker, D. J. P. The malnourished baby and infant Relationship with Type 2 diabetes. *Br Med Bull* **60**, 69–88 (2001).
 104. Uduwela, A. S., Perera, M. A. K., Aiqing, L. & Fraser, I. S. Endometrial-Myometrial Interface: Relationship to Adenomyosis and Changes in Pregnancy. *Obstetrical & Gynecological Survey* **55**, 390 (2000).
 105. Wood, C. Surgical and medical treatment of adenomyosis. *Hum. Reprod. Update* **4**, 323–336 (1998).
 106. Stewart, E. A. Uterine fibroids. *The Lancet* **357**, 293–298 (2001).
 107. Burel, A. *et al.* Role of HOXA7 to HOXA13 and PBX1 genes in various forms of MRKH syndrome (congenital absence of uterus and vagina). *Journal of Negative Results in BioMedicine* **5**, 4 (2006).
 108. MOSTOUFIZADEH, M. & SCULLY, R. E. MALIGNANT TUMORS ARISING IN ENDOMETRIOSIS. *Clinical Obstetrics and Gynecology* **23**, 951 (1980).
 109. GRIFFIN, J. E., EDWARDS, C., MADDEN, J. D., HARROD, M. J. & WILSON, J. D. Congenital Absence of the Vagina: The Mayer-Rokitansky-Kuster-Hauser Syndrome. *Ann Intern Med* **85**, 224–236 (1976).
 110. Kanichai, M., Ferguson, D., Prendergast, P. J. & Campbell, V. A. Hypoxia promotes chondrogenesis in rat mesenchymal stem cells: A role for AKT and hypoxia-inducible factor (HIF)-1 α . *J. Cell. Physiol.* **216**, 708–715 (2008).
 111. Shynlova, O., Mitchell, J. A., Tsampalieros, A., Langille, B. L. & Lye, S. J. Progesterone and gravidity differentially regulate expression of extracellular matrix components in the pregnant rat myometrium. *Biology of Reproduction* **70**, 986–992 (2004).
 112. Bulletti, C. *et al.* Abnormal uterine contractility in nonpregnant women. *Annals of the New York Academy of Sciences* **828**, 223–229 (1997).
 113. Izumi, G. *et al.* Cyclic Stretch Augments Production of Neutrophil

- Chemokines, Matrix Metalloproteinases, and Activin A in Human Endometrial Stromal Cells. *Am. J. Reprod. Immunol.* n/a–n/a (2015). doi:10.1111/aji.12359
114. Ott, H. C. *et al.* Perfusion-decellularized matrix: using nature's platform to engineer a bioartificial heart. *Nature Medicine* **14**, 213–221 (2008).
 115. Kheir, E. *et al.* Development and characterization of an acellular porcine cartilage bone matrix for use in tissue engineering. *J. Biomed. Mater. Res.* **99A**, 283–294 (2011).
 116. Hiraoka, T. *et al.* STAT3 accelerates uterine epithelial regeneration in a mouse model of decellularized uterine matrix transplantation. *J Clin Invest* **1**, (2016).
 117. Havelock, J. C. *et al.* Human myometrial gene expression before and during parturition. *Biology of Reproduction* **72**, 707–719 (2005).
 118. Loddenkemper, C. *et al.* Use of Oxytocin Receptor Expression in Distinguishing Between Uterine Smooth Muscle Tumors and Endometrial Stromal Sarcoma. *The American Journal of Surgical Pathology* **27**, 1458 (2003).
 119. Blanks, A. M., Shmygol, A. & Thornton, S. Myometrial function in prematurity. *Best Practice & Research Clinical Obstetrics & Gynaecology* **21**, 807–819 (2007).
 120. Schürch, W., Seemayer, T. A., Lagacé, R. & Gabbiani, G. The intermediate filament cytoskeleton of myofibroblasts: An immunofluorescence and ultrastructural study. *Vichows Archiv A Pathol Anat* **403**, 323–336 (1984).
 121. Eyden, B. P., Hale, R. J., Richmond, I. & Buckley, C. H. Cytoskeletal filaments in the smooth muscle cells of uterine leiomyomata and myometrium: An ultrastructural and immunohistochemical analysis. *Vichows Archiv A Pathol Anat* **420**, 51–58 (1992).
 122. Yu, J. *et al.* IL-6 downregulates transcription of NTPDase2 via specific promoter elements. *American Journal of Physiology - Gastrointestinal and Liver Physiology* **294**, G748–G756 (2008).
 123. Shimada, M. *et al.* IL-6 secretion by human pancreatic periacinar myofibroblasts in response to inflammatory mediators. *J Immunol* **168**, 861–868 (2002).

124. Catarzi, S. *et al.* Oxidative state and IL-6 production in intestinal myofibroblasts of Crohn's disease patients. *Inflammatory Bowel Diseases* **17**, 1674–1684 (2011).
125. IIVANAINEN, E. *et al.* Angiopoietin-regulated recruitment of vascular smooth muscle cells by endothelial-derived heparin binding EGF-like growth factor. *FASEB J.* **17**, 1609–1621 (2003).
126. Jeansson, M. *et al.* Angiopoietin-1 is essential in mouse vasculature during development and in response to injury. *J Clin Invest* **121**, 2278–2289 (2011).
127. Hellstrom, M., n, M. K., Lindahl, P., Abramsson, A. & Betsholtz, C. Role of PDGF-B and PDGFR-beta in recruitment of vascular smooth muscle cells and pericytes during embryonic blood vessel formation in the mouse. *Development* **126**, 3047–3055 (1999).
128. Rensen, S. S. M., Doevendans, P. A. F. M. & van Eys, G. J. J. M. Regulation and characteristics of vascular smooth muscle cell phenotypic diversity. *Neth Heart J* **15**, 100–108 (2007).
129. Frayon, S., Cueille, C., Gnidéhou, S., de Vernejoul, M.-C. & Garel, J.-M. Dexamethasone Increases RAMP1 and CRLR mRNA Expressions in Human Vascular Smooth Muscle Cells. *Biochemical and Biophysical Research Communications* **270**, 1063–1067 (2000).
130. Zhang, Z., Dickerson, I. M. & Russo, A. F. Calcitonin Gene-Related Peptide Receptor Activation by Receptor Activity-Modifying Protein-1 Gene Transfer to Vascular Smooth Muscle Cells. *Endocrinology* **147**, 1932–1940 (2006).
131. Nikitenko, L. L. *et al.* Differential and cell-specific expression of calcitonin receptor-like receptor and receptor activity modifying proteins in the human uterus. *Molecular Human Reproduction* **7**, 655–664 (2001).
132. Logan, P. C., Ponnampalam, A. P., Steiner, M. & Mitchell, M. D. Effect of cyclic AMP and estrogen/progesterone on the transcription of DNA methyltransferases during the decidualization of human endometrial stromal cells. *Molecular Human Reproduction* **19**, 302–312 (2013).
133. Aronica, S. M., Kraus, W. L. & Katzenellenbogen, B. S. Estrogen action via the cAMP signaling pathway: stimulation of adenylate cyclase and cAMP-

- regulated gene transcription. *Proceedings of the National Academy of Sciences* **91**, 8517–8521 (1994).
134. Aghajanova, L., Horcajadas, J. A., Esteban, F. J. & Giudice, L. C. The bone marrow-derived human mesenchymal stem cell: potential progenitor of the endometrial stromal fibroblast. *Biology of Reproduction* **82**, 1076–1087 (2010).
 135. Ngan, P. *et al.* The interactive effects of mechanical stress and interleukin-1 β on prostaglandin E and cyclic AMP production in human periodontal ligament fibroblasts in vitro: Comparison with cloned osteoblastic cells of mouse (MC3T3-E1). *Archives of Oral Biology* **35**, 717–725 (1990).
 136. Fitzgerald, J. B. *et al.* Mechanical Compression of Cartilage Explants Induces Multiple Time-dependent Gene Expression Patterns and Involves Intracellular Calcium and Cyclic AMP. *J. Biol. Chem.* **279**, 19502–19511 (2004).
 137. Walsh, D. A. & Van Patten, S. M. Multiple pathway signal transduction by the cAMP-dependent protein kinase. *FASEB J.* **8**, 1227–1236 (1994).
 138. Goel, M., Zuo, C. D. & Schilling, W. P. Role of cAMP/PKA signaling cascade in vasopressin-induced trafficking of TRPC3 channels in principal cells of the collecting duct. *Am. J. Physiol. Renal Physiol.* **298**, F988–96 (2010).
 139. Matsumoto, H. *et al.* Regulation of proliferation, motility, and contractility of human endometrial stromal cells by platelet-derived growth factor. *The Journal of Clinical Endocrinology & Metabolism* **90**, 3560–3567 (2005).
 140. WU, M. Effects of hydrostatic pressure on cytoskeleton and BMP-2, TGF- β , SOX-9 production in rat temporomandibular synovial fibroblasts1. *Osteoarthritis and Cartilage* **16**, 41–47 (2008).
 141. Wang, R. M. & Christman, K. L. Decellularized myocardial matrix hydrogels: In basic research and preclinical studies. *Advanced Drug Delivery Reviews* **96**, 77–82 (2016).
 142. Chan, B. P. & Leong, K. W. Scaffolding in tissue engineering: general approaches and tissue-specific considerations. *Eur Spine J* **17 Suppl 4**, 467–479 (2008).

143. Lu, S.-H. *et al.* Reconstruction of Engineered Uterine Tissues Containing Smooth Muscle Layer in Collagen/Matrigel Scaffold In Vitro. <http://dx.doi.org/10.1089/ten.tea.2008.0187> (2009).
doi:10.1089/ten.tea.2008.0187
144. Ye, T.-M., Pang, R. T. K., Leung, C. O. N., Liu, W. & Yeung, W. S. B. Development and characterization of an endometrial tissue culture model for study of early implantation events. *Fertil Steril* **98**, 1581–1589 (2012).
145. Takagi, S. *et al.* Reconstruction of functional endometrium-like tissue in vitro and in vivo using cell sheet engineering. *Biochemical and Biophysical Research Communications* **446**, 335–340 (2014).
146. Shimizu, T., Yamato, M., Kikuchi, A. & Okano, T. Cell sheet engineering for myocardial tissue reconstruction. *Biomaterials* **24**, 2309–2316 (2003).
147. Furukawa, K. S., Imura, K., Tateishi, T. & Ushida, T. Scaffold-free cartilage by rotational culture for tissue engineering. *J. Biotechnol.* **133**, 134–145 (2008).
148. Matsuura, K., Utoh, R., Nagase, K. & Okano, T. Cell sheet approach for tissue engineering and regenerative medicine. *J Control Release* **190**, 228–239 (2014).
149. Sumide, T. *et al.* Functional human corneal endothelial cell sheets harvested from temperature-responsive culture surfaces. *FASEB J.* **20**, 392–394 (2006).
150. Claassen, D. A., Desler, M. M. & Rizzino, A. ROCK inhibition enhances the recovery and growth of cryopreserved human embryonic stem cells and human induced pluripotent stem cells. *Molecular Reproduction and Development* **76**, 722–732 (2009).
151. Watanabe, K. *et al.* A ROCK inhibitor permits survival of dissociated human embryonic stem cells. *Nature Biotechnology* **25**, 681–686 (2007).
152. XiangyunLi, GuoliangMeng, RomanKrawetz, ShiyongLiu & Rancourt, D. E. The ROCK Inhibitor Y-27632 Enhances the Survival Rate of Human Embryonic Stem Cells Following Cryopreservation. <http://www.liebertpub.com/scd> **17**, 1079–1086 (2008).
153. Maekawa, M. *et al.* Signaling from Rho to the actin cytoskeleton through

- protein kinases ROCK and LIM-kinase. *Science* **285**, 895–898 (1999).
154. Grewal, S., Carver, J., Ridley, A. J. & Mardon, H. J. Human endometrial stromal cell rho GTPases have opposing roles in regulating focal adhesion turnover and embryo invasion in vitro. *Biology of Reproduction* **83**, 75–82 (2010).
 155. Yuge, A., Nasu, K., Matsumoto, H., Nishida, M. & Narahara, H. Collagen gel contractility is enhanced in human endometriotic stromal cells: a possible mechanism underlying the pathogenesis of endometriosis-associated fibrosis. *Hum. Reprod.* **22**, 938–944 (2007).
 156. Liu, H. C., Mele, C. A., Noyes, N. & Rosenwaks, Z. Endometrial secretory proteins enhance early embryo development. *J. Assist. Reprod. Genet.* **11**, 217–224 (1994).
 157. Menino, A. R. & Williams, J. S. Activation of plasminogen by the early bovine embryo. *Biology of Reproduction* **36**, 1289–1295 (1987).
 158. Diedrich, K., Fauser, B. C. J. M., Devroey, P., Griesinger, G. Evian Annual Reproduction (EVAR) Workshop Group. The role of the endometrium and embryo in human implantation. *Hum. Reprod. Update* **13**, 365–377 (2007).
 159. Sun, X., Bartos, A., Whitsett, J. A. & Dey, S. K. Uterine Deletion of Gp130 or Stat3 Shows Implantation Failure with Increased Estrogenic Responses. *Mol. Endocrinol.* **27**, 1492–1501 (2013).
 160. Cha, J., Sun, X. & Dey, S. K. Mechanisms of implantation: strategies for successful pregnancy. *Nature Medicine* **18**, 1754–1767 (2012).
 161. Daikoku, T. *et al.* Conditional deletion of Msx homeobox genes in the uterus inhibits blastocyst implantation by altering uterine receptivity. *Dev. Cell* **21**, 1014–1025 (2011).
 162. Song, H., Lim, H., Das, S. K., Paria, B. C. & Dey, S. K. Dysregulation of EGF Family of Growth Factors and COX-2 in the Uterus during the Preattachment and Attachment Reactions of the Blastocyst with the Luminal Epithelium Correlates with Implantation Failure in LIF-Deficient Mice. *Mol. Endocrinol.* **14**, 1147–1161 (2000).
 163. Partridge, E. A. *et al.* An extra-uterine system to physiologically support the extreme premature lamb. *Nat Commun* **8**, 15112 (2017).

164. Furukawa, K. S., Imura, K., Tateishi, T. & Ushida, T. Scaffold-free cartilage by rotational culture for tissue engineering. *J. Biotechnol.* **133**, 134–145 (2008).

Protocol

Cell culture

We performed sterile filtration of cell culture medium as well as Trypsin utilizing bottle-top filter in order to prevent any contaminations in the solutions. The bottle-top filter was subjected to autoclave at 120°C for 20 minutes in advance of using.

Cell culture solutions:

- PBS (-) (for 1000ml)
 - MilliQ water 1000ml
 - PBS powder 9.6g

⇒ Add the PBS powder directly into a sterilized glass bottle filled up with 1000ml of MilliQ water.

⇒ Autoclave it at 120°C for 20 minutes in order to sterilize.

- DMEM-LG (for 1000ml)
 - MilliQ water 900ml
 - DMEM-LG 9.98ml
 - NaHCO₃ 3.7g
 - Fetal Bovine Serum (FBS) 100ml
 - Antibiotic-Antimycotic (Aa) 10ml

⇒ After mixing the solution with a magnetic stirrer, adjust the pH of the solution to 7.1 by adding NaOH or HCl.

⇒ Sterilize the solution by using a bottle-top filter in the clean bench.

⇒ Add 100ml of FBS and 10ml of Aa into the Sterilized solutions.

⇒ Store it at 4°C and warm it at 37°C immediate before using.

Note: For rat endometrial stromal cell, rat bone marrow-derived mesenchymal stem cell, human bone marrow-derived mesenchymal stem cell, etc

- DMEM/F12 medium (Phenol free) (for 1000ml)
 - MilliQ water 950ml
 - DMEM/F12 (D2906; Sigma) 1 bottle
 - NaHCO₃ 1.2g
 - Fetal Bovine Serum (FBS) 50ml
 - Antibiotic-Antimycotic (Aa) 10ml

⇒ After mixing the solution with a magnetic stirrer, adjust the pH of the solution to 7.1 by adding NaOH or HCl.

⇒ Sterilize the solution by using a bottle-top filter in the clean bench.

⇒ Add 50ml of FBS and 10ml of Aa into the Sterilized solutions.

⇒ Store it at 4°C and warm it at 37°C immediate before using.

Note: For human endometrial stromal cell

Animal experiments

Rat endometrial stromal cells

Materials

- PBS (-)
- DMEM/F12 medium w/ 10% FBS and 1% Aa
- Type I collagenase (CLS-1; Worthington Biochemical Corporation)
- DNase I (10104159001; Roche)
- 40µm and 100µm cell strainer (Falcon)
- Sterile cloth (Hogi Medical)
- Sterile scalpel holders and No.10 scalpel blades

Procedures:

- a. Prepare for the DMEM/F12 medium containing collagenase (0.42% w/v) and DNase (0.02% w/v) in a 50ml tube.
- b. Cover the working area inside the bench with the sterile cloth and prepare a culture dish filled up with around 10ml of PBS (-).
- c. Dissect 9 weeks old female rat and harvest uterine horns.
- d. Wash the uterine horns with PBS (-).
- e. Inside the dish filled up with clean PBS (-), gently slice off pieces of the uterine tissues. (Very small pieces!)
- f. Transfer the minced uterine tissues into the tube with DMEM/F12 medium containing collagenase and DNase .
- g. Incubate at 37°C for 30 minutes.
- h. Filter through 100µm cell strainer (to remove tissue debris and glandular parts).
- i. Centrifuge at 2,150rpm for 5 minutes at 10°C.
- j. The supernatant was discarded and resuspended with DMEM/F12 medium
- k. Filter through 40µm cell strainer (to remove myometrium).
- l. Resuspend with DMEM/F12 medium and transfer to the culture dish.

- m. Incubate for 30 minutes for stromal cells to attach onto the dish, the old medium is removed and replace with fresh medium (to eliminate epithelial cells).
- n. The culture medium is changed every 3 – 4 days and passage cells when reaching 70 – 80% confluent.

Rat behavioral Core Protocols

1. Estrous Cycle staging

Rats typically have a 4 – 6 day cycle that consists of 4 stages;

- Estrus: cornified and non-nucleated epithelial cells
- Proestrus: round and nucleated epithelial cells
- Diestrus I (metestrus): low cell number, lots of cell debris
- Diestrus II : mostly lymphocytes

With rats, the most highly receptive time is proestrus (usually 2pm-6pm).

Ovulation in the rat is spontaneous and occurs about 10 hours after the beginning of the estrus.

2. Vaginal smear:

is carried out to distinguish the four different stages of estrous cycle by noting characteristic cell types (cell shape and density as well as presence of blood).

- Prepare for 150 – 200µl of PBS (-) using a disposable pipette
- Grab a rat's tail and insert slightly into a rat's vagina.
(No need to insert deeply)
- Pipette up and down about 5 times.
- Remove the pipette from the vagina and transfer the PBS into culture dish.
- Examine under a microscope.

3. Mating:

- Mating needs to start when the proestrus is confirmed from a female rat.
- Transfer the female rat into the cage where a male rat stays.
- Carry out the smear next day to find out sperms from the male rat.
- Separate the male and female rat into each cage.
- Wait for 4 days for the zygote to move to the uterine horns for implantation.

4. Collecting rat embryo:

- If the sperms are observed, the female rat is separated from the male rat.
- Prepare for KSOM embryo culture medium (Merck Millipore).
- Make 4 droplets of KSOM medium on a culture dish and fill up another dish with KSOM medium.
- Warm them up inside the incubator.
- Sacrifice the female rat between 10am – 2pm.
 - ** 10am – 12pm: more 4 ~ 8 cell stages of embryo
 - 12pm – 2pm: more morula or blastocyst
- Dissect two uterine horns from the rat and put them into a culture dish filled up with PBS (-).
- By using 200µl pipette, pipette up and down the lumen of uterine horn with PBS (-).
- Find out embryo under a microscope.
 - ** Usually obtain 6 – 20 embryo.
- By using 2.5µl pipette, gently pick up each embryo and transfer to one of four drops of KSOM culture medium.
- Transfer the embryo from one drop to the other one (1 => 2 => 3=> 4). This process removes most of bloods or any dusts.
- Incubate the embryo in fresh KSOM culture medium in a humidified incubator at 37°C with 5% CO₂.

Note: The gestation period is normally 22 days, but can vary from 21-23 days.

Tissue engineered construct preparation

Making scaffold-free tissue

Preparation

- Lumox dish (94.6077.410; SARSTEDT)
- Cloning ring (diameter 5mm or 10mm; lwaki)
- Y-27632 (257-0051; Wako)

For Human endometrial stromal cells (hESCs):

- a. Prepare for 70 – 80% confluent culture dish.
- b. Wash with a certain amount of PBS twice.
- c. Add 2 – 3ml of 0.25% trypsin onto the culture dish and wait for cells to be detached from the dish (3 – 5 minutes).
- d. After checking that all the cells are detached, add about 10ml of culture medium into the dish and mix them well, and collect all the solutions with cells into a tube.
- e. Centrifuge the tube at 1,150rpm for 5 minutes.
- f. Aspirate the supernatant of the solutions.
- g. Add 10ml of culture medium into the tube, and resuspend it by pipetting up and down.
- h. Count the number of cells in the tube.
- i. Prepare for a sterilized lumox dish and a cloning ring (10mm).
- j. Seed 4.0×10^4 hESCs resuspended with 400 μ l of culture medium inside the cloning ring placed on the lumox dish.
- k. Incubate for 2 or 4 days to make a monolayer of hESCs in a humidified incubator at 37°C with 5% CO₂.
- l. After 2 or 4 days, repeat a-h.
- m. Resuspend 1.0×10^6 hESCs in 400 μ l of fresh culture medium containing
- n. 10 μ M Y27632.
- o. Remove the old medium inside and outside the ring on the lumox dish

- p. Add 400µl of the resuspended medium with cells inside the ring and also fill up with fresh medium containing 10µM Y27632 outside the ring, too.
- q. Wait for 3 hours for hESCs to form a single layer by settling down and then remove the ring gently.
 - ** If too long, cells may die due to lack of nutrients and oxygen supply.
- r. Incubate for 2 days to form the first single layer.
- s. Repeat l-q until stacking up to 3 layers of hESCs to reconstruct a scaffold-free tissue.

For rat endometrial stromal cells (rESCs) and human bone marrow-derived stem cells (hMSCs):

- a. Prepare for 70 – 80% confluent culture dish.
- b. Wash with a certain amount of PBS twice.
- c. Add 2 – 3ml of 0.25% trypsin onto the culture dish and wait for cells to be detached from the dish (3 – 5 minutes).
- d. After checking that all the cells are detached, add about 10ml of culture medium into the dish and mix them well, and collect all the solutions with cells into a tube.
- e. Centrifuge the tube at 1,150rpm for 5 minutes.
- f. Aspirate the supernatant of the solutions.
- g. Add 10ml of culture medium into the tube, and resuspend it by pipetting up and down.
- h. Count the number of cells in the tube.
- i. Prepare for a sterilized lumox dish and a cloning ring (10mm).
- j. Seed 4.0×10^4 cells resuspended with 400µl of culture medium inside the cloning ring placed on the lumox dish.
- k. Incubate for 2 or 4 days to make a monolayer of cells in a humidified incubator at 37°C with 5% CO₂.
- l. After 2 or 4 days, repeat a-h.
- m. Resuspend 1.0×10^6 cells in 400µl of culture medium.
- n. Remove the old medium inside and outside the ring on the lumox dish

- o. Add 400µl of the resuspended medium with cells inside the ring and also fill up with fresh medium outside the ring, too.
- p. Wait for 3 hours for hMSCs to form a single layer by settling down and then remove the ring gently.
 - ** If too long, cells may die due to lack of nutrients and oxygen supply.
- q. Incubate for 2 days to form the first single layer.
- r. Repeat l-q until stacking up to 3 layers to reconstruct a scaffold-free tissue.

Note:

- *Since rESCs or hMSCs have a relatively weak cell-cell interaction force compared to hESCs, it does not require the use of Y27632.*
- *Cells such as rat bone marrow-derived mesenchymal stem cell has a weak cell-cell interaction force, it requires a longer time of waiting time after seeding cells inside the ring. (>9 hours)*

Dynamic culture

Applying cyclic strain

In this study, we applied cyclic strain using the Flexcell tension system (FX-4000™; Flexcell International Corporation) placed in a humidified incubator at 37°C with 5% CO₂. The Flexcell is computer-operated and applied its strain by vacuum.

Cell Preparation:

- Prepare for 70 – 80% cell confluency on a culture dish.
- Wash with a certain amount of PBS twice.
- Add 2 – 3ml of trypsin onto the culture dish and wait for cells to be detached from the dish (3 – 5 minutes).
- After checking that all the cells are detached, add about 10ml of culture medium into the dish and mix them well, and collect all the solutions with cells into a tube.
- Centrifuge the tube at 1,150rpm for 5 minutes.
- Aspirate the supernatant of the solutions.
- Add 10ml of culture medium into the tube, and resuspend it by pipetting up and down.
- Count the cells in the tube.
- 1.0×10^5 cells were subcultured per well in a 6-well Flexcell plate
- Incubate for 3 – 4 days to be confluent in a humidified incubator at 37°C with 5% CO₂.

Running Flexcell tension machine:

- Check that the cells are confluent in a 6-well Flexcell plate.
 - Aspirate the medium and add a fresh culture medium before running Flexcell.
 - Gently put a lubricant (51360; Loctite) on the bottom of the plate.
 - Set the plate into the Flexcell tension system.
- **Unless the plate is not tightly fit, the vacuum pump can not load any tension due to air leakage.

- Turn on the PC, Flexcell tension machine, and vacuum pump.
- Set the Flexcell software (FX-3000);
 - ✓ Regiment: 15% strain
 - ✓ Frequency: 0.1 Hz for endometrial stromal cells (or 1Hz for MSCs)
 - ✓ Baseplate: BioFlex (35mm)
- Start the system.

Note: Make sure you empty the water inside a water trapper everyday.

Histological Analysis

Cryosectioning

Preparation:

- PBS (-)
- 10% neutral buffer formalin (Sigma)
- 30% Sucrose
- O.C.T. compound (4583; Sakura Tissue TEK)
- Plastic mold trays (4566; Sakura)
- Liquid nitrogen
- Isopentane

Making frozen blocks:

- Wash the tissue sample with PBS (-) (2 times)
- Transfer the sample into the 10% formalin and store it at 4°C overnight.
- Remove the formalin and wash it once with PBS.
**available to store in PBS at 4°C for longer time
- Transfer the sample into 30% sucrose solution and wait for 2 hours until the sample is sank on the bottom of the solution (or at 4°C overnight).
- Fill the plastic mold tray with O.C.T. compound and try to remove air bubbles.
- Place the sample onto the mold tray and wait for 2 hours at room temperature.
**The surface to section should be facing down
- Re-positioning the sample embedded inside O.C.T. compound.
- Pre-chill isopentane with liquid nitrogen using the steel container set-up until the white spots start to form in the isopentane.
**Do NOT directly add the isopentane into liquid nitrogen
- Snap freeze the sample by contacting the mold tray with the isopentane using forceps.
- Frozen block is stored at -80°C.

Sample sectioning:

- Turn on the cryostat (Leica) and set the temperature to -20°C .
- Place a bit of O.C.T. compound on the surface of the sample holder to stick the sample on the top facing downwards.
- Using the weight, press down the sample for 30 seconds to stick firmly.
- Set the holder onto the stage with the desired orientation.
- Adjust the dial setting to $10\mu\text{m}$ for trimming off the block and $5\mu\text{m}$ for sectioning the sample.
- Once the section is sliced off, place it on a glass slide.
- Try to place 2-4 sections on a glass slide.
- Place the glass slides with the samples on top of the vent in a clean bench and allow it to air dry for overnight (at least 1 hour).
**This will ensure the samples attach firmly to the slides.
- Store the sample at -30°C .

Hematoxylin & Eosin (HE) staining

Preparation:

- Mayer's Hematoxylin
- Diluted Eosin (E-solution)
 - Milli-Q water 2ml
 - 99.5% Ethanol 3ml
 - 1% Eosin Y Solution 1ml
 - Acetic acid 6 μ l
- 80% Ethanol, 90% Ethanol, 100% Ethanol, Lemosol, Xylene
- Mountquick set

Methods:

- Incubate the glass slides in room temperature for 15mins (stored at -30°C)
- Put the glass slides in the slide's rack
- Fill up a beaker with tap water and immerse the rack into the beaker for 5 minutes
- After removing the water, drip Mayer's Hematoxylin to cover each samples in room temperature for 5minutes
- Blot away the Hematoxylin solution and put the slides into the rack.
- Wash the slides in the tap water for 5mins.
- Drain the excess water.
- Add the diluted E-solution onto the sample in room temperature for 3mins.
- Blot away the E-solution and put the slides into the rack.
- Put the rack into 80% ethanol for 1min. (No water washing)
 - 90% ethanol for few seconds
 - 100% ethanol for few seconds
 - Lemosol for few seconds
 - Xylene for few seconds
- Let them dry under the draft for 10 – 60 seconds (try not to over-dry the samples)
- Mount the samples with mountquick and cover with a cover slide.
- Air dry the slides for 30 minutes prior to storing at room temperature.

Toluidine Blue (Tb) staining

Preparation:

- 0.05% Toluidine blue (pH4.2)
- Mountquick set

Methods:

- Incubate the glass slides in room temperature for 15mins (stored at -30°C)
- Put the glass slides in the slide's rack
- Fill up a beaker with tap water and immerse the rack into the beaker for 5 minutes
- After removing the water, drip the Toluidine blue solution to cover each samples in room temperature for 5mins
- Blot away the Toluidine blue solution and put the slides into the rack.
- Wash the slides in the tap water for 5mins.
- Drain the excess water.
- Let them dry under the draft for 10 – 60 seconds (try not to over-dry the samples)
- Mount the samples with mountquick and cover with a cover slide.
- Air dry the slides for 30 minutes prior to storing at room temperature.

Masson's Trichrome (MT) staining

Preparation:

- Weigert's Iron Hematoxylin Solution 1 (Muto chemicals; 40341)
- Weigert's Iron Hematoxylin Solution 2 (Muto chemicals; 40351)
- Masson Stain Solution B (Muto chemicals; 40252)
- 2.5% Phosphotungstic Acid Solution (Muto chemicals; 40181)
- Aniline Blue solution (Muto chemicals; 40202)
- 0.75% Orange G solution (Muto chemicals; 40232)
- Mordant 1 (Muto chemicals; 40061)
- Mordant 2 (Muto chemicals; 81411)
- 1% Acetic acid
 - Acetic acid 1ml
 - Distilled water 99ml
- 70% Ethanol, 90% Ethanol, 100% Ethanol, Lemosol, Xylene
- Mountquick set

Methods:

- Incubate the glass slides in room temperature for 15mins (stored at -30°C)
- Put the glass slides in the slide's rack
- Fill up a beaker with tap water and immerse the rack into the beaker for 5 minutes
- After removing the water, draw around samples on the glass slides with DAKO pen
- Drip Mordant 1 solution to cover each samples at room temperature for 30 minutes under the humidified condition.
- Wash the slides in the running tap water for 3 minutes.
- Air dry at room temperature for 2 minutes
- Prepare for Weigert's Iron Hematoxylin solution 1 & 2 by mixing in the 1:1 proportion.
- Add Weigert's Iron Hematoxylin solution to the samples for 10 minutes.

- Wash the slides in the running tap water for 10 minutes.
- Drip Mordant 2 solution to the samples for 1 minute.
- After removing the Mordant solution, add 0.75% Orange G solution for 2 minutes
- Wash the solutions with 1% acetic acid for 5 seconds (for 3 times)
- Drip Masson Stain Solution B onto the samples for 30 minutes.
- Wash the solutions with 1% acetic acid for 5 seconds (for 3 times)
- Add 2.5% Phosphotungstic Acid Solution to the samples for 8.5 minutes.
- Wash the solutions with 1% acetic acid for 5 seconds (for 3 times)
- Add Aniline Blue solution to the samples for 15 minutes.
- Wash the solutions with 1% acetic acid for 5 seconds (for 3 times)
- Wash again with 70% Ethanol quickly and put the slides into the rack.
- Put the rack into 70% ethanol for 7 minutes followed by;
 - 90% ethanol for 7 minutes
 - 100% ethanol for 7 minutes
 - Xylene for 7 minutes
- Let them dry under the draft for 10 – 60 seconds (try not to over-dry the samples)
- Mount the samples with mountquick and cover with a cover slide.
- Air dry the slides for 30 minutes prior to storing at room temperature.

Verhoeff-Van Gieson (VVG) staining

Preparation:

- Weigert's Iron Hematoxylin Solution 1 (Muto chemicals; 40341)
- Weigert's Iron Hematoxylin Solution 2 (Muto chemicals; 40351)
- Van Gieson's Stain Solution A (Picric acid) (Muto chemicals; 40361)
- Van Gieson's Stain Solution B (Fuchsin) (Muto chemicals; 40371)
- Maeda's Resorsin • Fuchsin Solution (Muto chemicals; 40321)
- 70% Ethanol, 90% Ethanol, 100% Ethanol, Lemosol, Xylene
- Mountquick set

Methods:

- Incubate the glass slides in room temperature for 15mins (stored at -30°C)
- Put the glass slides in the slide's rack
- Fill up a beaker with tap water and immerse the rack into the beaker for 5 minutes
- After removing the water, draw around samples on the glass slides with DAKO pen
- Immerse the rack into the 70% Ethanol for a few seconds.
- Drip Maeda's Resorsin • Fuchsin Solution solution to cover each samples at room temperature for 60 minutes under the humidified condition.
- Wash the slides by dripping 100% Ethanol to remove the excessive staining solution and again wash in the running tap water for 3 minutes.
- Prepare for Weigert's Iron Hematoxylin solution 1 & 2 by mixing in the 1:1 proportion.
- Add Weigert's Iron Hematoxylin solution to the samples for 5 minutes.
- Wash the slides in the running tap water for 10 minutes.
- Prepare for Van Gieson's stain solution A & B by mixing in the 10:1 proportion. (e.g. 100ml of A solution + 10 – 15ml of B solution)
- Drip Van Gieson's solution to the samples for 10 minutes.
- Wash the solutions with water for a few seconds

- Put the rack into 70% ethanol for 1 minute followed by;
 - 90% ethanol for few seconds
 - 100% ethanol for few seconds
 - Lemosol for few seconds
 - Xylene for few seconds
- Let them dry under the draft for 10 – 60 seconds (try not to over-dry the samples)
- Mount the samples with mountquick and cover with a cover slide.
- Air dry the slides for 30 minutes prior to storing at room temperature.

Immunohistochemistry (IHC)

Preparation:

- DAKO pen
- 10mM citrate buffer
 - Tri-sodium citrate (dehydrate) 2.94g
 - Distilled water 1L
 - Mix to dissolve and adjust pH to 6.0 with 1M HCl
 - Add 0.5ml of Tween-20 and mix well
 - Store at room temperature for 3 months or at 4°C for longer storage
- 3% H₂O₂/MeOH
- PBS (-)
- 0.1% TBST
 - Add 100ml 10X TBS to 900ml distilled water
 - Add 1ml Tween-20 and mix
- PBST+1% BSA
 - Add 25µl Tween 20 into 25ml PBS
 - Add 250mg BSA with the mixture on the shaker
- Blocking buffer (DAKO)
- Primary antibody
- Secondary antibody (Envision+ System – HRP Labelled Polymer Anti-Rabbit; DAKO)
- DAB
- Mayer's hematoxylin (Sigma-aldrich)
- Mountquick set

Primary antibody:

Cytokeratin18: ab181597 (1:500)

Vimentin: ab92547 (1:500)

Smooth muscle actin: ab5694 (1:500)

Ki67: ab15580 (1:250)

ERa: ab32063 (1:200)

Methods:

- Incubate the glass slides at room temperature for 15 minutes (stored at -30°C)
- Pre-heat 10mM citrate buffer on a hotplate to 60°C – 80°C
- Put the glass slides in the slide's rack
- Fill up a beaker with tap water and immerse the rack into the beaker for 5 minutes
- Put the rack into 10mM citrate buffer for 60 minutes
- Draw around samples on the glass slides with DAKO pen
- Wash the slides with PBS at 3 minutes (for 2 times)
- Drip 3% H₂O₂/MeOH for 10 minutes
- Wash the slides with PBS - 0.1% TBST - 0.1% TBST for 3 minutes each
- Drip the blocking buffer and incubate for 1 hour in room temperature inside humidifying chamber
- Prepare for primary antibody by diluting it with PBST+1% BSA as protocol
- Drain the excess blocking reagent
- Drip the primary antibody and incubate in room temperature for 1 hour
(or overnight at 4°C)
- Wash the slides with 0.1% TBST at 3 minutes (for 3 times)
- Drip the secondary antibody and incubate in room temperature for 1 hour (in dark situation)
- Wash the slides with 0.1% TBST at 3 minutes (for 3 times)
- Prepare DAB solution as protocol
- Drip the DAB solution for 1 – 3 minutes (in dark situation)
- Put the glass slides into the rack and immerse in tap water for 10 seconds
- Drain the water and drip Hematoxylin for 20 seconds
- Put the glass slides into the rack and immerse in tap water for 5 minutes
- Let them dry under the draft for 10 – 60 seconds (try not to over-dry the samples)
- Mount the samples with mountquik and cover with a cover slide.

Immunocytochemistry/immunofluorescence (ICC/IF)

Preparation:

10% Formalin

0.2% Triton-X

PBS

Blocking reagent (1% BSA + PBS)

 Add 10mg BSA into 10ml PBS

Primary antibody

Secondary antibody

DAPI

 50ml PBS + 10 μ l DAPI

VectorShield (DAKO)

Primary antibody

Actin (1:500)

 2 μ l stock + 998 μ l PBS-BSA 1%

Methods:

- Remove medium
- Wash with PBS (for 2 times)
- Fix cells with 10% formalin for 15 minutes
- Wash with PBS (for 3 times)
- Permeabilize 0.2% Triton-X for 3 minutes
- Wash with PBS (for 3 times)
- Add blocking reagent and incubate at room temperature for 1 hour
- Removed the blocking reagent and drain the excess reagents.
- Drip the primary antibody and incubate in room temperature for 1 hour
 (or overnight at 4°C)
- Wash with PBS (for 3 times)
- Add the secondary antibody (+ actin staining if needed) and incubate in room temperature for 1 hour (in dark situation)

- Wash with PBS (for 3 times)
- Counterstain with DAPI for 5 minutes (in dark situation)
- Rinse the coverslip with PBS and invert a drop of mounting media (VectorShield)
- Store the slides in the dark at -30°C

Reverse transcription - Polymerase chain reaction (rt-PCR)

A. Preparation:

- Cryopress equipment
- Liquid nitrogen
- PBS (-)
- TRIzol reagent (Invitrogen)
- Chloroform
- Isopropanol (2-propanol)
- RNase-free water
- TOYOBO ReverTra Ace qPCR Master Mix
- Thunderbird SYBR qPCR Mix (QPS-201; TOYOBO)

B. (i) Sample Preparation monolayer sample:

- Remove the culture medium in a 6-well plate (or culture dish) immediately after finishing the experiment
- After flushing with PBS (-), add a 1ml of TRIzol in the dish.
- By pipetting up and down, try to detach and dissolve all the cells attaching onto the dish.
- Collect the TRIzol reagent with the cells into 1.5ml tube.
- Perform RNA extraction or store it at -30°C or -80°C.

B. (ii) Sample Preparation tissue sample:

- Prepare for sterilized cryopress equipments as well as liquid nitrogen.
 - Place a sample into the mortar frozen by liquid nitrogen and fill it with a bit of liquid nitrogen.
 - Once the sample completely freezes over, fit in the pestle.
 - Place the holder under the cryopress and push the lever downwards such that the vibrator touches the pestle. This will grind the sample to fine small pieces.
- ** Be careful not to push down too long, or the samples may fly out.

- Scrap the small pieces off the pestle and into the mortar. Fill the mortar with a bit of liquid nitrogen to gather and freeze the grinded samples.
- Push the lever downwards again until the samples becomes a fine powder. (about 5~10 times)
- Transfer the grinded sample into a RNase-free 1.5ml tube.
- Fill the tube with 1ml of TRIzol reagent and dissolve it.
- Perform RNA extraction or store it at -30°C or -80°C.

(**Optional** for the samples with high content of fat, proteins, or extracellular material. But **DO NOT** perform this if you are performing DNA isolation)

- Centrifuge the samples at 12,000 x g for 10 minutes at 4°C
** The resulting pellet contains ECM, polysaccharides, and high molecular weight DNA, while the supernatant contains the RNA.
- Transfer the cleared supernatant to a new tube.
- Perform RNA extraction or store it at -30°C or -80°C.

C. mRNA extraction:

- Prepare for chloroform (e.g. TRIzol: Chloroform = 1 ml : 0.2 ml)
- Add 0.2ml of chloroform to the tube and shake vigorously by hand for 10 sec (You will see entirely pinkish color in the tube)
- Wait for 1 – 2 mins at room temperature for the mixture to be separated into whitish (top) and pinkish phase (bottom).
- Centrifuge the tube at 12,000xg for 15 mins at 4°C.
- Transfer the upper aqueous phase in the tube into a new tube, and try to obtain 350 – 500µl.
- Add 350µl of 100% isopropanol to the RNA aqueous. (e.g. RNA aqueous mixture : isopropanol = 1 : 1)
- Shake the tube vigorously by hand, and then vortex it.
- Incubate for 10 – 15 mins at room temperature. (or store at -30°C)
- Centrifuge the tube at 12,000 x g for 10 mins at 4°C
- (You will see whitish pellets formed at the bottom of the tube.)
- Dump the solutions gently from the tube not to lose the RNA pellets.

- Wash the pellet by adding 1ml of 75% ethanol and gently shake the tube by hand.
- Centrifuge the sample at 9,000 x g for 5 mins at 4°C.
- Carefully dump the solutions and make sure to remove all the ethanol left in the tube.
- Add a certain amount of RNase-free water (13 – 100µl) depending on the amount of pellets obtained, and re-suspend it by 10-20 times of pipetting up and down.
- Measure the concentration and purity of the RNA using the NanoDrop.
- Store it at -80°C.

Nanodrop:

A₂₃₀ : detecting the contamination of guanidine isothiocyanate, salts, sugars, or other organic solvents.

A₂₆₀ : detecting total RNA

A₂₈₀ : detecting protein or phenol contamination.

A₃₂₀ : checking for abnormal absorption.

For RNA with high purity

$$A_{260}/A_{280} = 1.8 \sim 2.0$$

$$A_{260}/A_{230} > 2.0$$

D. cDNA conversion (TOYOBO ReverTra Ace qPCR Master Mix):

- According to the concentration of samples obtained from NanoDrop, calculate to 500ng of RNA in a 0.2ml tube with RNase-free water up to a total volume of 6 μ l.
(i.e. concentration = mass / volume; mass = 500ng)
- Denature the RNA by incubating at 65°C for 5 mins and then chill on ice.
- Add 2 μ l of 4 x DN Master mix with gDNA remover into the tube to make 8 μ l of total volume.
- Incubate at 37°C for 5 mins and then chill on ice.
- Add 2 μ l of 5 x RT Master mix into the tube to make 10 μ l of total volume.
- Incubate the sample at 37°C for 15 mins, followed by 50°C for 5 mins and 98°C for 5 mins
- Store the cDNA samples at -30°C.

E. RT-PCR (ABI StepOnePlus – SYBR Green Fast):

- cDNA samples and standard
 - Make working samples by diluting the cDNA samples to 1/20 with RNase-free water in a sterile 0.2ml tube.
 - By mixing 1 – 2 μ l of each cDNA sample together to make the standard stocks. (100 \times standard)
 - Make further 10 times dilutions twice to obtain 10 \times and 1 \times standard using RNase-free water. (10 \times standard and 1 \times standard)
- Master mix
 - RNase-free water 1.2 μ l
 - ROX 0.2 μ l
 - Forward Primer (10 μ M) 0.3 μ l
 - Reverse Primer (10 μ M) 0.3 μ l
 - SYBR Green 5.0 μ l
- Protocol:
 - Prepare for a 96-well plate, and transfer 3 μ l of cDNA and standards (100 \times , 10 \times , 1 \times) into the plate

- Transfer 7 μ l of the target gene of primer master mix into the 96-well plate.
- Seal the sealer properly and mix the solution in the plate by shaking up and down.
- Spin down the plate and place them into the ABI StepOnePlus machine.
- On the computer, open the ABI software and start the run after setting the target and sample names as well as plate setting.